Seismic data processing

Special course IV

3dr year Geophysics students

General seismic data processing sequence

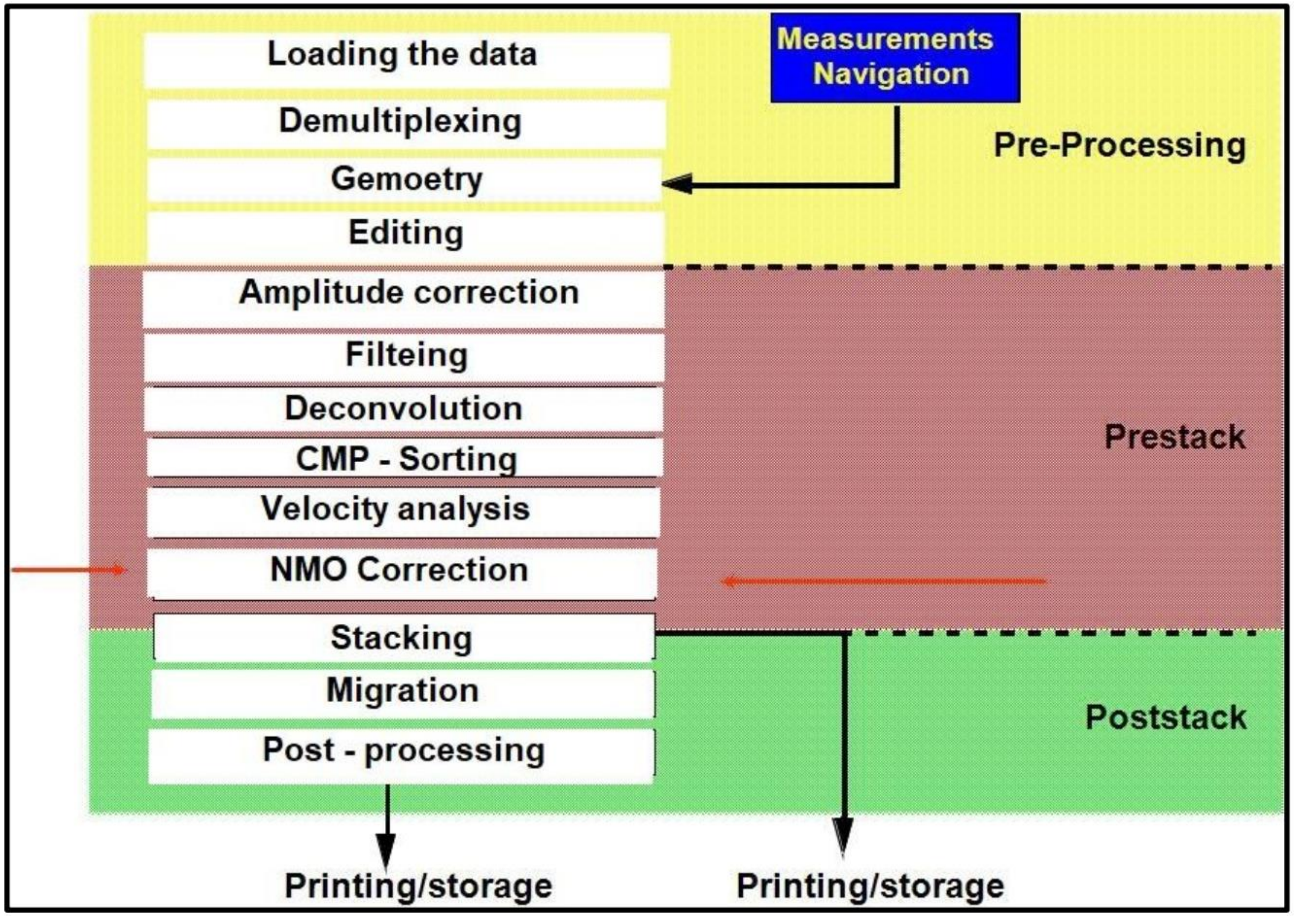

Seismic reflection processing

Flow overview

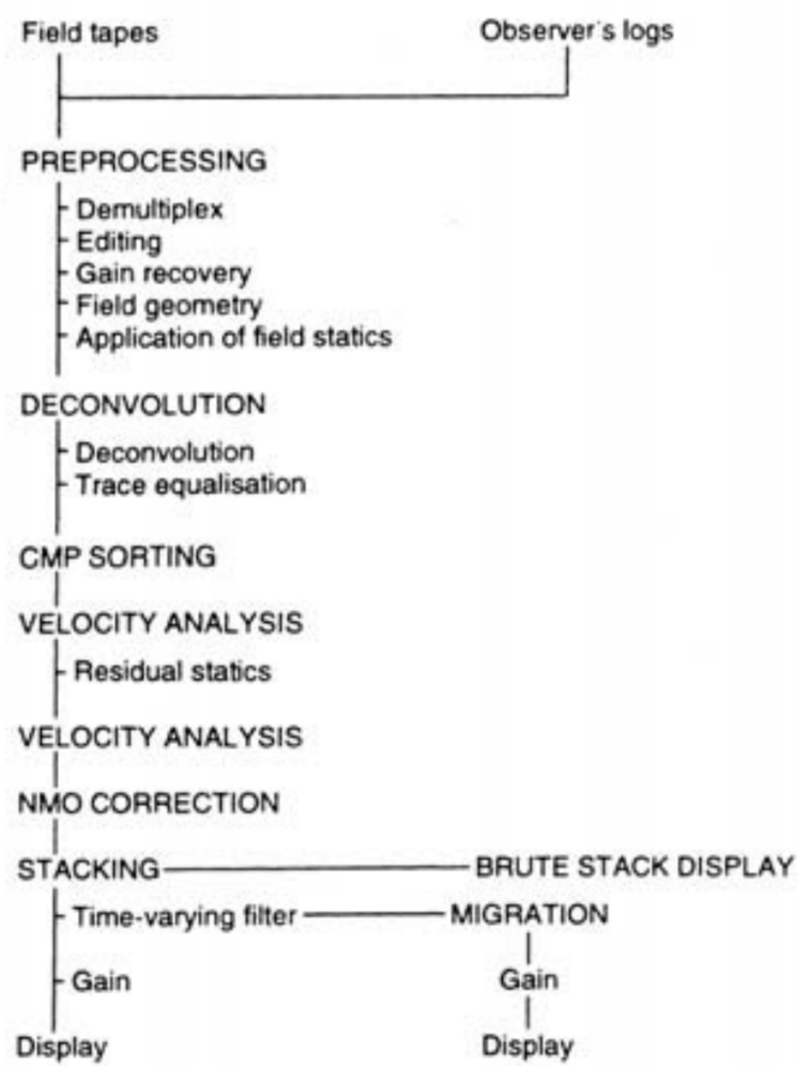

These are the main steps in processing

The order in which they are applied is variable

1. Demultiplexing

- The name given to sorting the traces from time ordered storage (all receiver stations at a given time) to receiver ordered format (all times for a given receiver) or trace sequential format.

- Many modern instruments do this in the field, but much data still comes in from the field multiplexed. SEG A and SEG B formats are multiplexed, SEG Y is a trace sequential format, and SEG D can be either way.

- This process <u>takes the data coming from the receivers and puts them into trace order</u>.

- Normally the data are written to tape at this stage in one of the designated industry formats so that the raw records are maintained to form the basis of possible later reprocessing.

- If starting from field tapes, reformatting includes <u>converting the data from standard industry format into whatever format the processing system uses</u> (Bacon et all 2003).

Demultiplexing

…bookkeeping!

Four geophones: A, B, C, D, recording samples 1, 2, 3, 4 …

- The recoding device stores samples in the order recorded
- Demultiplexing is separating all the samples to produce a time sequence for each geophone

$$\mathbf{A_1B_1C_1D_1A_2B_2C_2D_2A_3B_3C_3D_3A_4B_4C_4D_4 \ldots.}$$

$$\mathbf{A_1A_2A_3A_4 \ldots.}$$

$$\mathbf{B_1B_2B_3B_4 \ldots.}$$

$$\mathbf{C_1C_2C_3C_4 \ldots.}$$

$$\mathbf{D_1D_2D_3D_4 \ldots.}$$

Industry standards (SEG) usually allows for painless translation of the data

2. Data editing

Trace editing: Noisy traces, Traces with transient glitches or mono frequency signals are deleted, correcting reversals polarity.

In real data there may be bad traces or missing traces. Some shots may be bad , or there may be consistent or systematic errors in the data.

The processer should check the data by dividing it in to groups of shots. The divided groups checked one by one by viewing them, so the dead shot and the noisy traces will be detect.

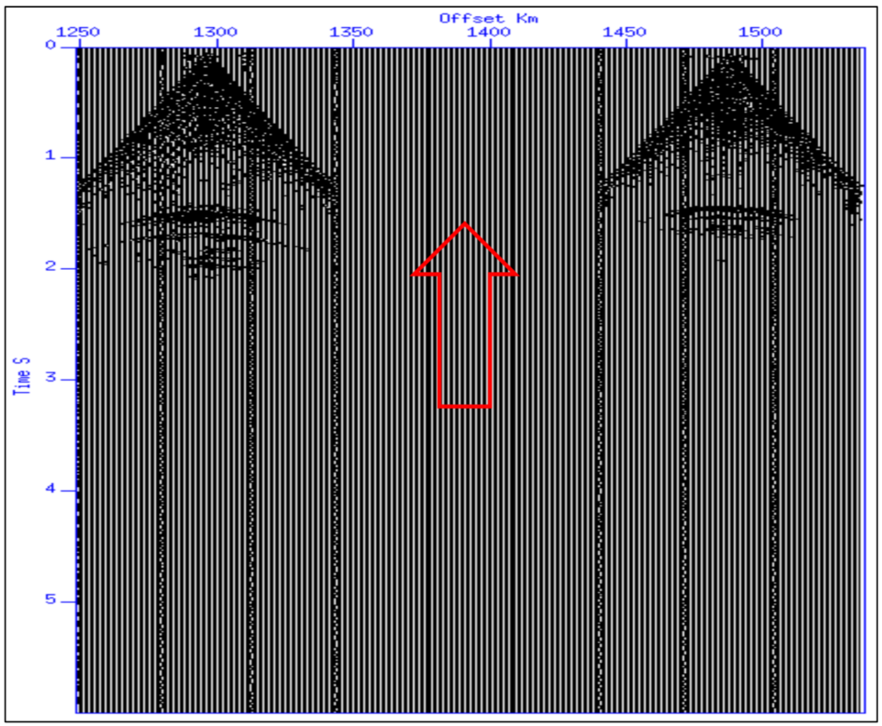

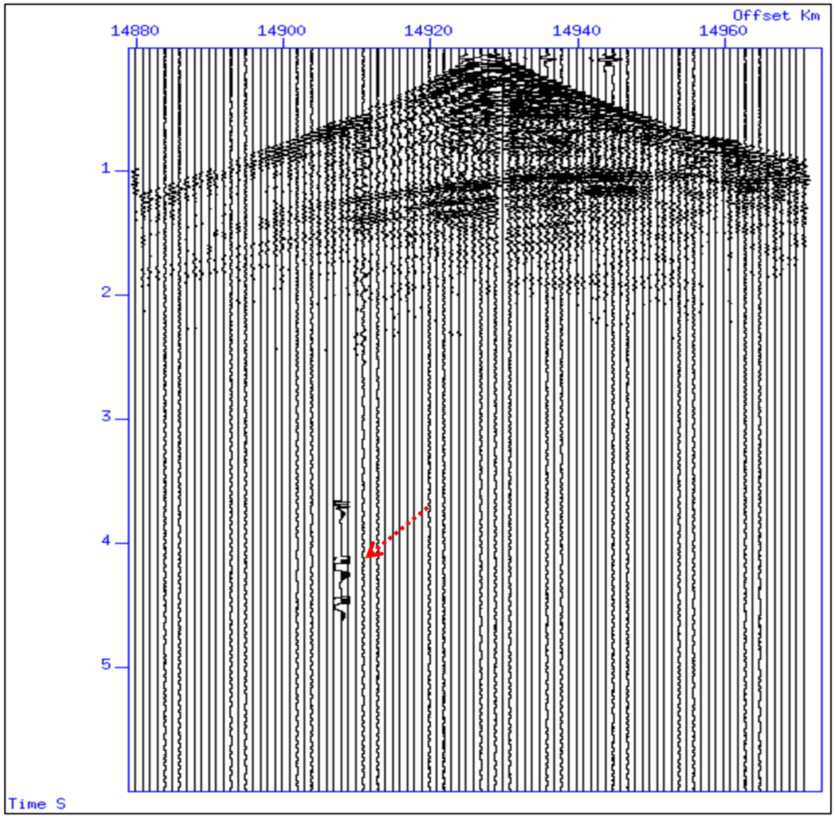

3. Geometry Definition

- Geometry information tells us how the Multiple Coverage was achieved by defining the coordinates of shot and receivers, relationship between file numbers and shot locations, relationship between shots and receivers, missing shots and or receivers and attributes for shots and receivers e.g. elevations, depths etc (Westren geco, 2007).

4. Field Layout

4.1 Spread types

The spread types is related to the arrangement of geophone groups in relation to the source point (Sheriff, 2002), or to the geometrical pattern of groups of geophones relative to the seismic source.
The output from a single shot is recorded simultaneously by the spread during seismic acquisition (Schlumberger, 2017).

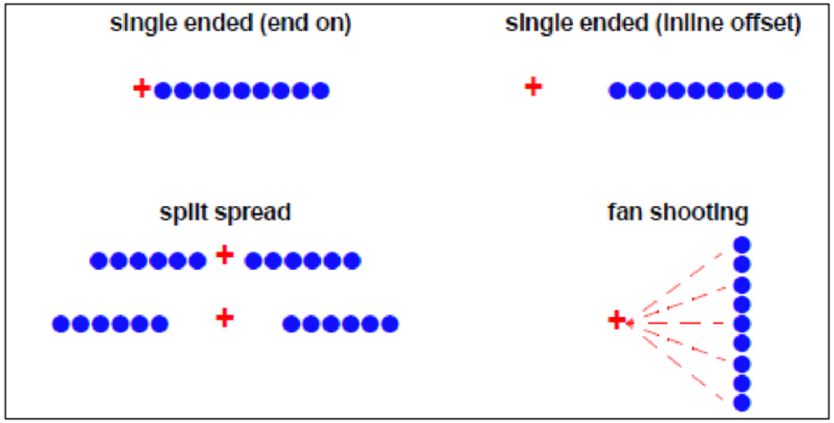

- The three common types of Spread types (field geometry) .
- The seismic source is at one end, and receivers are only on one side of the source it is End on type.
- Split spread or Straddle spread has been the most commonly used spread before the coming into operation of digital recording. In this case, the source is at the center and geophones are symmetrically placed on either side of it.
- Geophones may be offset with respect to the source when so desired.
- Records from a split spread reflection survey are used to detect the dipping reflectors and to find the amount of slope.
- The detection points receivers are laid out in fan-like arrays at distances from a common source point. This spread called Fan shooting.

4. Field Layout

4.2 CDP recording and gathers type

- In multichannel seismic acquisition where beds do not dip, the common reflection point at depth on a reflector, or the halfway point when a wave travels from a source to a reflector to a receiver.
- In the case of flat layers, the common depth point is vertically below the common midpoint.
- In the case of dipping beds, there is no common depth point shared by multiple sources and receivers (Schlumberger, 2017).

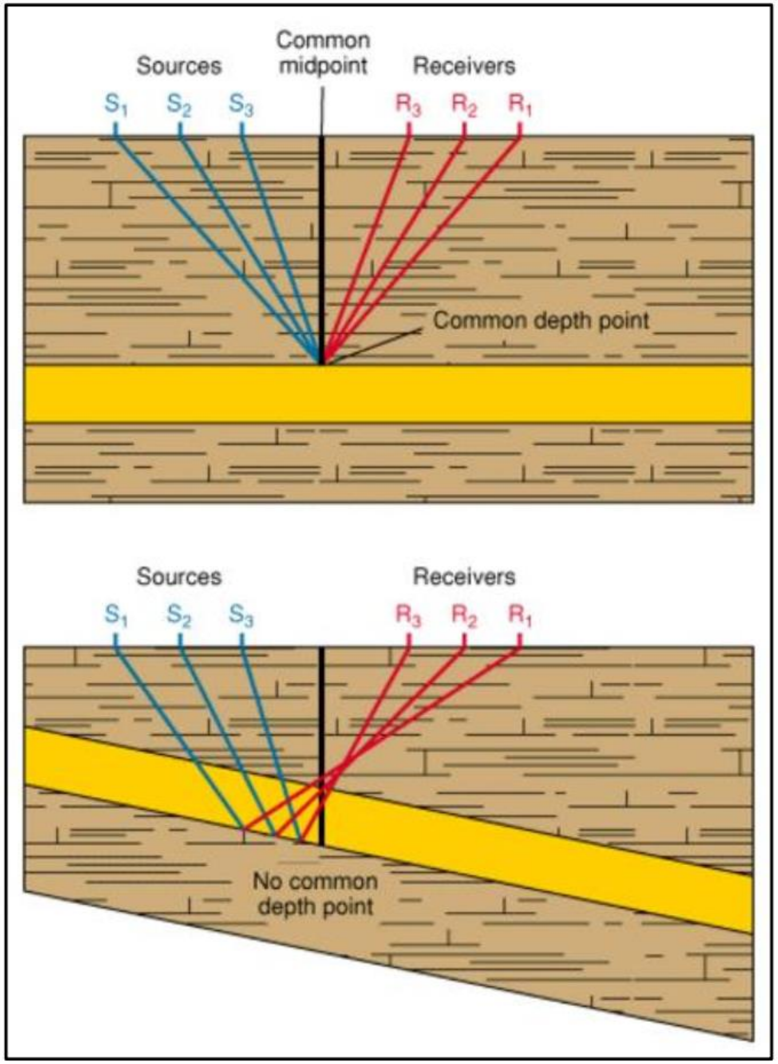

The seismic traces can be viewed in different gathers.
A gather is a collection of seismic traces which share some common geometric attribute which are sorted from field records.

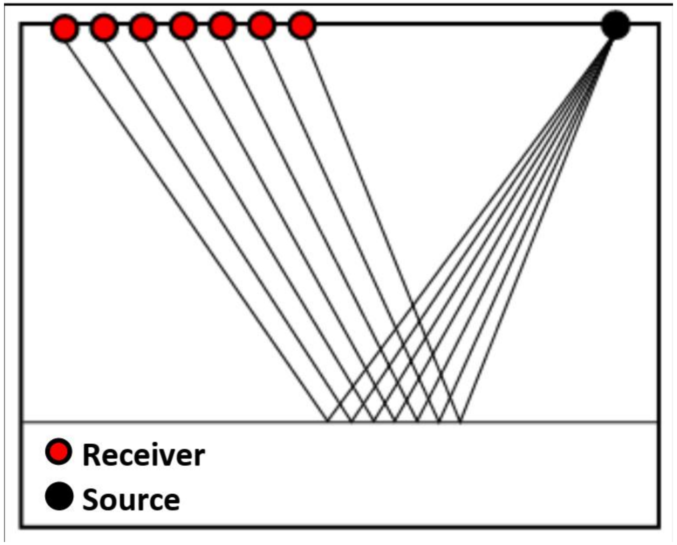

These gather are :

- Common source or receiver gathers basic quality assessment tools in field acquisition.

- When the traces of the gather come from a single shot and many receivers, it is called a common shot gather. A single receiver with many shots is called a common receiver gather.

- It is very easy to inspect traces in these displays for bad receivers or bad shots (Schlumberger, 2017).

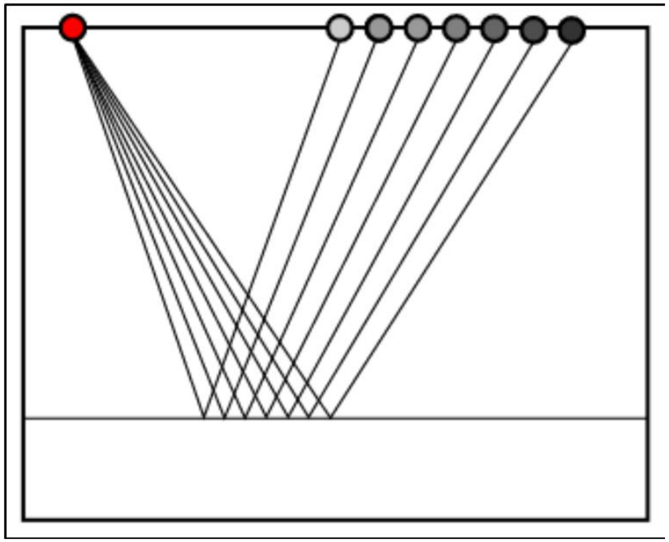

- <u>**Common midpoint gather**</u> the conventional gather traces sorted by surface geometry to approximate a single reflection point in the earth.

- Data from several shots and receivers are combined into a single gather.

- The traces are sorted <u>by offset</u> in order to perform velocity analysis for data processing and hyperbolic moveout correction.

- Only shot–receiver geometry is required to construct this type of gather (Schlumberger, 2017).

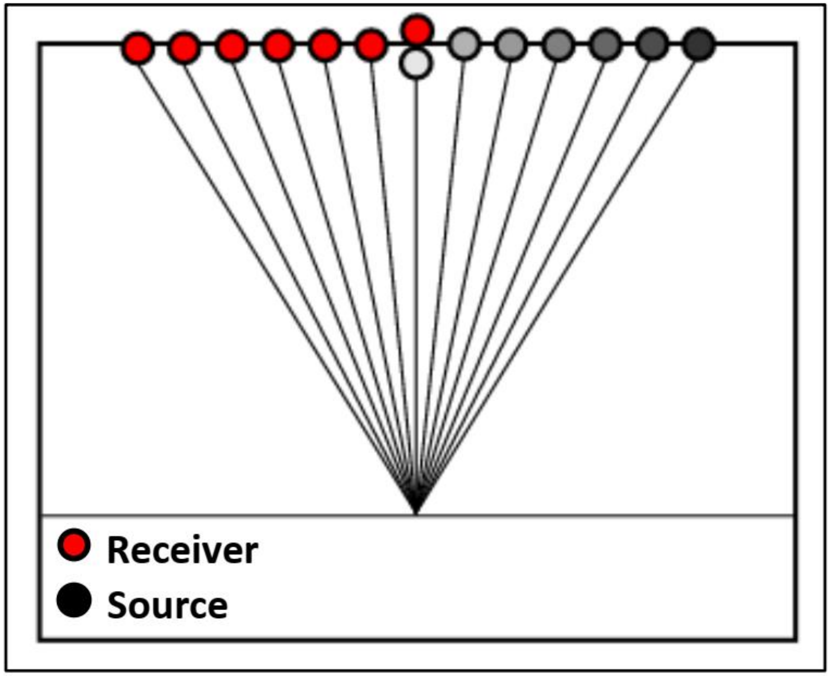

- Common offset gather used for basic quality control, because it approximates a structural section.

- Since all the traces are at the same offset, it is also sometimes used in AVO analysis; one can quickly inspect the approximate spatial extent of a candidate AVO anomaly.

- If the near offset trace is used for each shot, this is called a brute stack (Schlumberger, 2017).

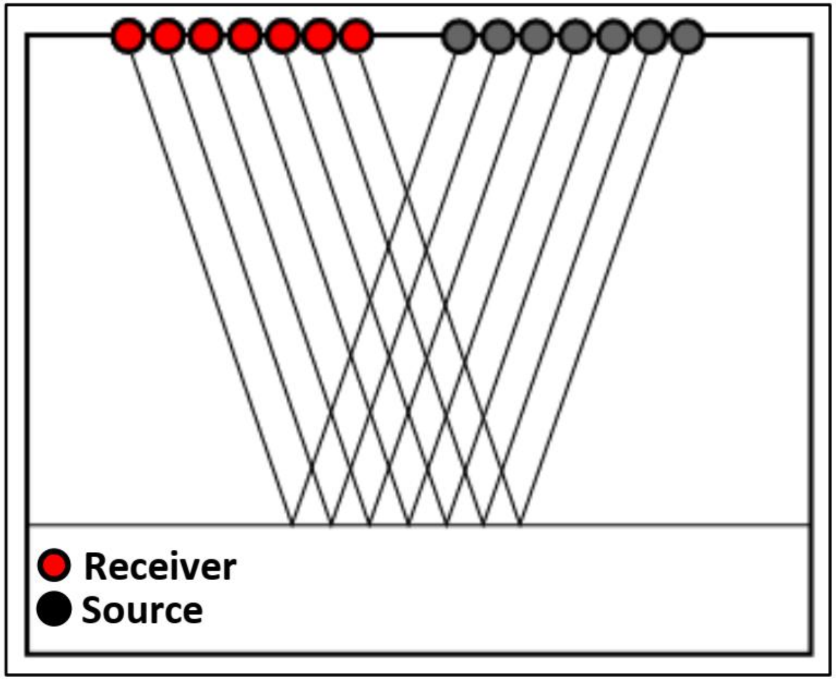

5. Amplitude Recovery

- The amplitude recovery is applied to seismic data to compensate for attenuation, spherical divergence and other effects.

- The goal is to get the data to a state where the reflection amplitudes relate directly to the change in rock properties giving rise to them (Schlumberger glossary, 2017).

- With regard to equalizing amplitudes on one trace, it may be obvious that <u>reflection late in the section will be of a much smaller in amplitude</u> than the ones <u>early in the section</u>, simply due to energy losses in the subsurface.

- The most important energy losses are due to geometrical spreading, absorption of the rocks and transmission losses.

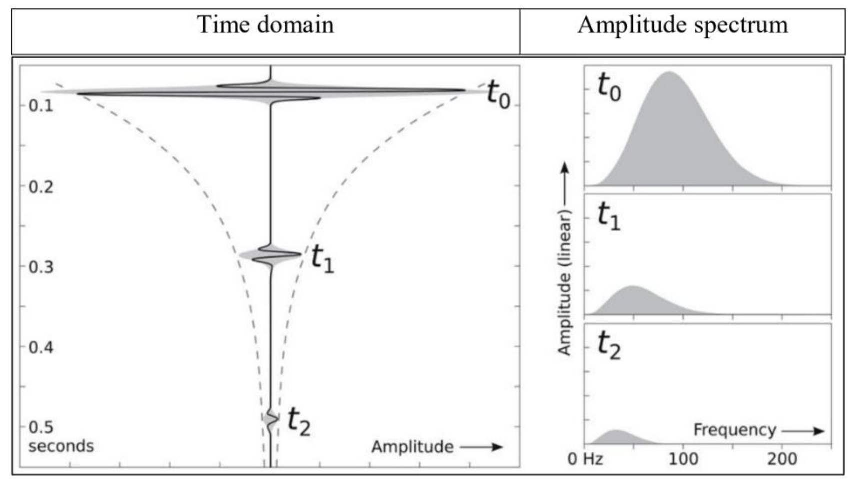

Amplitude decay (Reine, 2013).

Preprocessing
Gain recovery

"Turn up the volume" to account for seismic attenuation

1. Could calculate the energy/amplitude loss using geometric spreading and apply a correction
2. **Automatic gain control (AGC)** apply a gain to equalize amplitude along the trace

Pre-AGC

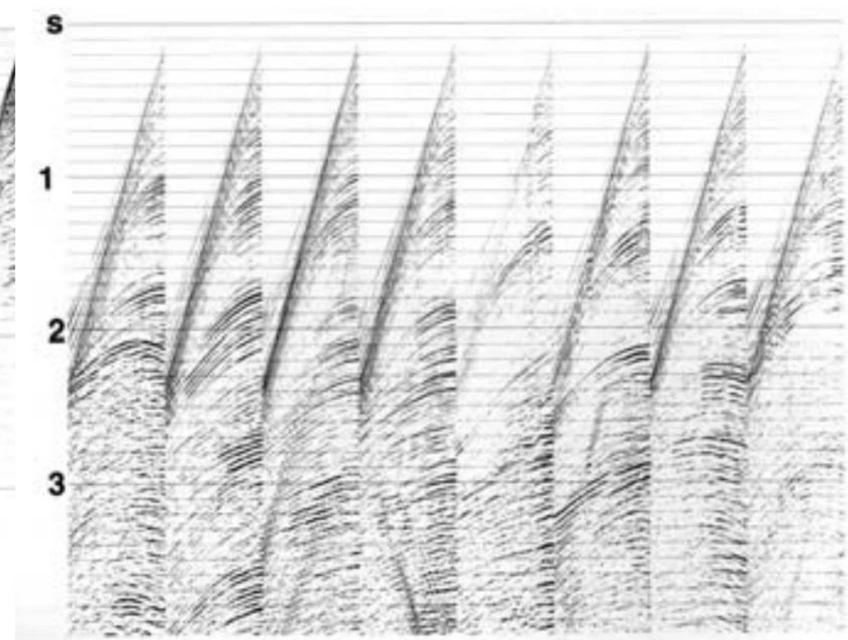

Post-AGC

- Geometrical spreading is spreading of the wavefront since the energy of a wave is inversely proportional to $1/r^2$ (in a homogeneous medium). This means that the amplitude is decaying as $1/r$.
- There is an assumption that the data is processed as if it was measured in a two-dimensional world, which means a spreading is proportional to $1/\sqrt{r}$ for the amplitude.
- A correction is made on the traces with a spreading function. This geometrical spreading function is specified as a travel time and a specific average velocity function (Drijkoningen and Verschuur, 2003).
- The other (gain) correction is applied to correct for absorption, and this one is corrected with an exponential gain function, where the factor in the exponential is related to the average absorption coefficient of the rocks.
- Then, the last correction is to deal with the transmission losses at interfaces in the subsurface although, this correction is usually included in the exponential gain for the absorption losses (Drijkoningen and Verschuur, 2003).

6- Seismic Noise

- Noise attenuation is an important step in seismic data processing, and must be held in a way so that at the end of the acquisition and processing sequence, the desired signal can be reliably interpreted and the noise is suppressed as much as possible.
- There are main types of noise such as multiples, ground roll and scattered energy.
- How much low-velocity noise can be suppressed depends on the choice of field arrays, the stack response, filtering and on various processing steps, (Vermeer 2002).

- Noise is any disturbance on the seismic record which tends to obscure primary reflections from rock strata. It may be conveniently divided into two sorts random noise and coherent (Ashcroft, 2011).
- Coherent noise is generated by the shot itself. S waves, Love and Rayleigh waves (ground roll) and reflections from surface irregularities are all forms of coherent noise.
- In shallow refraction work these slow, and therefore late arriving waves usually prevent the use of any event other than the first arrival of energy (Milsom, 2003).

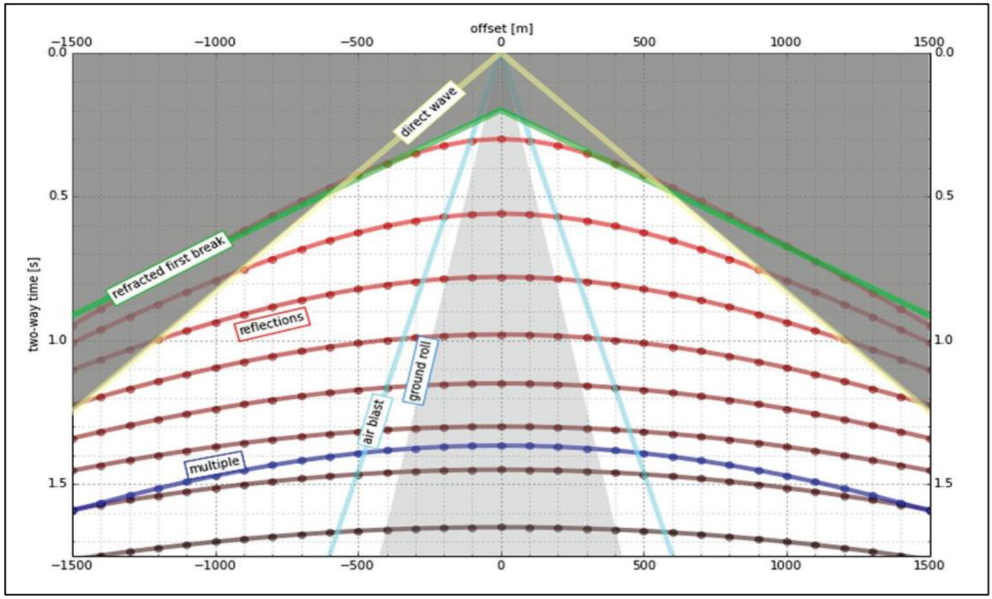

Seismic noise type (Bianco, 2014)

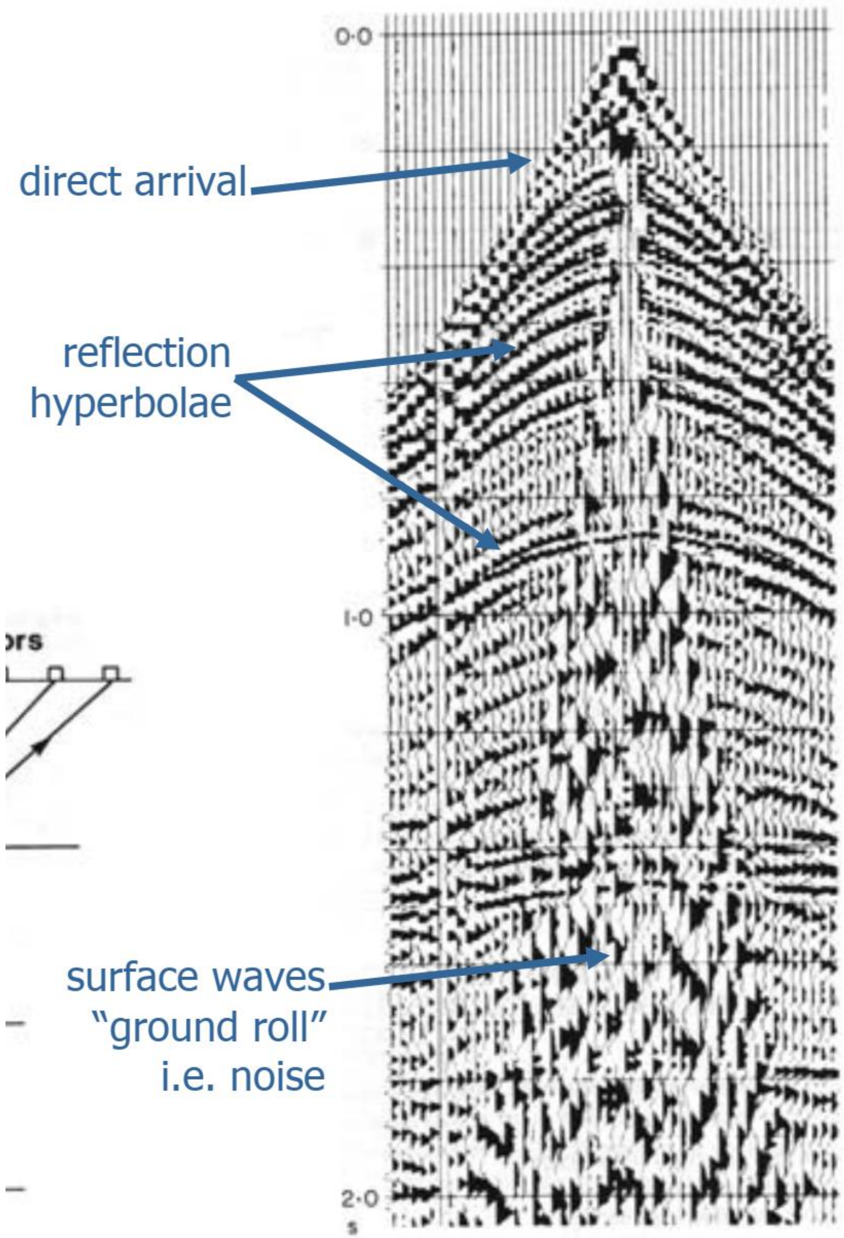
direct arrival
reflection
hyperbolae
surface waves
"ground roll"
i.e. noise
0·0
1·0
2·0
s

- Random noise is noise generated by activities in the environment where seismic acquisition work is being carried out. Movements of traffic, animals and people all generate random noise and can, to varying extents, be controlled. It should at least be possible to prevent the survey team contributing, by giving warning using a whistle or hooter (Milsom, 2003).

- This noise appears in a seismic record as spikes. In a marine acquisition, random noise can be created by ship props, drilling, other seismic boats, and wind or tidal waves.

- Radom noises in seismic data are recognized principally by the absence of coherency or continuity from one seismic trace to the next.

- Random noise can be reduced or removed from data by stacking the traces, filtering during processing or using arrays of geophones during acquisition (Onajite, 2014).

- The signal-to-noise ratio, abbreviated S/N, is the ratio of the signal energy in a specified portion of the record to the total noise energy in the same portion.
- Whenever the signal-to-noise ratio is small, poor records are resulted. (Telford et al,1990).

7- Resolution in seismic reflection surveys

- The ability of separating two closely spaced features in depth (time) as well as in space.

- The minimum separation distance between two seismic events (two distinct features on the seismic section).

- The sharper the reflected wavelet, and higher S/N ratio, the better the resolution will be.

- Wavelength λ is defined by the equation $\lambda = v/f$, where 'v' velocity and 'f' frequency of the wave passing through a medium.
- There are two types of the resolution: vertical and horizontal resolution.

A- Vertical Resolution

$t = 200$ m

The seismic pulse has a wavelength, λ=200 m. When the layer is relatively thick, the two reflections are distinct in the combined seismic trace (right hand panel).

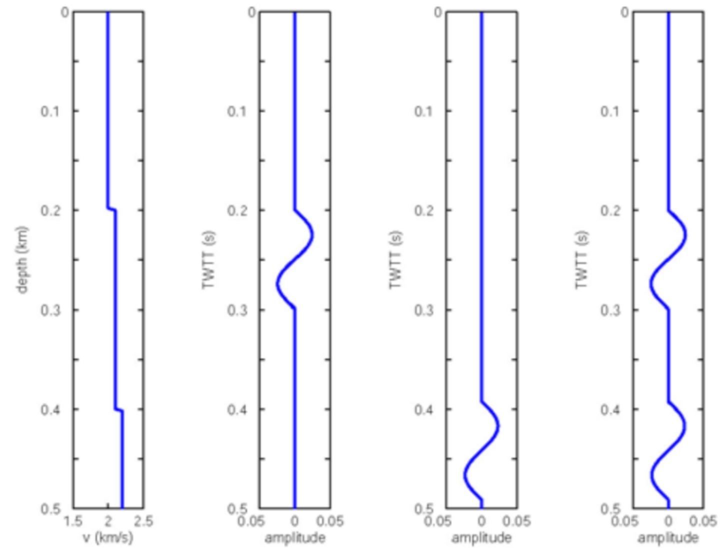

$t = 20$ m

When the layer is very thin (t = 20 m), the two reflections overlap and two separate reflections cannot be identified.

In this case, it is not possible to determine that two layers are present.

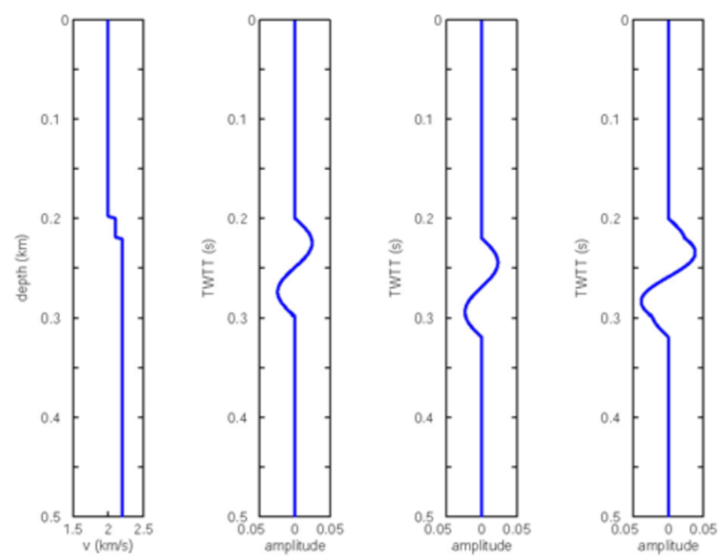

A- Vertical Resolution

$t = 50$ m

Note that the transition occurs when the crest of second arrival coincides with the trough of the first arrival.

This is produced by the second reflection travelling a distance $2t$ greater than the first reflection.

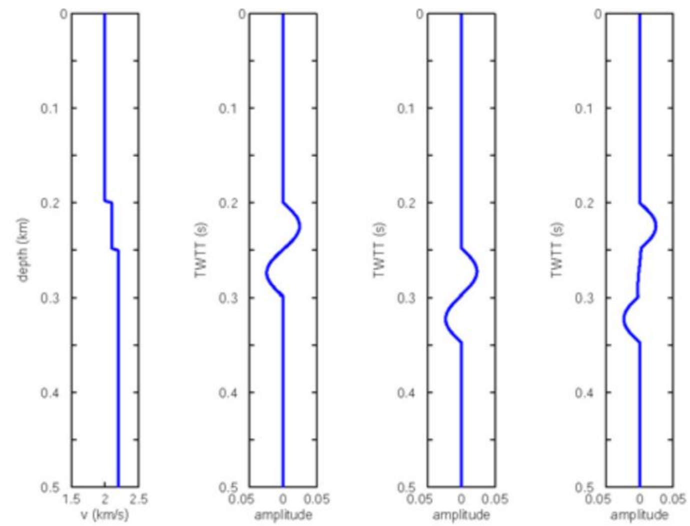

Two waves can be distinguished from each other if they are separated by distance ***λ/2.***
Now the reflection from the lower interface has travelled an additional distance of 2*t*.
Thus the best resolution occurs when $2t = \lambda/2$ which gives ***t = λ/4***

$t = 60$ m

The second reflection can just be detected.

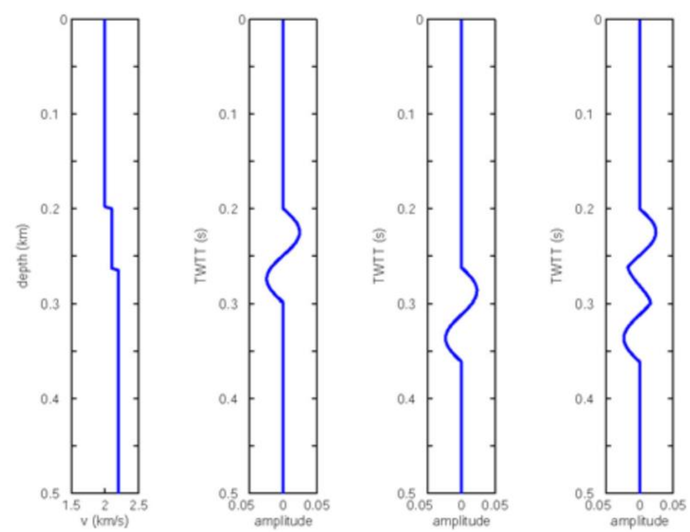

B- Horizontal resolution

Two factors can limit horizontal resolution in a reflection survey. One is due to the physics of seismic wave propagation (Fresnel zones), and the other is due to the geophone spacing.

Fresnel zones

- Fresnel zone is defined as the subsurface area, which reflects energy that arrives at the earth's surface within a time delay equal to half the dominant period (T/2).
- In this case ray paths of reflected waves differ by less than **λ/2**. Commonly accepted value is one-fourth the signal wavelength *(λ/4)*.

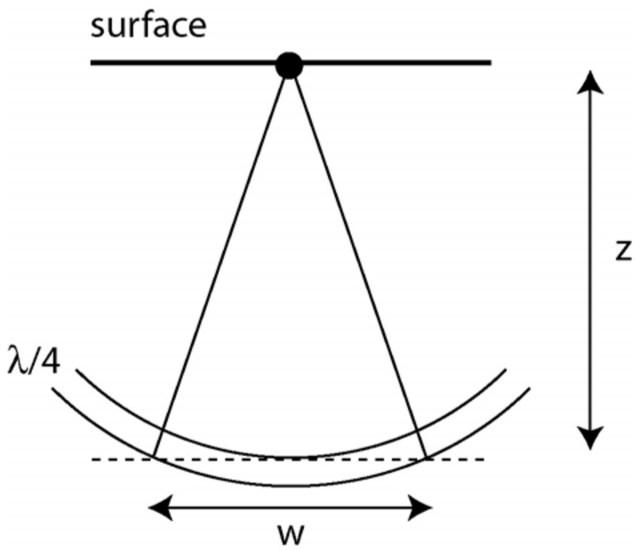

The reflection essentially occurs from a circular disk, over which in phase reflections occur. This is called the **Fresnel zone** and has a width $w = 2z\lambda$

The width of this zone is the smallest feature that can be detected with the surface. -- Higher resolution will be achieved by using short wavelengths. However this will result in more attenuation, and the signals will have limited penetration.

B- Horizontal resolution

Detector spacing

- The reflection points on an interface will have a horizontal spacing equal to half the geophone/hydrophone spacing.

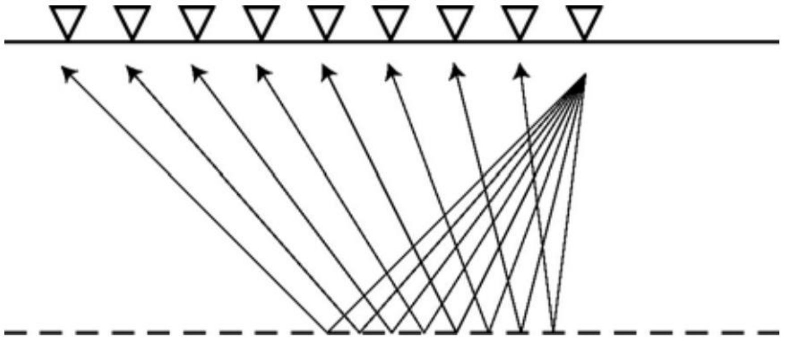

- By making this spacing **less than** the Fresnel zone, the survey resolution will not be limited by the layout, but by the physics of the wave propagation.

8. Statics and their removal

- ***Elevation statics*:**

Geophones at an elevation above a datum (or reference level) will detect the incoming signal later than a geophone on the datum.

- ***Weathering statics*** :

weathering of near surface rocks produces a zone of low velocities that is variable in thickness.

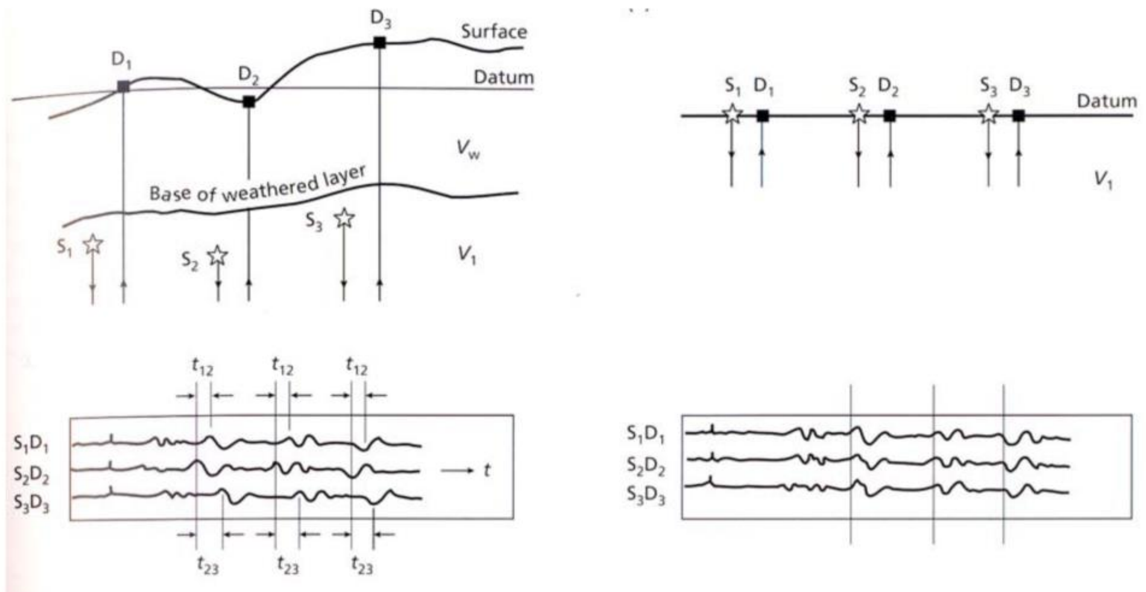

Kearey Figure 4.15

Correction of statics

●Elevation statics can be removed by accurate surveying with GPS or differential GPS.

●Weathering statics can be estimated from a variety of techniques, including measuring the refracted arrival (head wave) that travels along the base of the weathered layer.

Static corrections

Correct for surface topography and the weathered surface layer

Surface topography

Time correction to each trace:

$$t_g = \left(E_g - E_d\right)/V$$

Source depth

$$t_s = \left(E_s - E_d\right)/V$$

total correction

$$t_e = t_s + t_g$$

Shift each trace by this amount to line up deeper reflectors

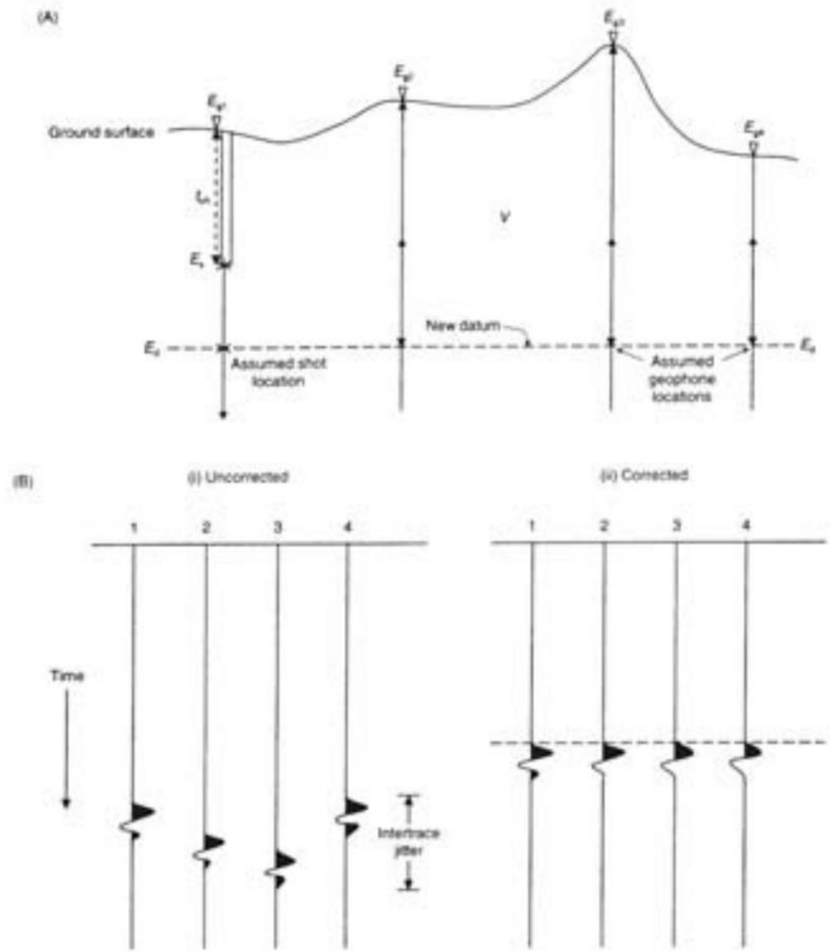

Static corrections

To make corrections we need to know the velocity of the surface weathered material

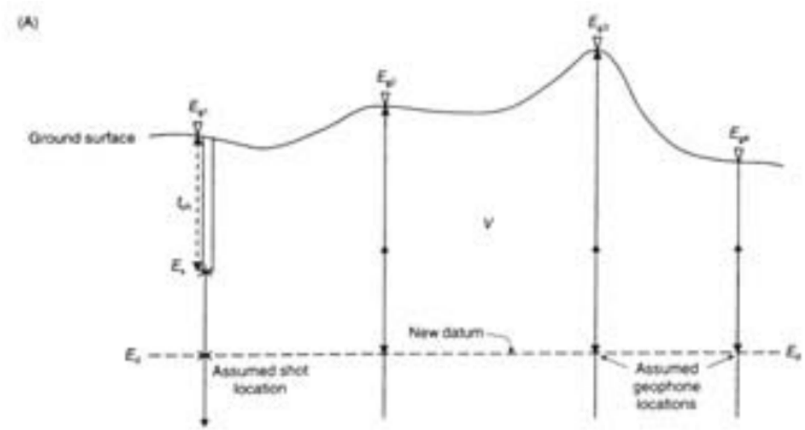

Uphole traveltime

$$V = d / t_{uh}$$

Refraction studies

Used to determine near surface velocities and variations in the thickness of the weathered layer.

Finally,

Data smoothing statics

- An automated process which lines up adjacent peaks
- Can only be applied when reflections are already within a wiggle

In residual static analysis, traces are automatically aligned to produce the most continuous seismic event. Example below is from *Kearey Figure 4.16*

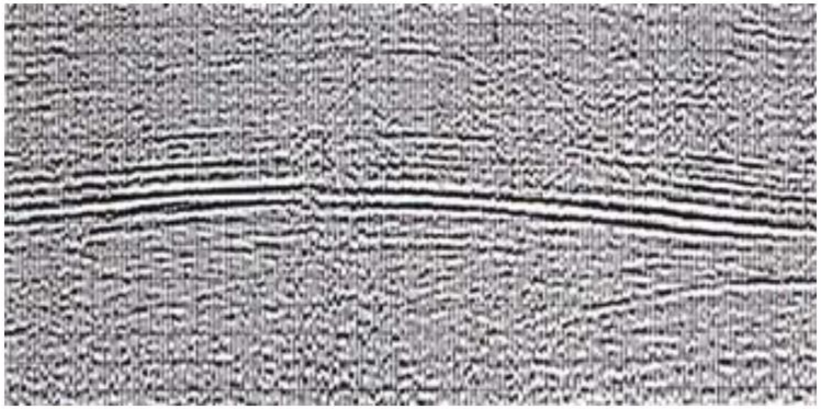

Before

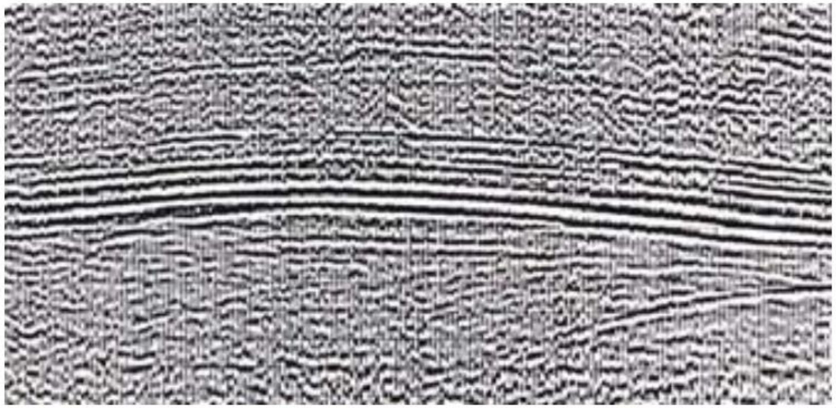

After residual static analysis

Static corrections

An example

Pre-correction

Post-correction

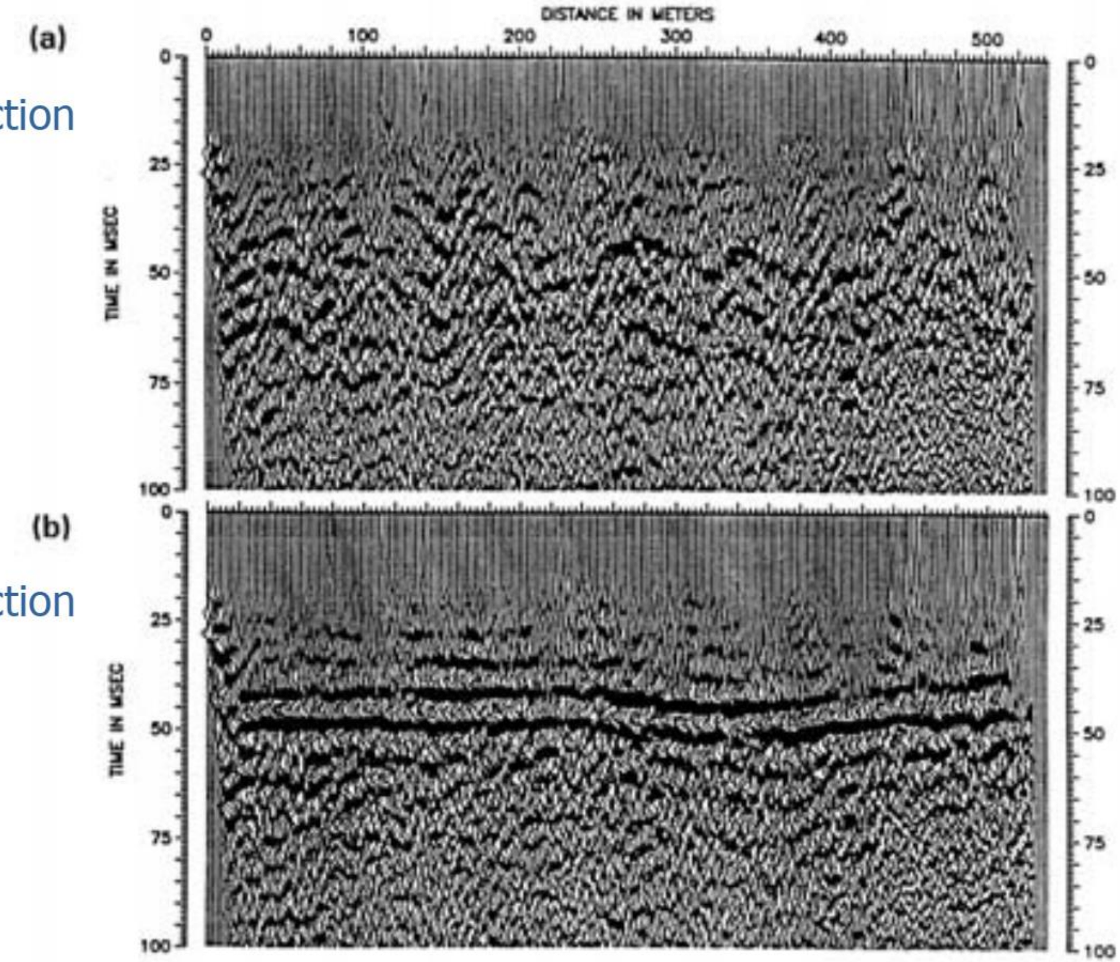

Fig. 4.17 Effect of applying residual static corrections on CDP reflection data recorded at a waste-dump site in Zealand, Denmark. Time section (a) before application of statics and (b) after application of statics. (After Ploug, 1991.)

9. Seismic Noise Filtering

1 Frequency Filter

- In order to separate noise from useful reflected signal, criteria of their frequency range and velocity may be utilized.
- If the low frequency, high energy noise, such as surface waves, has frequencies which are well separated from reflection signal frequencies, they may be filtered out during initial recording itself.
- However, it is found that noise spectrum often overlaps the signal spectrum, and for this reason the frequency filtering is of limited value only (Upadhyay, 2004).
- The filter response may be expressed either in the time domain or in the frequency domain.
- If the response is known in one domain it is possible to express it in the other domain.
- For accomplishing the filter operation, both the seismic signal and filter response characteristics should be expressed in the common domain, either in the time domain or in the frequency domain (Upadhyay, 2004).

There are many varieties of filters:

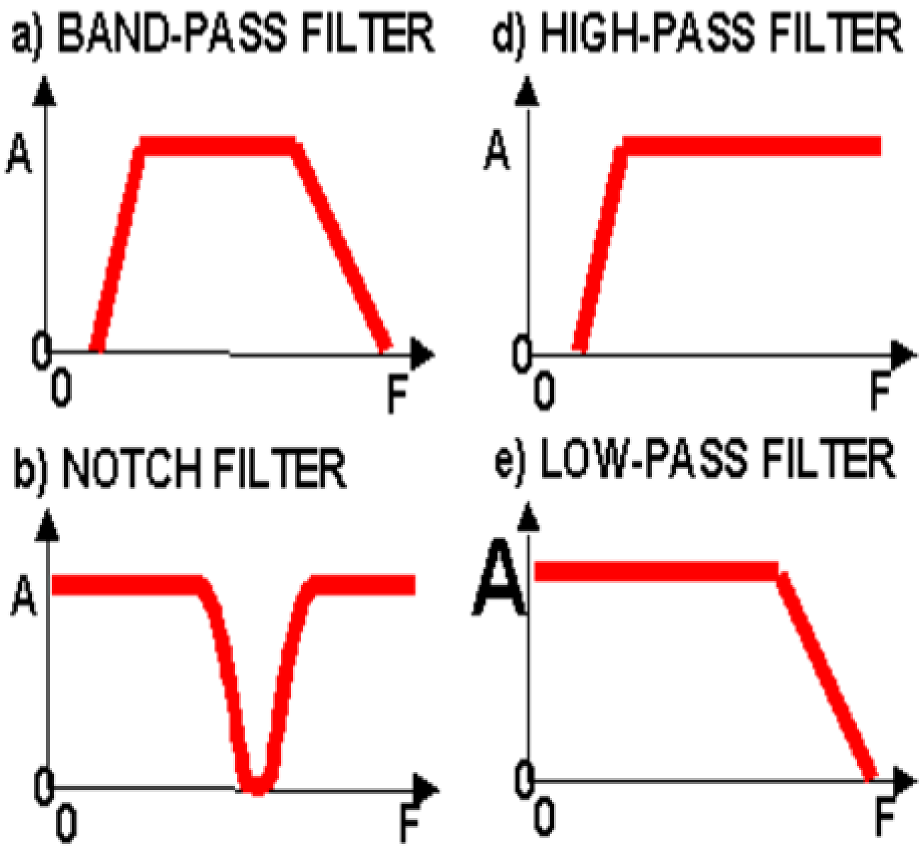

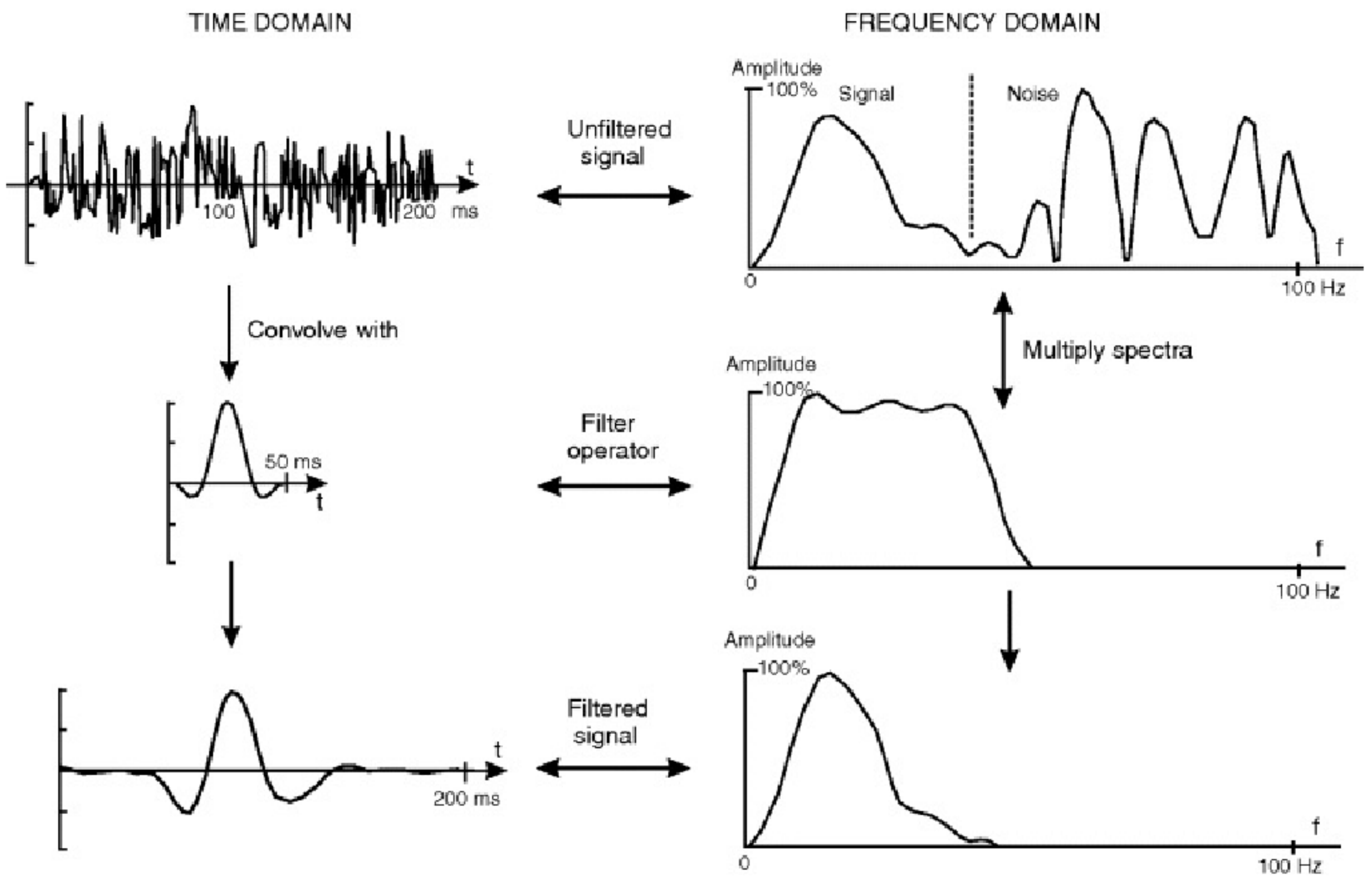

Filtering in time and in frequency domain (Ashcroft, 2011)

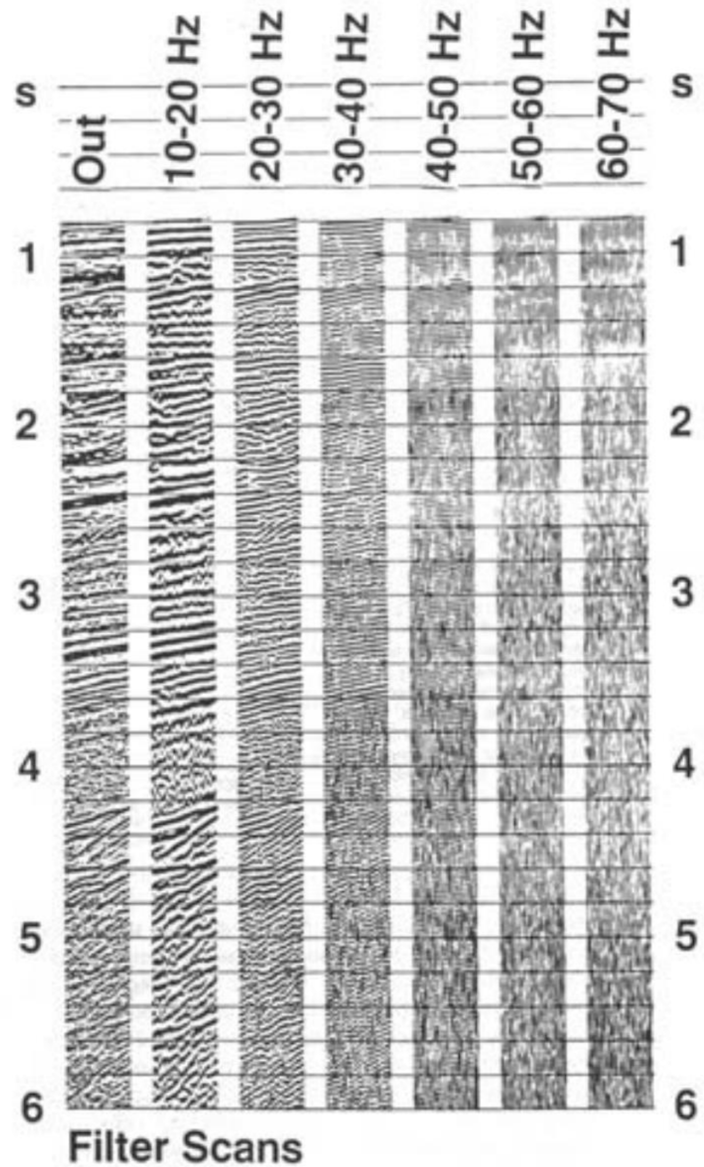

7-6 Example of filter scans (right) on raw field data (left). The bandpass of the filter used for each panel is annotated at the head of each panel. The low-frequency signals are at least 10 Hz (and probably lower). The high-cut of the filter should be time-variant here: higher than 60–70 Hz could be cut after 1.5 s; higher than 50–60 Hz could be cut after 1.5 s; higher than 50–60 Hz could be cut after 2.4 s; higher than 40–50 Hz could be cut after 4 s. (*Western Geophysical.*)

2-Frequency-Wavenumber (F-K) Filter (Dip filter)

- An F–K filter is designed to suppress unwanted events in the frequency wavenumber (F–K) domain. When applying multidimensional Fourier transforms, such as from (*t*, *x*) to (*f*,k), linear events in the original domain will also be linear events in the transformed domain, except that the orientations of each event in the two domains are perpendicular to each other (Chun & Jacewitz, 1981).
- If there are linear noises, or if there are noises with dip (offset or time) less than a certain angle, such as ground rolls, we can mute such noise in the F–K domain, and then transfer the remaining data back to the *t*–*x* domain. Hence F–K filtering is also called dip-filtering when it is used to remove linear events of certain dip angle (Zhou, 2014).

Linear events and their orientation before and after 2D Fourier transform (a) in time domain before transformation (b) in wavenumber domain after transformation (Zhou, 2014).

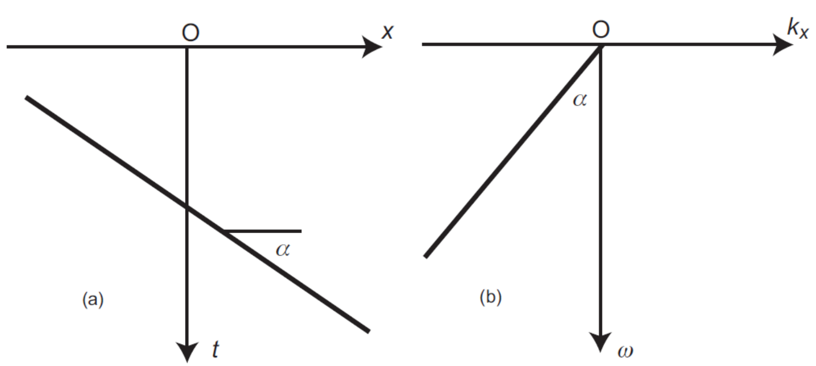

•A seismic pulse travelling with velocity *v* at an angle α to the vertical will propagate across the spread with an apparent velocity ($V_a = v/\sin\alpha$) .
•Along the spread direction, each individual sinusoidal component of the pulse will have an apparent wavenumber k_a related to its individual frequency *f*, where ($f = V_a k_a$). Hence, a straight-line curve with a gradient of V_a will be formed from the plot of frequency against apparent wavenumber for the pulse.

- Any seismic event propagating across a surface spread will be characterized by an F-K curve radiating from the origin at a particular gradient determined by the apparent velocity with which the event passes across the spread. The overall set of curves for a typical shot gather containing reflected and surface propagating seismic events is shown in the figure, (Kearry et.al 2002).

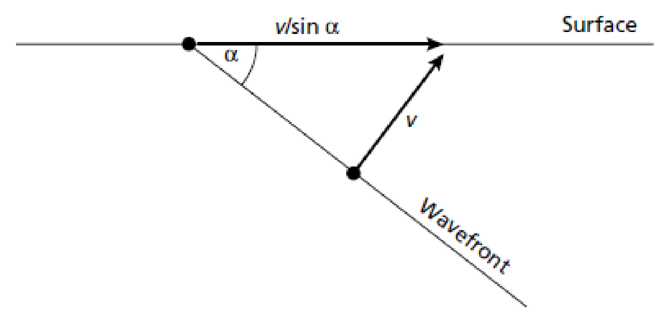

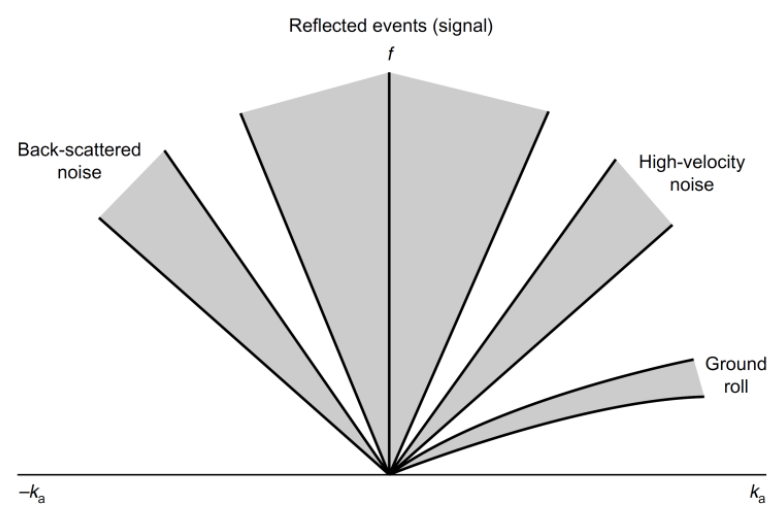

•It is apparent that different types of seismic event fall within different zones of the *f–k* plot.

•This fact provides a means of filtering to suppress unwanted events on the basis of their apparent velocity.

- The normal means by which this is achieved, known as <u>*f–k* filtering</u>, is:
- to perform a 2D Fourier transformation of the seismic data from the *t–x* domain to the *f–k* domain,
- then to filter the *f–k* plot by removing a wedge-shaped zone or zones containing the unwanted noise events
- and finally to transform back into the *t–x* domain, (March & Bailey 1983).

FK TRANSFORM

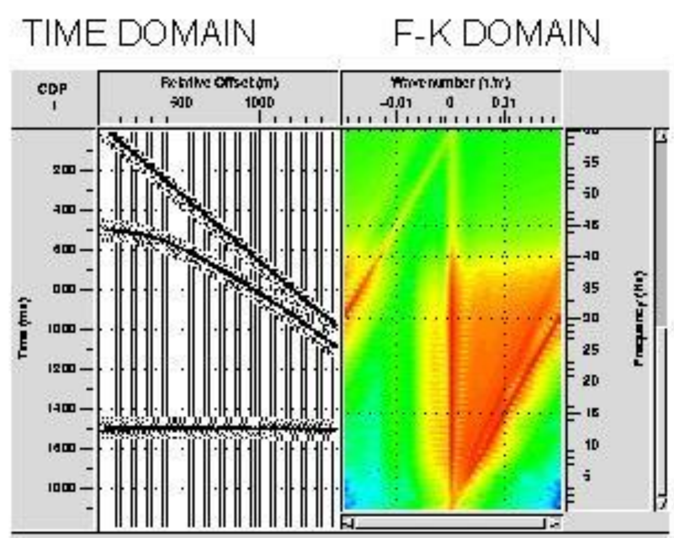

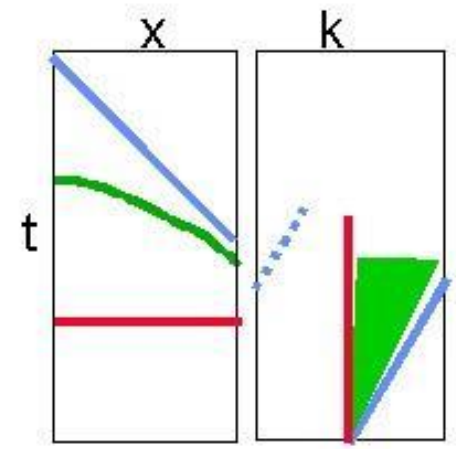

10. Muting

- **Muting** is the process of <u>excluding parts of the traces that contain only noise or more noise than signal</u>.
- The far geophone groups are quite distant from the energy source. On the traces from these receivers, refractions may cross and mix with reflection information from shallow reflectors.
- However, the nearer traces are not so affected.
- When the data are stacked, the far traces are muted (zeroed) down to a time at which reflections are free of refractions.

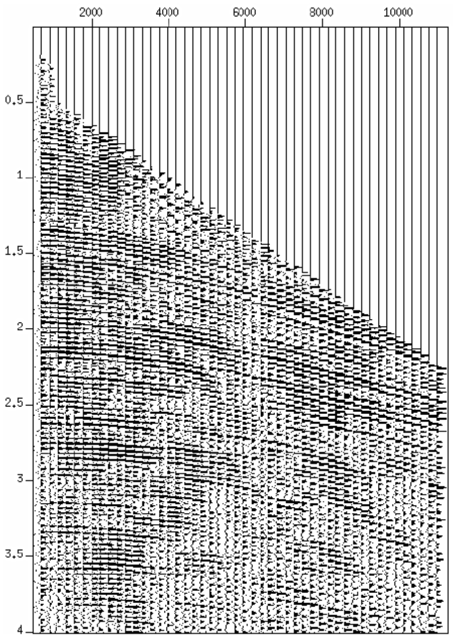

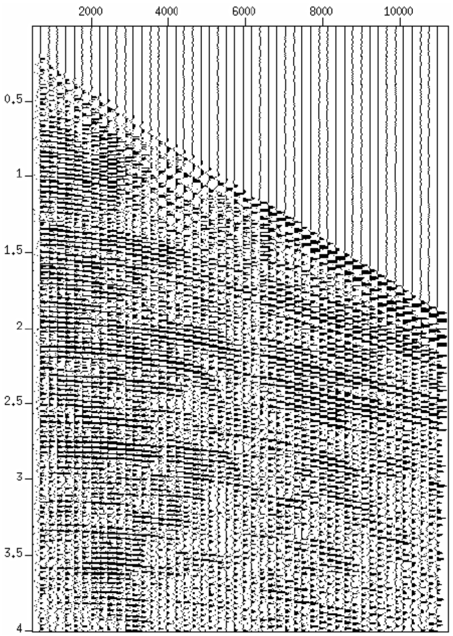

Two seismic sections. A) on the left side after using mute, B) on the right without mute (Forel et al, 2005).

11. Deconvolution

- Deconvolution is process designed to enhance the vertical resolution of the seismic data by attenuating the undesirable signals such as short period multiples. It is also called inverse filtering (Sheriff, 2002).

Reflectivity and convolution

The seismic wave is sensitive to the sequence of impedance contrasts

➔ The **reflectivity series** (R)

(A)

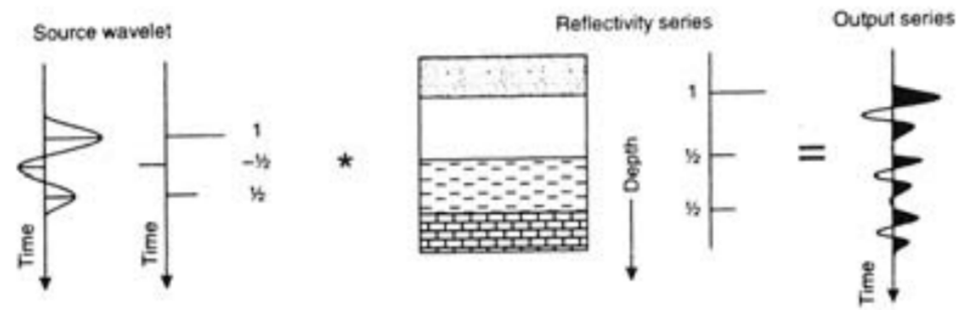

We input a source wavelet (W) which is reflected at each impedance contrast

The seismogram recorded at the surface (S) is the convolution of the two

S = W * R

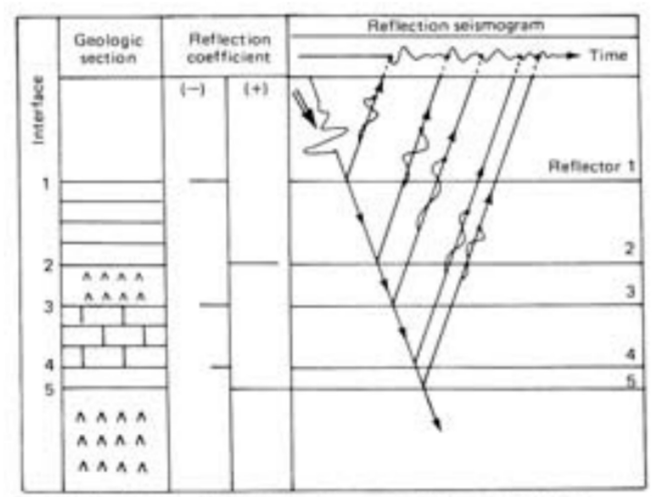

Fig. 4.18 Schematic of a model geological section, a reflectivity log, and a synthetic seismogram. The last is produced by convolving the input wavelet with the reflection effects at each interface derived from the reflectivity log. (Modified from Al-Sadi, 1982.)

Deconvolution

…undoing the convolution to get back to the reflectivity series – what we want

Spiking or whitening deconvolution

Reduces the source wavelet to a spike. The filter that best achieves this is called a **Wiener filter**

Our seismogram **S = R*W** (reflectivity*source)

Deconvolution operator, D, is designed such that **D*W = δ**

So **D*S = D*R*W = D*W*R = δ*R = R**

Time-variant deconvolution

D changes with time to account for the different frequency content of energy that has traveled greater distances

Predictive deconvolution

The arrival times of primary reflections are used to predict the arrival times of multiples which are then removed

Spiking deconvolution

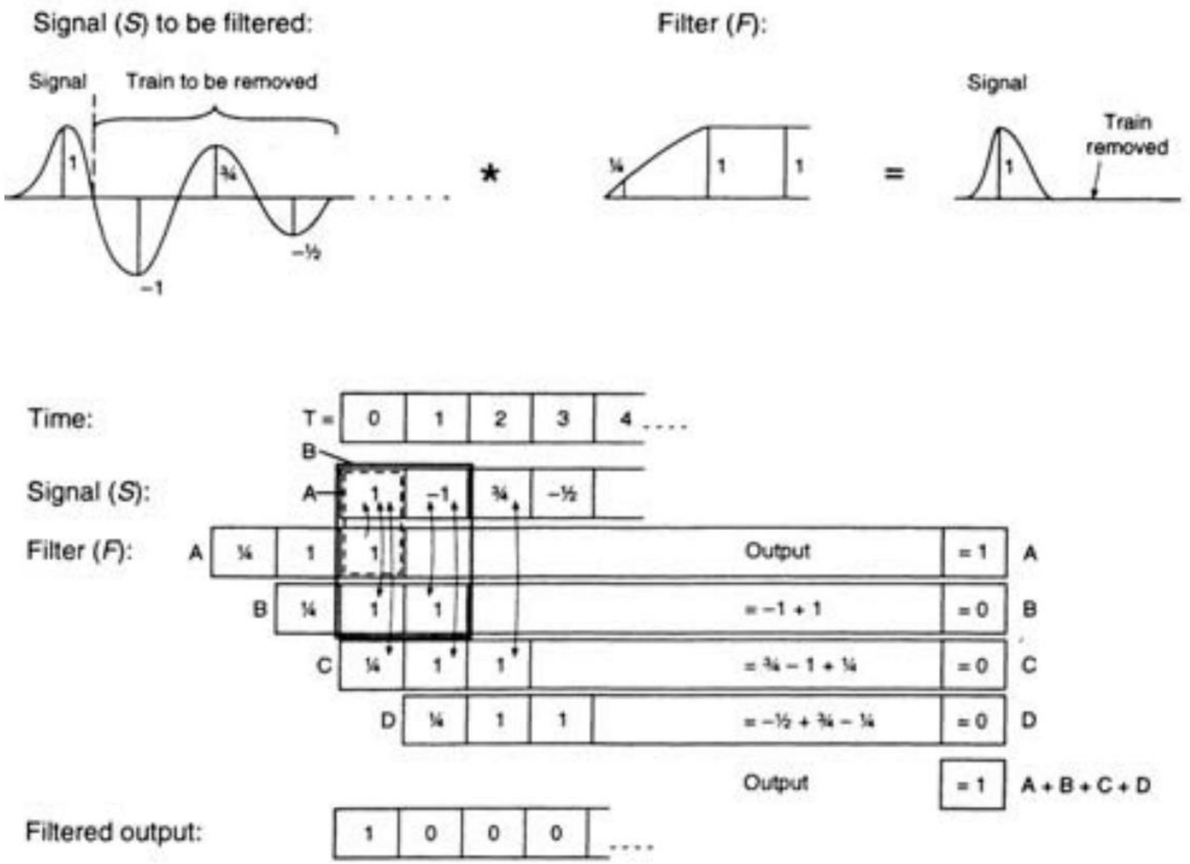

Figure 6.30 (*opposite*) Filtering out a reverberant signal:

At each relevant time sample (i.e. at $T = 1$ or $2, \ldots$) the signal amplitude S is multiplied by the corresponding segment of the filter F. Hence for $T = 1$, the calculation is simply of the form signal x filter $(S*F)$ such that output $= [1 \times (-1)] + (1 \times 1) = -1 + 1 = 0$. Taking this a stage at a time, we have:

Stage A: At $T = 0$, the first element of the filter (1) is multiplied by the corresponding sample of the signal (1), hence the output = 1

Stage B: At $T = 1$, the first element of the filter (1) is multiplied by the corresponding sample of the signal (-1) giving a value of -1. This is added to the product of the second element of the filter (1) and its corresponding sample of the signal (1) to give a value of 1 and on overall output of $-1 + 1 = 0$

Stage C: As for Stage B but shifted by one time sample ($t = 2$)

Stage D: As for Stage C but shifted by one time sample ($t = 3$)

Source-pulse deconvolution

Examples

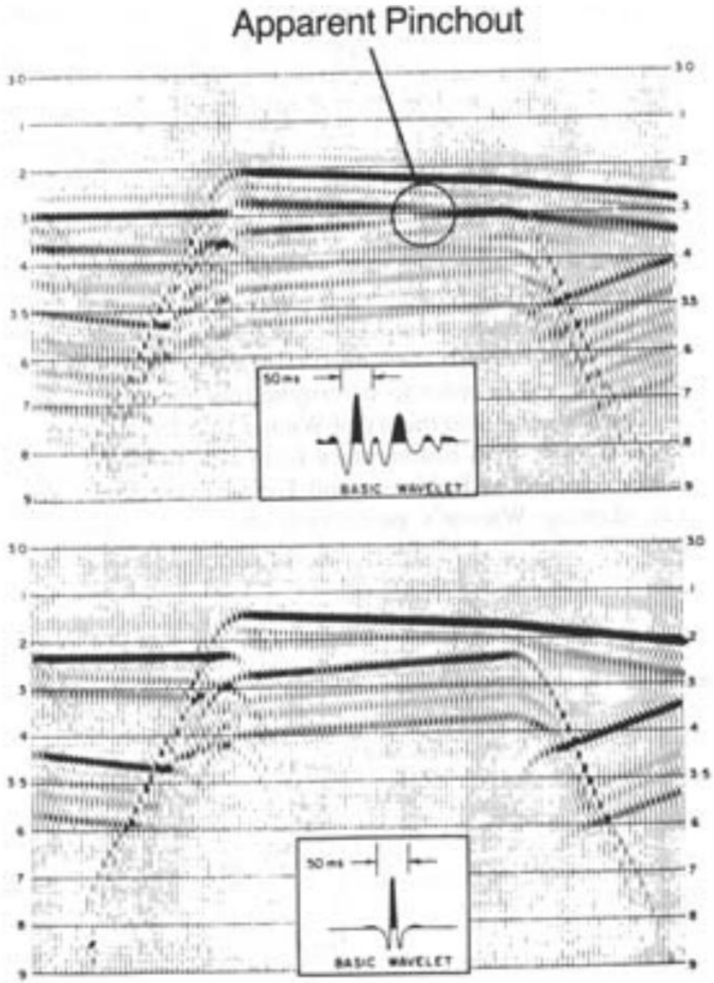

Source wavelet becomes spike-like

Original section

Deconvolution: Ringing removed

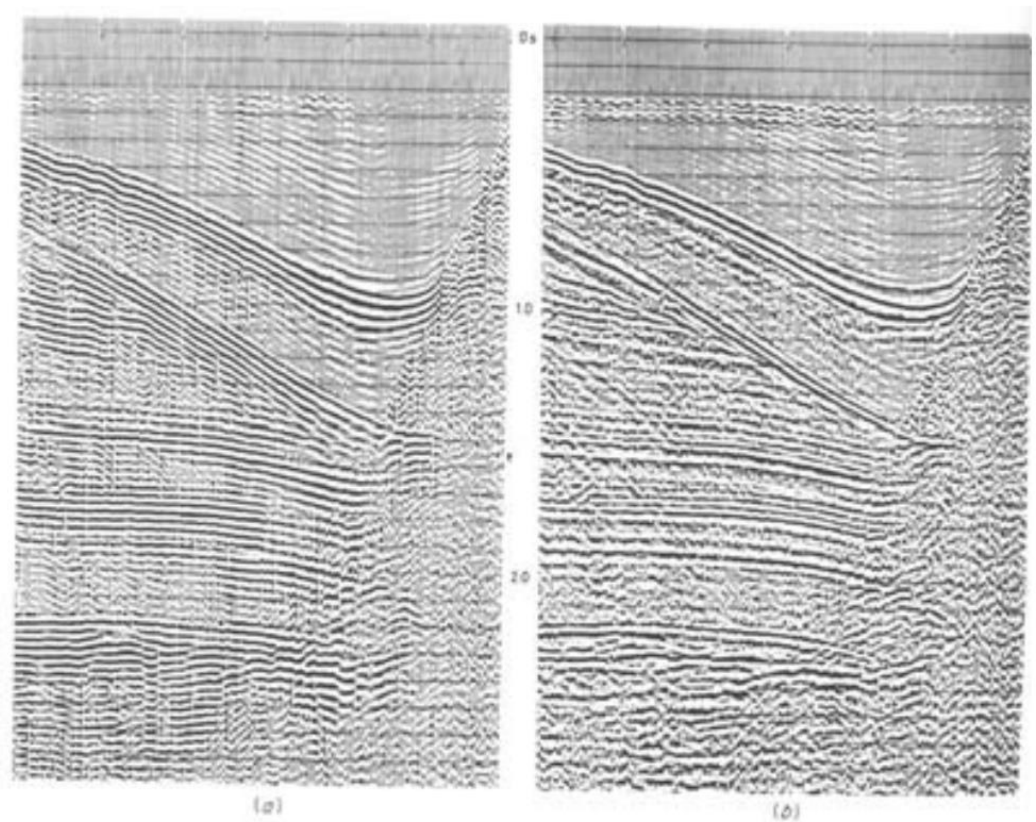

Deconvolution using correlation

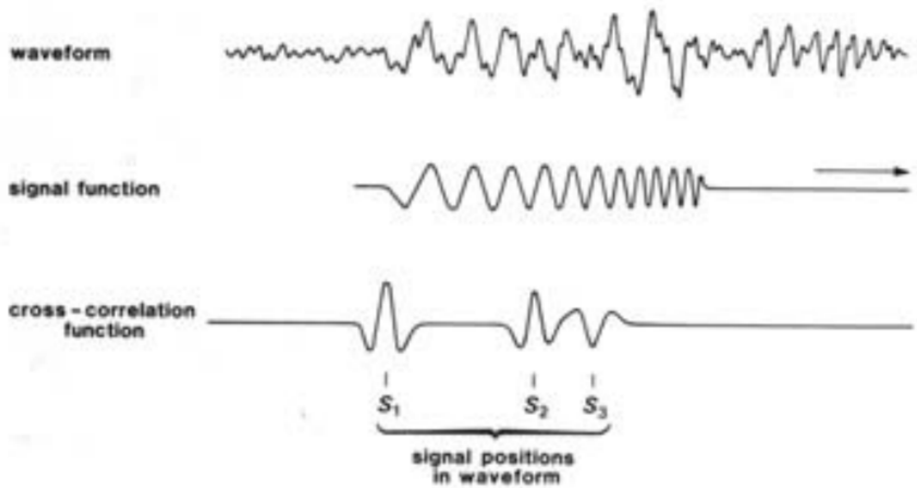

If we know the source pulse

Then cross-correlating it with the recorded waveform gets us back (closer) to the reflectivity function

If we don't know the source pulse

Then autocorrelation of the waveform gives us something similar to the input plus **multiples**.

Cross-correlating the autocorrelation with the waveform then provides a better approximation to the reflectivity function.

Multiples

Due to multiple bounce paths in the section

➔ Looks like repeated structure

These are also removed with deconvolution

- easily identified with an autocorrelation
- removed using cross-correlation of the autocorrelation with the waveform

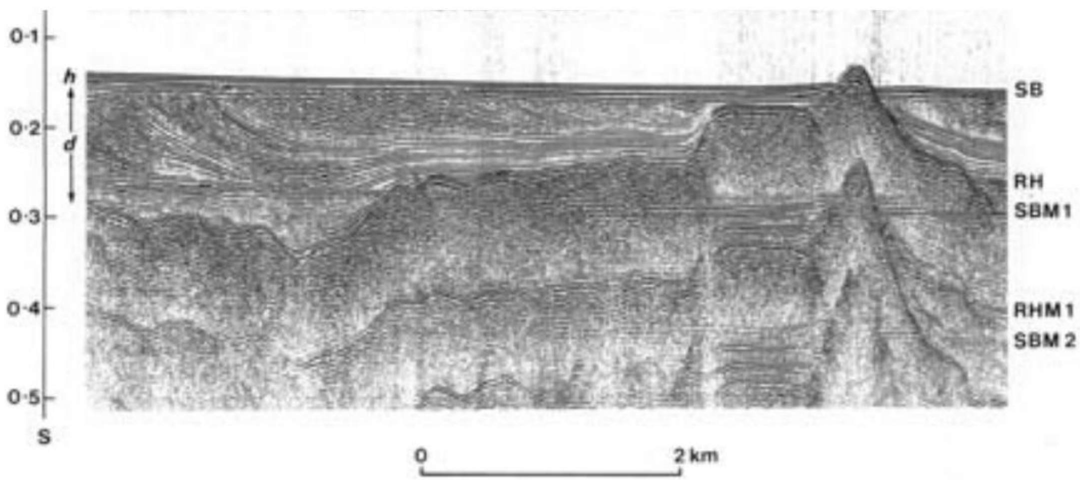

Sea-bottom reflections

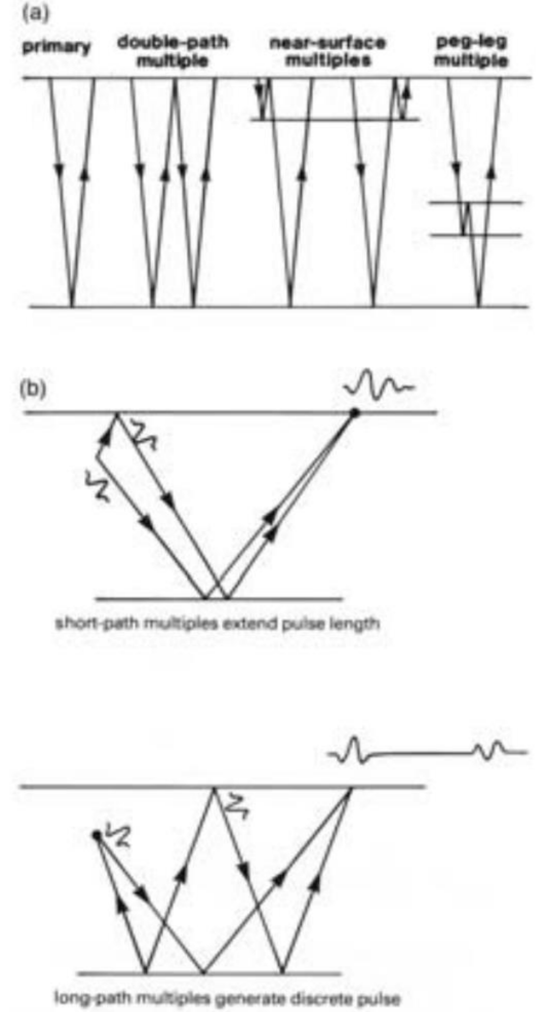

11- CMP Sorting

- The acquisition of Seismic data with multifold coverage is usually done in shot-receiver (s, g) coordinates.
- Seismic data processing, on the other hand, conventionally is done in midpoint offset coordinates.
- The required coordinate transformation is achieved by sorting the data into CMP gathers.
- On the base of the field geometry information, every single trace is assigned to the midpoint of between the shot and receiver locations.
- Those traces that have the same midpoint location are summed together, making up a CMP gather (Yilmaz, 2001).

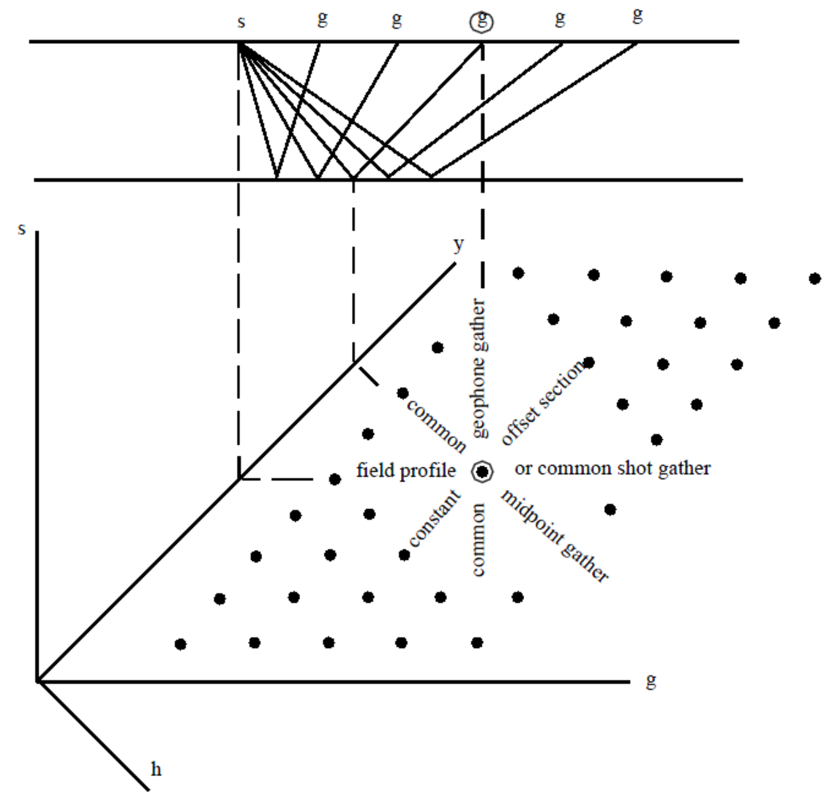

- Figure describes the recording geometry and ray paths that is associated with a flat reflector.

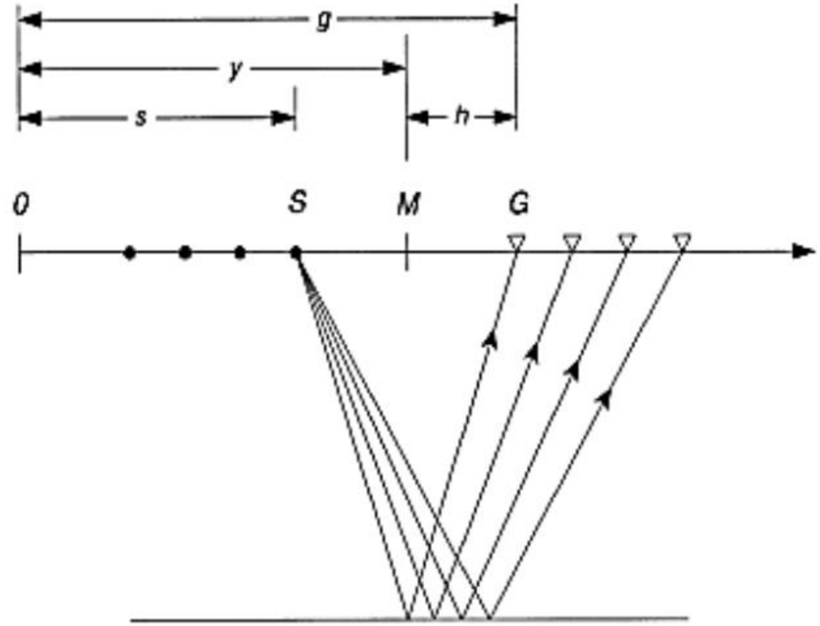

a

- Figure shows the CMP gather and ray paths that is associated with a flat reflector (Yilmaz, 2001).

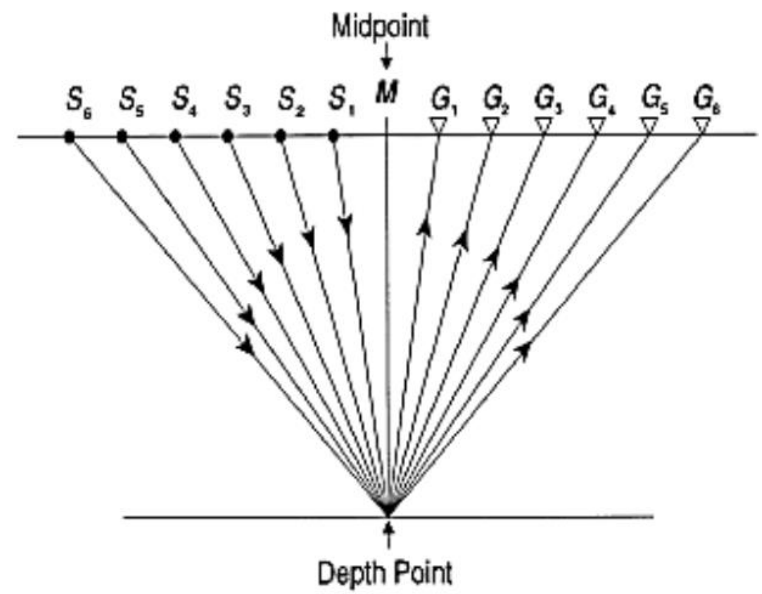

b

- A seismic source is located at the front of a 6-channel array.
- The spacing of geophones is Δx along the entire array.
- If we have N geophones and that array moves a distance $n\ \Delta x$ between shots, then you can show that the number of rays that share the same common mid-points

  $= N.\ \Delta x / 2n.\ \Delta x = N/2n.$

(geophone spacing * no. geophones / 2 * shot spacing)

- This quantity is also called the **fold** or the **coverage** (in percent).
- This survey will give 3 rays for each mid-point.
- This is called **3-fold CMP coverage** or 300% coverage.

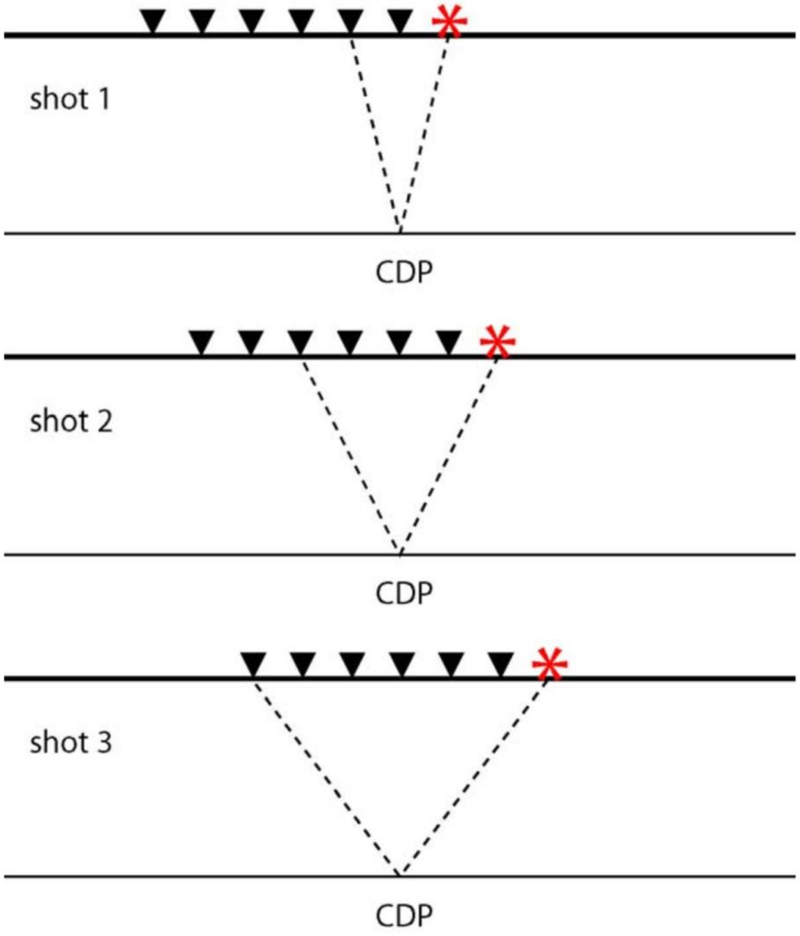

Fold controls **the signal-to noise ratio (S/N),** if the fold is doubled, a 41% increase in S/N is accomplished.
Doubling the S/N ratio requires quadrupling the fold, assuming that the noise is distributed in a random fashion (incoherent noise) (Cordsen et al., 2000).

12- NMO-Correction

- In reflection seismology, the normal moveout (NMO) is describing the effect that the distance between the source and the receiver (the offset) has on the arrival time of a reflection in the form of an increase of time with offset.
- The NMO depends on complex combination of factors which include the velocity that is above the reflector, the offset, the dip of the reflector and the azimuth of the source-receiver in relation to dip of the reflector (Yilmaz 2001).
- For a flat and a horizontal reflector, the travel time equation is:

$$t^2 = t_0^2 + \frac{x^2}{v^2}$$

Where x = offset.
v = velocity of the medium above the interference.
t_0 = time travel at the zero offset.

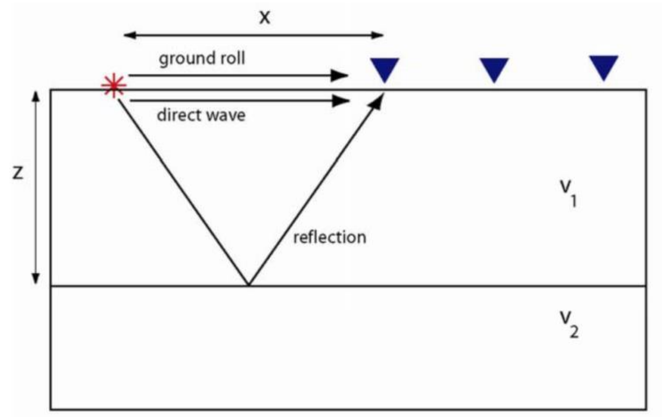

- A P-wave reflects from the interface between layer 1 and layer 2. The angle of incidence and reflection are equal.
- Using Pythagoras' theorem, the distance travelled by the seismic signal on the downward leg of the journey is **:**

$$d = \sqrt{z^2 + \frac{x^2}{4}}$$

- From symmetry, the total distance travelled is *2d*. The whole journey is travelled at velocity v_1, so the travel time is given by

$$t_{ref} = 2\frac{\sqrt{z^2 + \frac{x^2}{4}}}{v_1} = \frac{\sqrt{4z^2 + x^2}}{v_1}$$

- t_{ref} has a minimum value when $x = 0$. In this situation, the seismic signal travels **vertically** and makes an angle of 90° with the interface. This geometry is called **normal incidence** and the travel time is $t_{ref} = t_0 = 2\, z / v_1$
- The travel time can be written:

$$t_{ref}^2 = t_0^2 + \frac{x^2}{v_1^2}$$

Where x = offset.
v = velocity of the medium above the interference.
t_0 = time travel at the zero offset.

$$t_{ref} = \frac{\sqrt{4z^2 + x^2}}{v_1} = \frac{2z}{v_1}\sqrt{1 + (\frac{x}{2z})^2} = t_0\sqrt{1 + (\frac{x}{2z})^2}$$

$$t_{ref} = t_0\left[1 + (\frac{x}{2z})^2\right]^{1/2} = t_0\left[1 + (\frac{x}{v_1 t_0})^2\right]^{\frac{1}{2}}$$

We can simplify the equation for t_{ref} by using a power series expansion (Taylor's Theorem) and assuming that $x / v_1 t_0$ is relatively small.

$$t_{ref} = t_0\left[1 + (\frac{x}{v_1 t_0})^2\right]^{\frac{1}{2}} = t_0\left[1 + (\frac{x}{v_1 t_0})^2\right]^{\frac{1}{2}} = t_0\left[1 + \frac{1}{2}(\frac{x}{v_1 t_0})^2 + ...\right]$$

If the higher order terms are ignored, then we can write that:

$$t_{ref} = t_0\left[1 + \frac{1}{2}(\frac{x}{v_1 t_0})^2\right] = t_0 + \frac{x^2}{2v_1^2 t_0}$$

Re-arranging gives an expression for t_{ref} - t_0 which is termed the **normal moveout**

$$t_{ref} - t_0 = \frac{x^2}{2v_1^2 t_0}$$

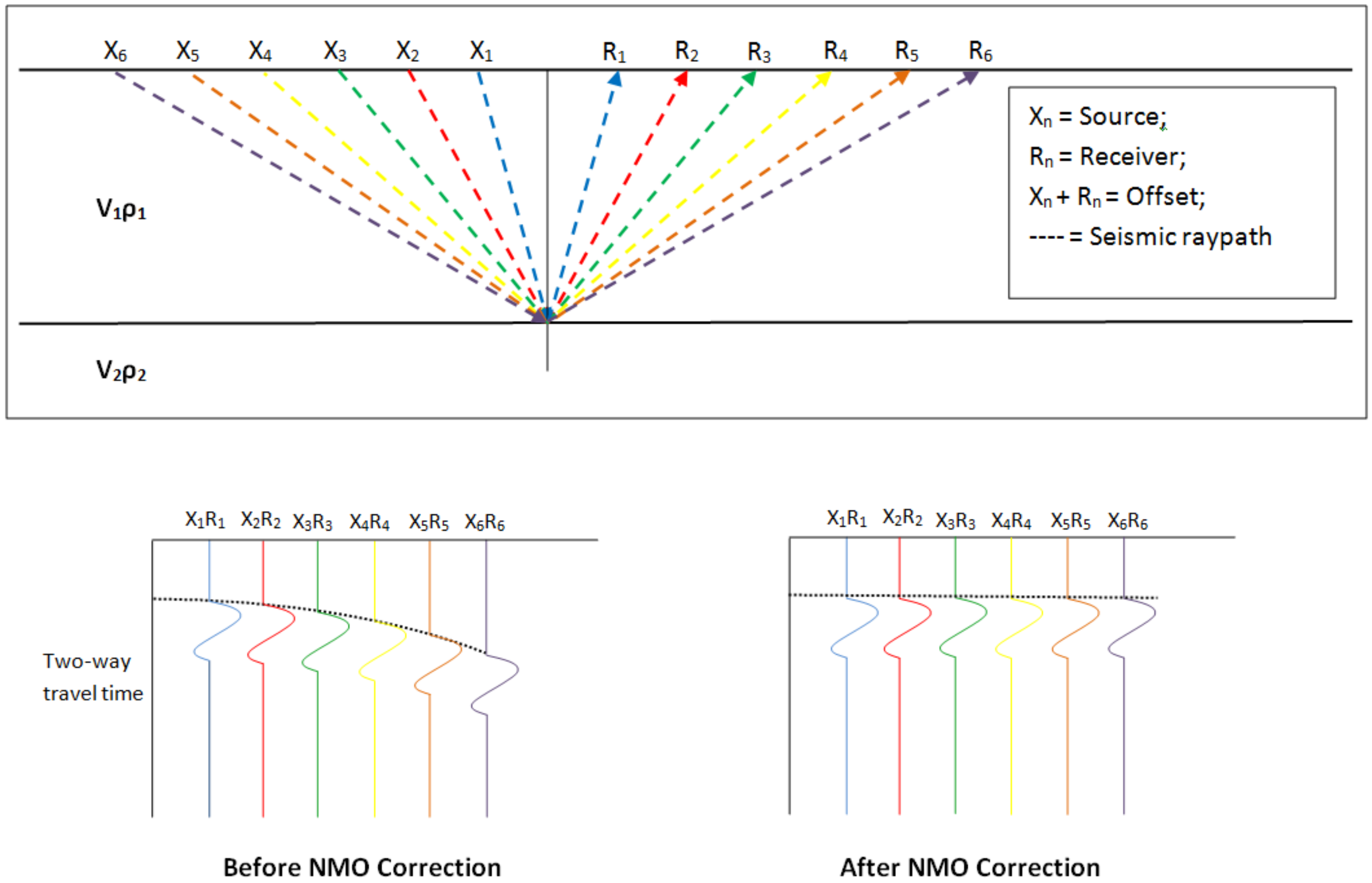

Seismic data that is sorted by CMP then corrected by NMO (Seg.Wiki).

Interval velocity and average velocity

- The **interval velocity** is the **actual velocity** in a specific layer and is defined as $v_i = z_i / \tau_i$
- For the whole ray path we can define an **average velocity** as

$$\overline{V} = \frac{\sum z_i}{\sum \tau_i} = \frac{\sum v_i \tau_i}{\sum \tau_i}$$

- Another way of averaging the velocity is to use the **root-mean-square** average. This is defined as:

$$\overline{V}_{rms,n} = \left[\frac{\sum_{i=1}^{n} v_i^2 \tau_i}{\sum_{i=1}^{n} \tau_i} \right]^{\frac{1}{2}}$$

- and is needed to compute interval velocities, as described below. For the case of n = 2

$$\overline{V}_{rms,2} = \left[\frac{v_1^2 \tau_1 + v_2^2 \tau_2}{\tau_1 + \tau_2} \right]^{\frac{1}{2}}$$

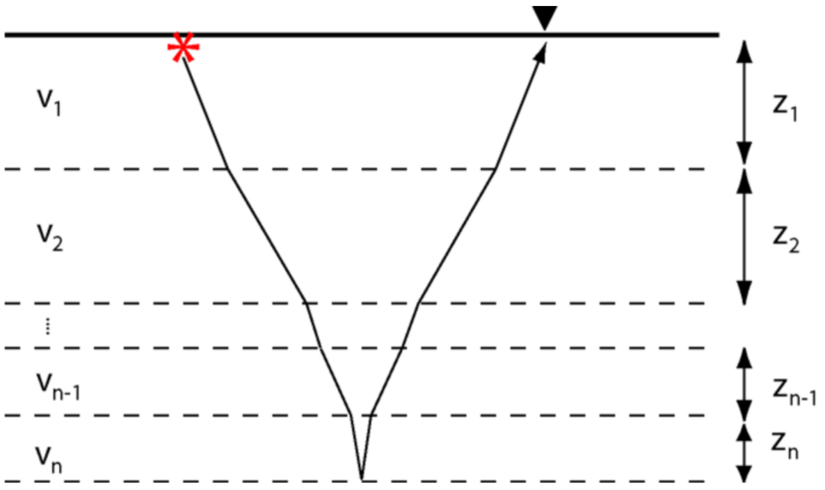

Normal move-out for multiple layers and the Dix equation

- When the seismic signals travel close to the vertical direction, we can show that the normal moveout for the *nth* reflection is:

$$\Delta t = t - t_n = \frac{x^2}{2 t_n \overline{V}_{rms,n}^{\,2}}$$

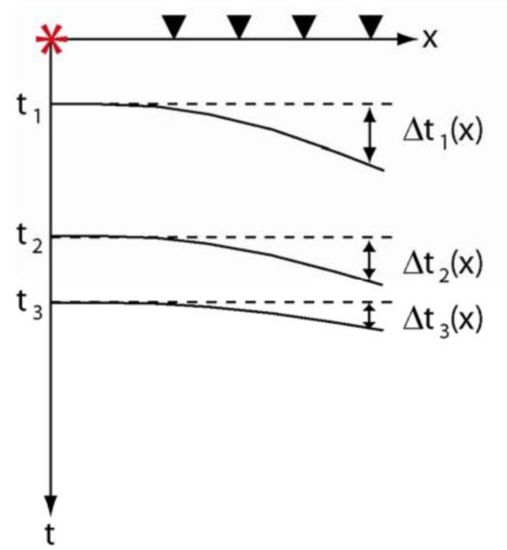

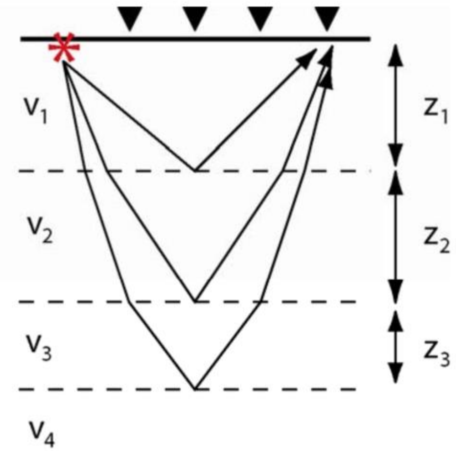

Dix equation states :

$$v_n = \left[\frac{V_{rms,n}^2 t_n - V_{rms,n-1}^2 t_{n-1}}{t_n - t_{n-1}} \right]^{\frac{1}{2}}$$

13- Stacking

- The traces in a CMP can be corrected for NMO once the velocity is known, in order to correct each trace to the equivalent of a **zero-offset trace**.
- These traces will have the same reflection pulses at the same times, but with different random and coherent noise.
- Combining all these traces in a CMP together will decrease the noise and increase the signal-to-noise ratio (SNR).
- This process is termed **stacking** (Kearry et.al, 2002).

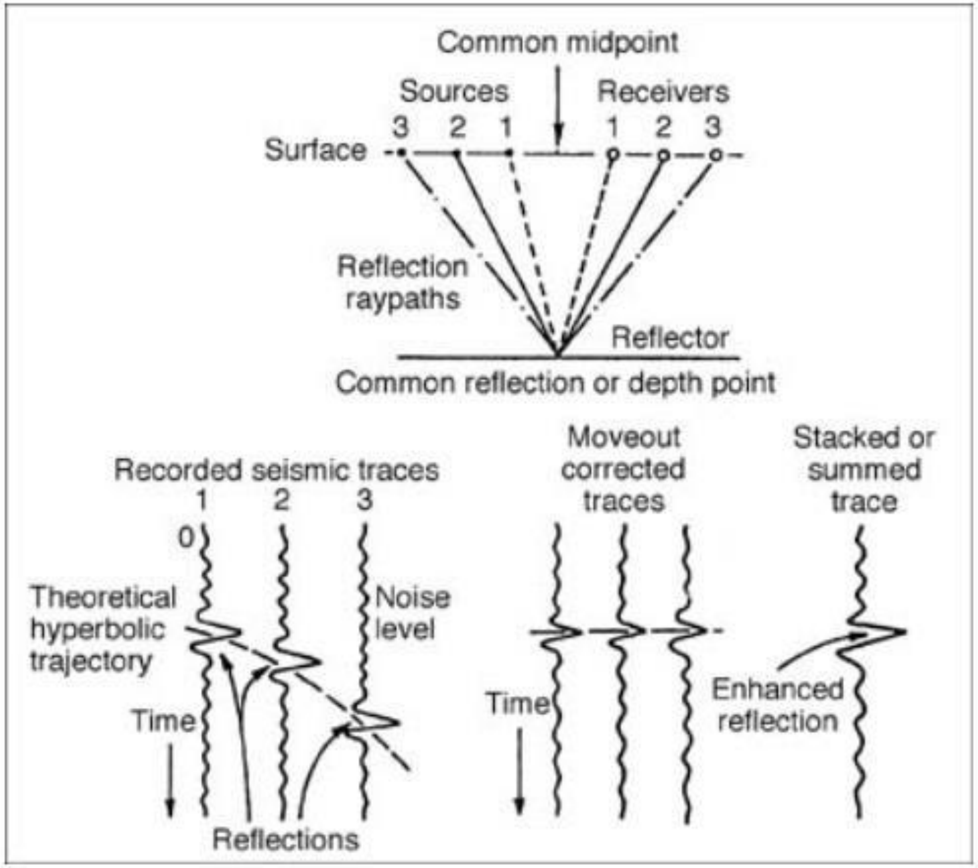

The stacking process after sorting to CMP and applying NMO. (Schlumberger Oilfield Glossary)

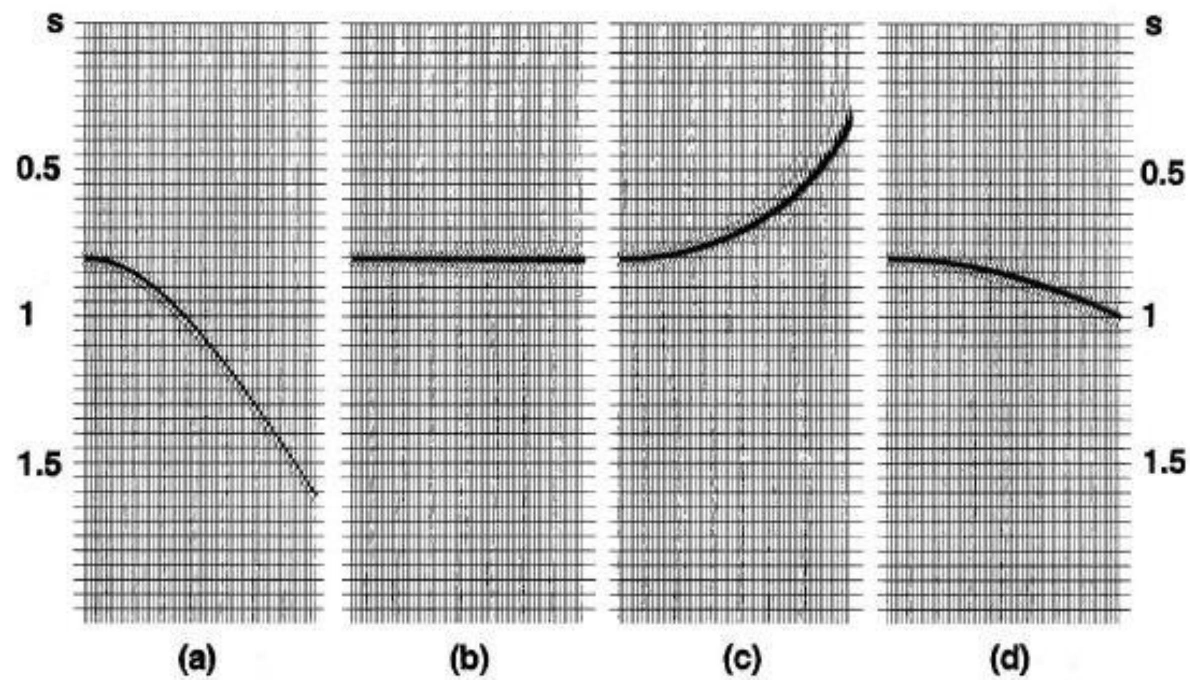

(a) CMP gather of single event with a 2264 m/s velocity
(b) NMO corrected gather by using the best velocity
(c) over corrected gather by using low velocity 2000 m/s
(d) under corrected gather using high velocity 2500 m/s, after (Yilmaz 2001).

(b) Data sorted into common mid-point gathers
Velocity analysis, apply NMO corrections
Stack to get zero offset trace (4-fold)
Combine into seismic section

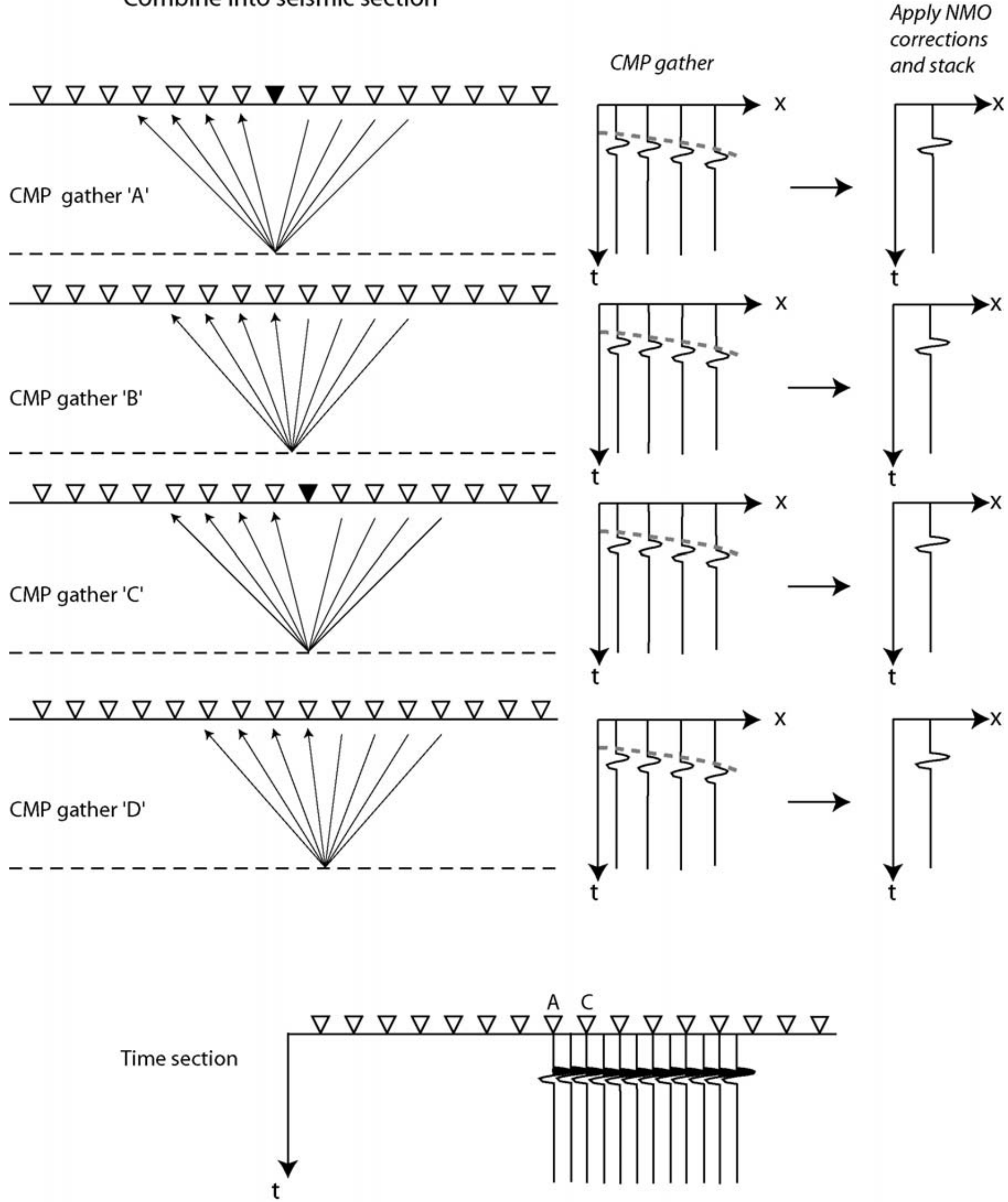

Stacking velocity

Multiple layer case

Note: the sensitivity to velocity decreases with depth

Stacking velocity panels: constant velocity gathers

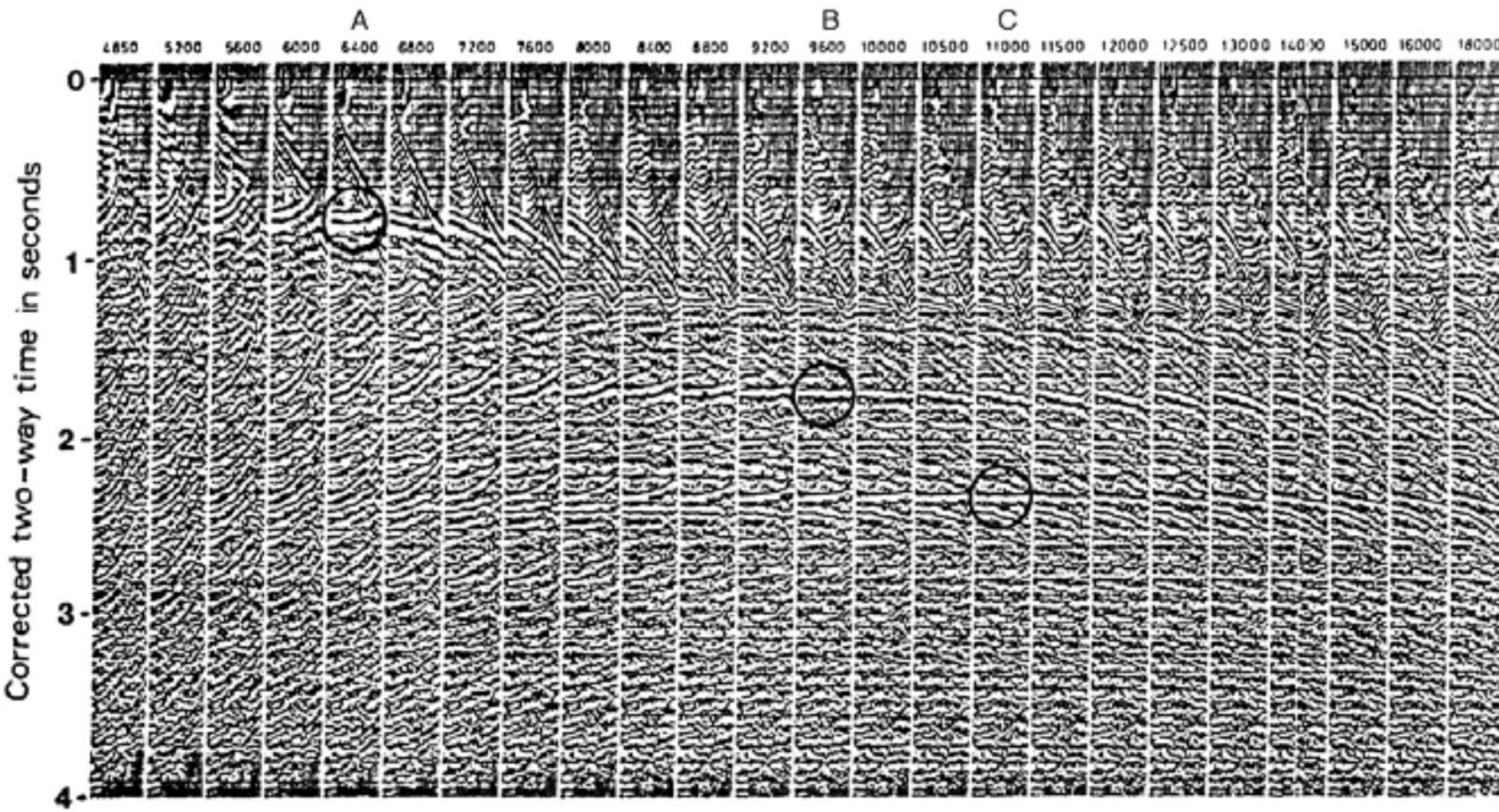

14- Velocity Analysis

- Velocity analysis is the calculation of stacking or NMO velocity from measurements of normal moveout.

- It generally deals with finding the best velocity associated with the best-fit hyperbola to common-midpoint data.

- However, even in the absence of noise and errors, time-offset data is not hyperbolic except in the case of constant velocity, and the stacking velocity value is often somewhat dependent on the amount of data included in the analysis.

- The stacking velocity is roughly the rms velocity when all reflectors are horizontal and when velocity varies only with depth.

There are many velocity analysis methods:

- $T^2 - X^2$ Analysis Method.
- Constant Velocity Stack.
- Velocity Spectrum Method.
- Dix's Expanding Spread Technique.
- Seismic Velocity Inversion.
- T - ΔT Method.

Velocity Spectrum Method

- The initial result of velocity analysis is a set of velocity functions that are determined at specific CMP locations within the survey.
- Velocity functions are defined by sets of time, velocity pairs that are picked for significant primary reflections.
- Linear interpolation between these points defines velocities for every sample in the CMP traces.
- The velocity spectrum approach is based on the correlation of the traces in a CMP gather.

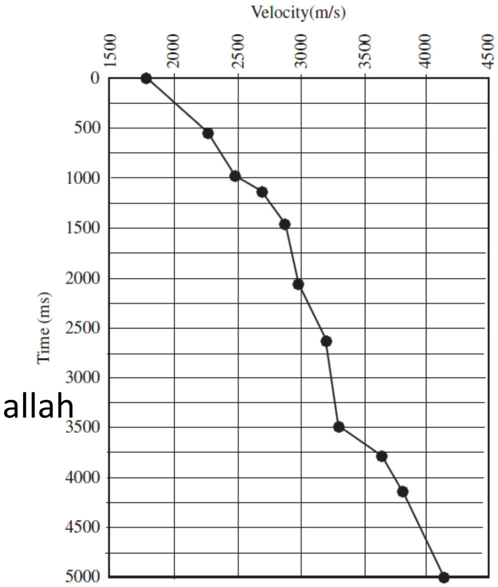

Velocity function (Gadallah and Fisher, 2009)

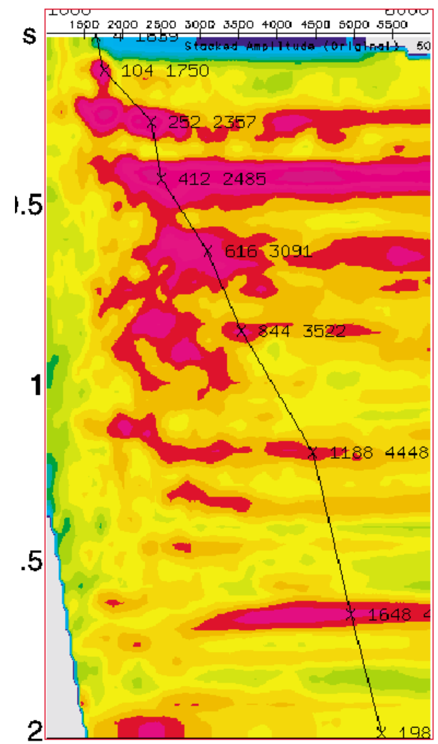

Picking velocity of primary reflection (Yilmaz, 2001).

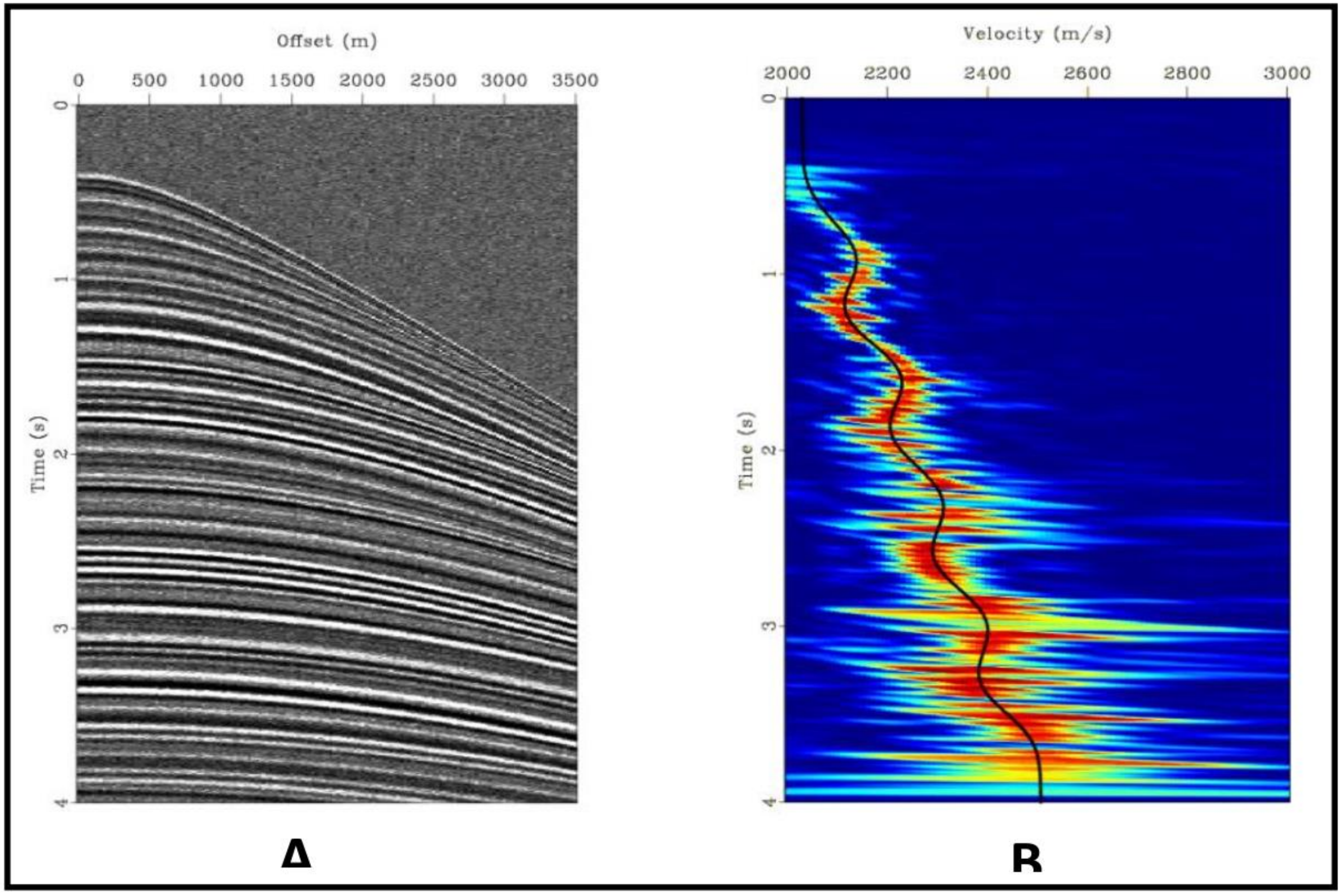

(A) synthetic CMP gathers (B) semblance scans for CMP gathers. Black curves indicate velocity picks after (Fomel 2009).

15- Travel time curve for a dipping reflector

- *t(x)* is greater than *t(-x)* and the travel time curve is asymmetric about x = 0
- the minimum travel time does not occur at x = 0 m (why?)
- also note that the reflection received at $x = 0$ m did not originate beneath x = 0.
- To account for this effect a technique called **migration** is used.
- The **dip moveout** is defined as

$$\Delta T_d = t_x - t_{-x} = \frac{2x\sin\theta}{v_1}$$

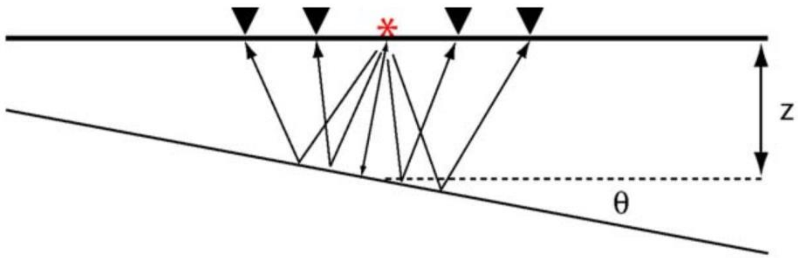

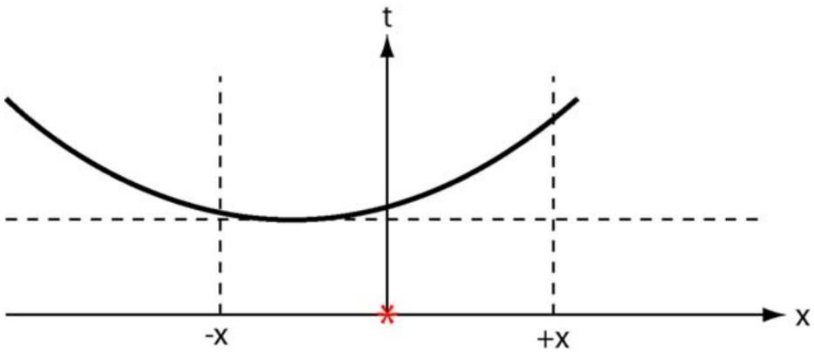

$$t = \frac{\sqrt{x^2 + 4z^2 + 4xz\sin\theta}}{v_1}$$

$$t \approx t_0 + \frac{(x^2 + 4xz\sin\theta)}{2v_1^2 t_0}$$

Why is migration needed?

Dipping layers are imaged with an incorrect dip

- Consider a shot (S) and receiver (R) that are located close together. A reflector has a true dip angle = α_t and is at a depth z below the shot point.
- Seismic energy that returns to R will reflect at 'A' where the ray path is at 90º to the reflector.
- However, in a **seismic section**, a reflection in plotted as it was **directly below** the shot-receiver point , which in this case is 'B'.
- Note the line A-B is the arc of a circle, centered at RS.
- The result is the reflector is imaged by the seismic data with an apparent dip of α_s that is <u>less than the true dip</u>.

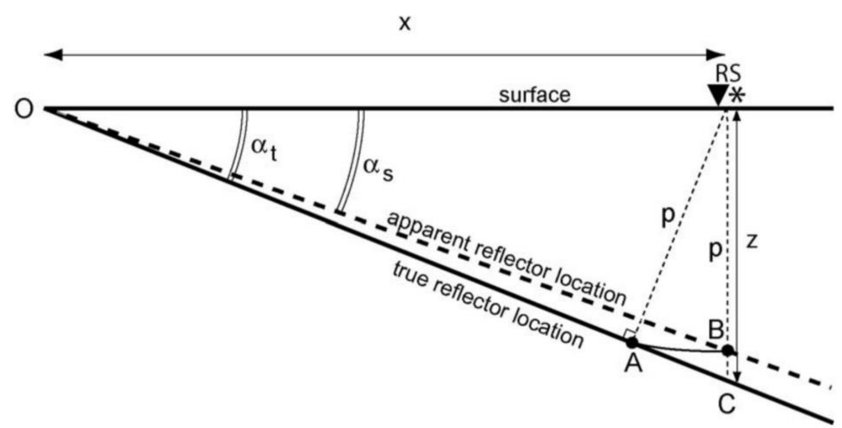

Reflectors appear to have an **apparent dip** **that is less than the true dip**.

Why is migration needed?

Multiple reflections in same zero offset trace

- When a syncline has very limited topography, only one reflection is observed in each zero offset trace (i.e. shot and receiver are placed very close together and moved along the profile)

- With more rugged topography, a normal reflection will occur at three locations when the source and receiver are above the syncline. This produces the characteristic "***bow tie***" in the travel times.

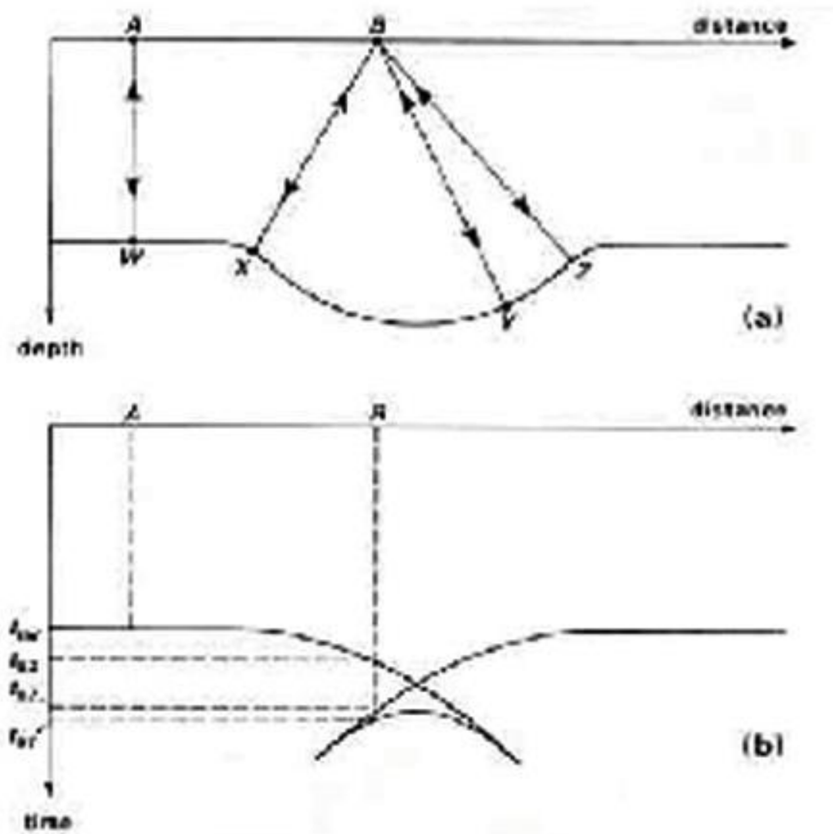

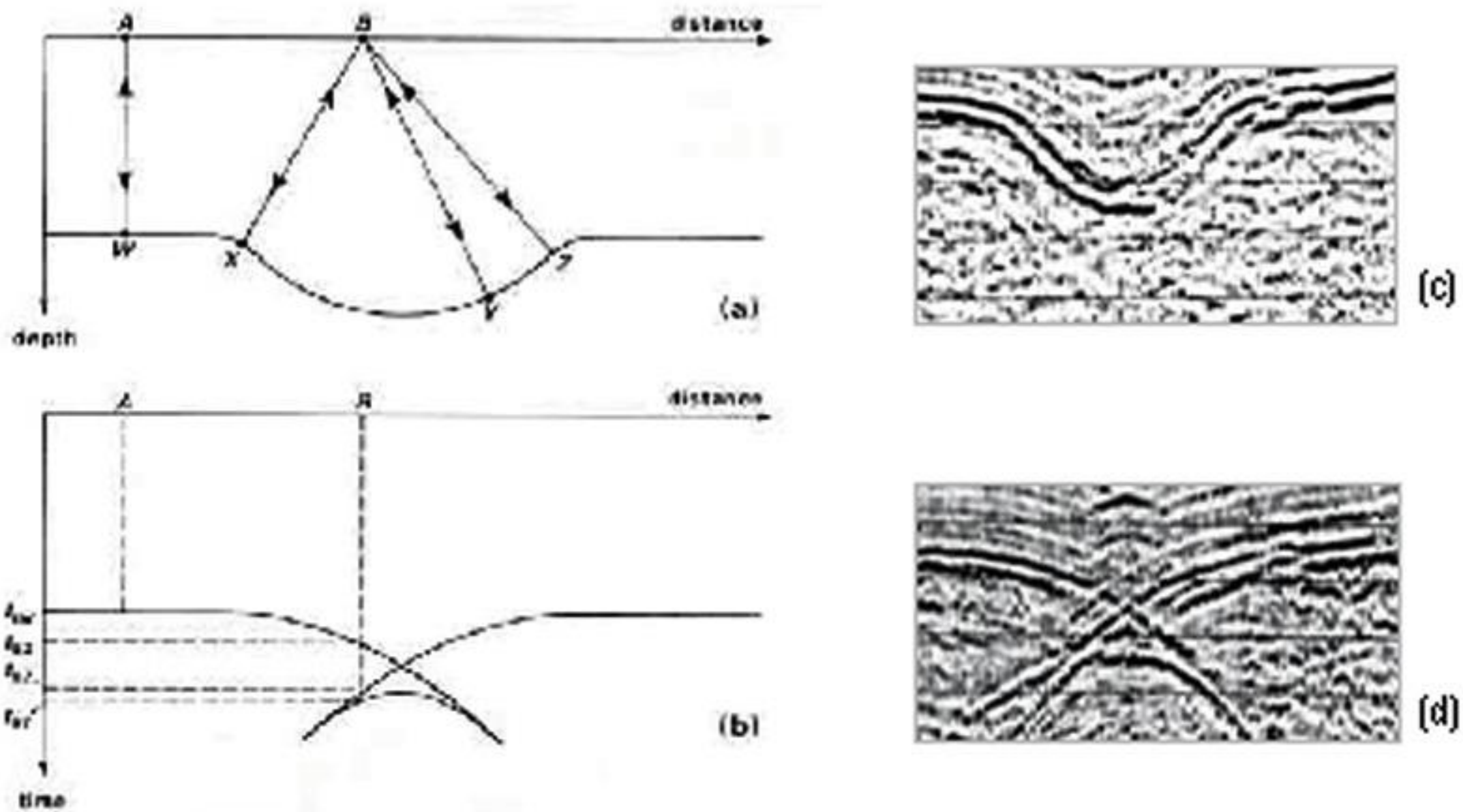
A
B
distance
W
X
Y
Z
(a)
depth
distance
(b)
time
(c)
(d)

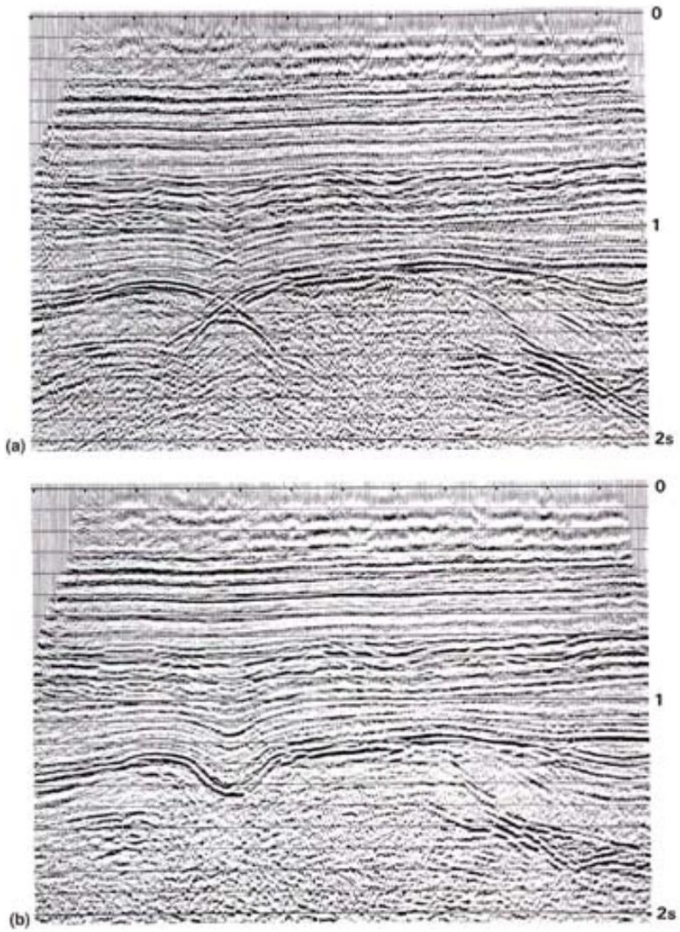

Wave equation migration in a location where structures generally sub-horizontal. Note that bow-ties are essentially removed by the migration (Kearey chapter 4).

Why is migration needed?

Diffractions

- **Diffractions occur from point reflectors and corners**.
- The figure shows a small sphere that is diffracting seismic waves. The diffractor has the property that it scatters energy in all directions.
- Some of this energy returns to the location of the shot (*) along the same path.
- When the shot-receiver array is moved along the profile with zero-offset, the travel time curve above has a travel time which plots as a hyperbola
- A hyperbola will also result when the shot-receiver offset is varied (*e.g.* a shot gather or CMP gather).

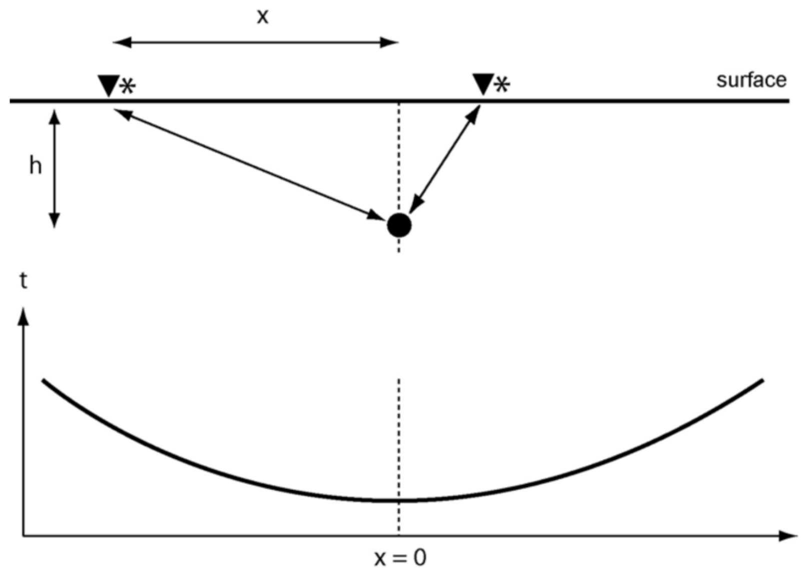

$$t_{diff} = \frac{2\sqrt{x^2 + h^2}}{v_1}$$

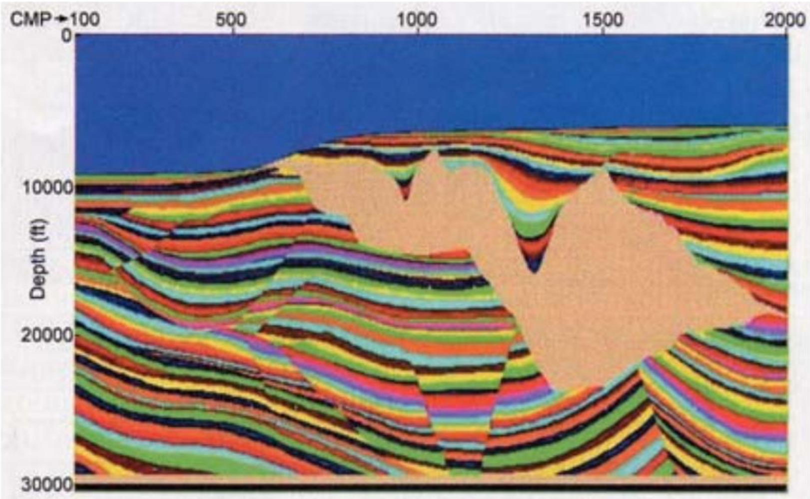

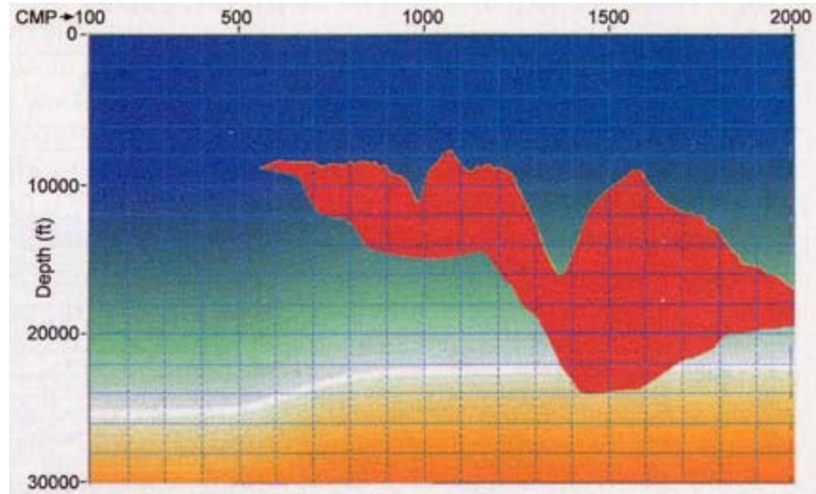

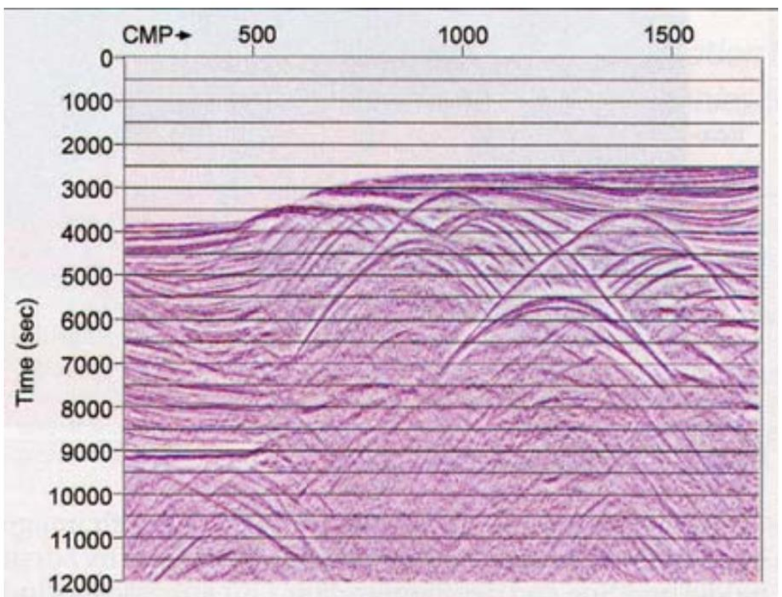

In the zero-offset time section, note the **diffraction hyperbolae** that originate in the sharp corners in the upper surface of the salt sheet. Very few coherent reflectors can be seen beneath the salt.

The diffraction hyperbola is the steepest dipping event that can be recorded on a seismic record section.

Migration methods

- It is mathematical process that attempts to reconstruct the reflector geometry from measurements of the reflected seismic energy.
- The simplest technique works by assuming that from the travel time, we know that the reflection point must lie somewhere on a hemispherical surface. By migrating several points this allows us reconstruct the reflector surface.
- If applied to a diffraction, this will **collapse the hyperbola to a point**.

- Some commonly used methods of migration include:

  - diffraction migration
  - wave equation migration
  - Kirchhoff migration

Each migration technique can be further divided into **time** and **depth** migration

- *time migration*: the vertical axis on the migrated section is still time.

- *depth migration*: estimates of velocity are used to convert time to depth during migration.

Migration can also be applied before or after stacking the CMP gathers:

Post-stack depth migration **:**

- The zero offset traces derived from the CMP stacks are migrated.
- This has the advantage of lower computer time and the higher signal-to-noise ratio can make the migration more stable.
- However the process of stacking assumes a relatively flat interfaces. This is valid in geological structures that have sub-horizontal stratigraphy, but is not valid in complex, highly 3-D environments.

Pre-stack depth migration:

- This migrates individual traces prior to stacking.
- Requires major amount of computation, but is necessary in complex 3-D environments.

Example from a PGS advert in The Leading Edge.

Note that structures with steeper dip are imaged more reliably with pre-stack depth migration.

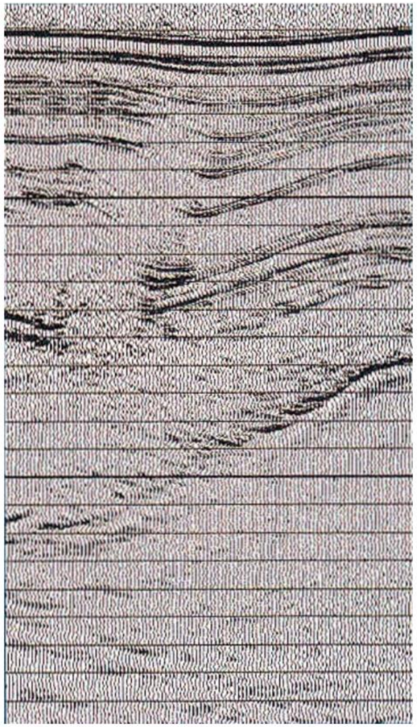

Post-stack depth migration

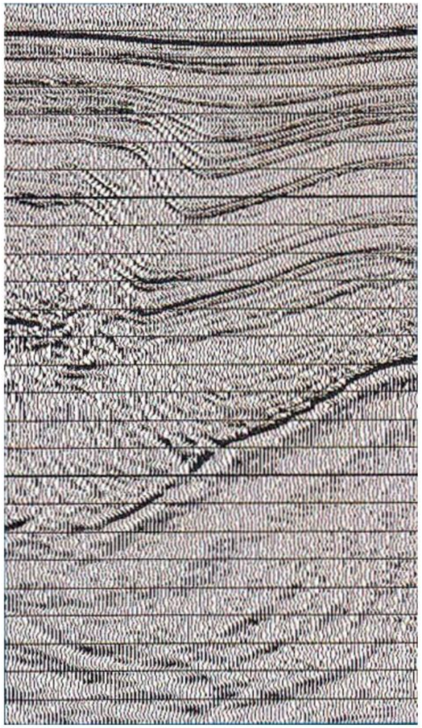

Pre-stack depth migration

Example: Migration of reflection from a rugged interface

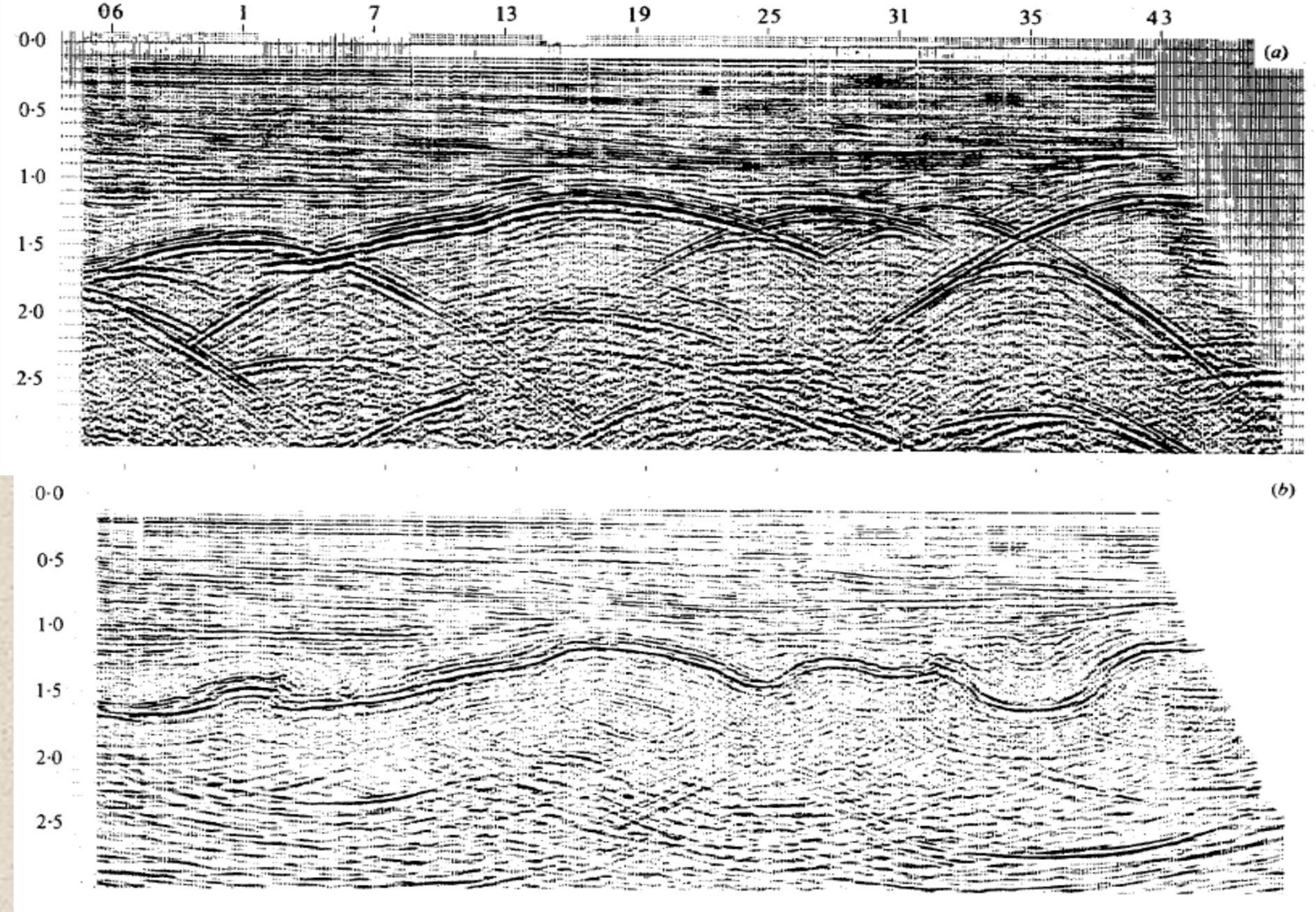

(a) Unmigrated section; (b) Migrated section.

Multiples do not migrate correctly and along with other errors in migration this can produce "***smiles***" which are upward directed hyperbolae. This is illustrated in Figure 4.84 from Telford.

Example: Migration of reflection from a rugged interface

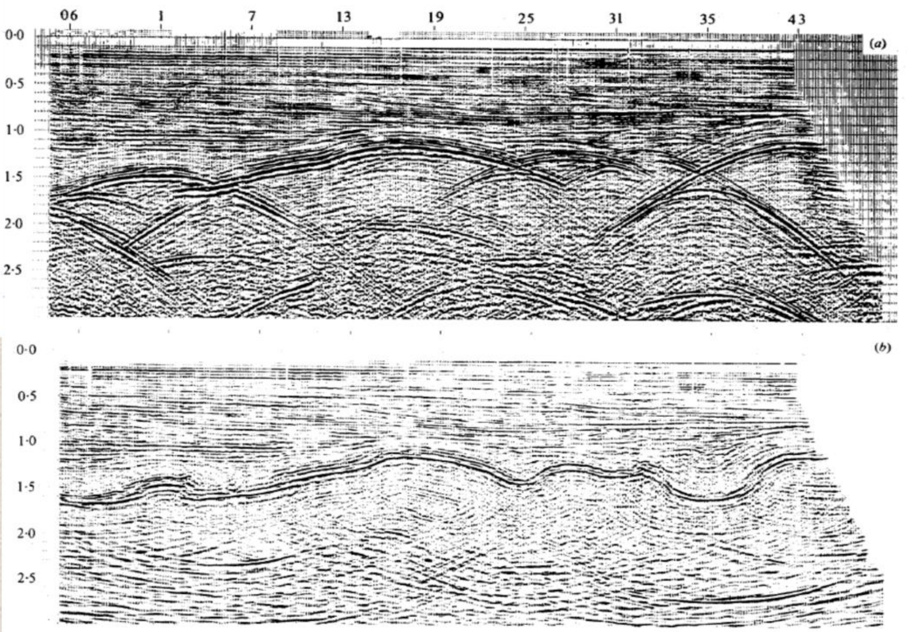

(a) Unmigrated section; (b) Migrated section.

Vertical seismic profile (VSP)

- The seismic sensors are in the borehole while the seismic source is still at the surface.
- First, different types of VSP's are discussed.
- Next, it is explained how to obtain a reflectivity profile from raw VSP data.
- The result serves as a calibration for the surface seismic image: in VSP's we know both depth and time, so the velocity is much better known than from surface seismic.

- The (VSP) surveys have some special advantages over surface seismic reflection surveys.
- One key advantage is the ability to separate the downgoing (direct) and upgoing (reflected) wavefields that enable the calculation of the true reflection amplitude or seismic impedance (Hinds et al., 1999).
- By placing geophones in a borehole, favourable recording conditions are achieved: Shorter paths; Lower attenuation, higher frequencies; Less effects of weathering; Receiver spread may run across the horizon of interest.

Different types of Vertical Seismic Profiles (VSP's)

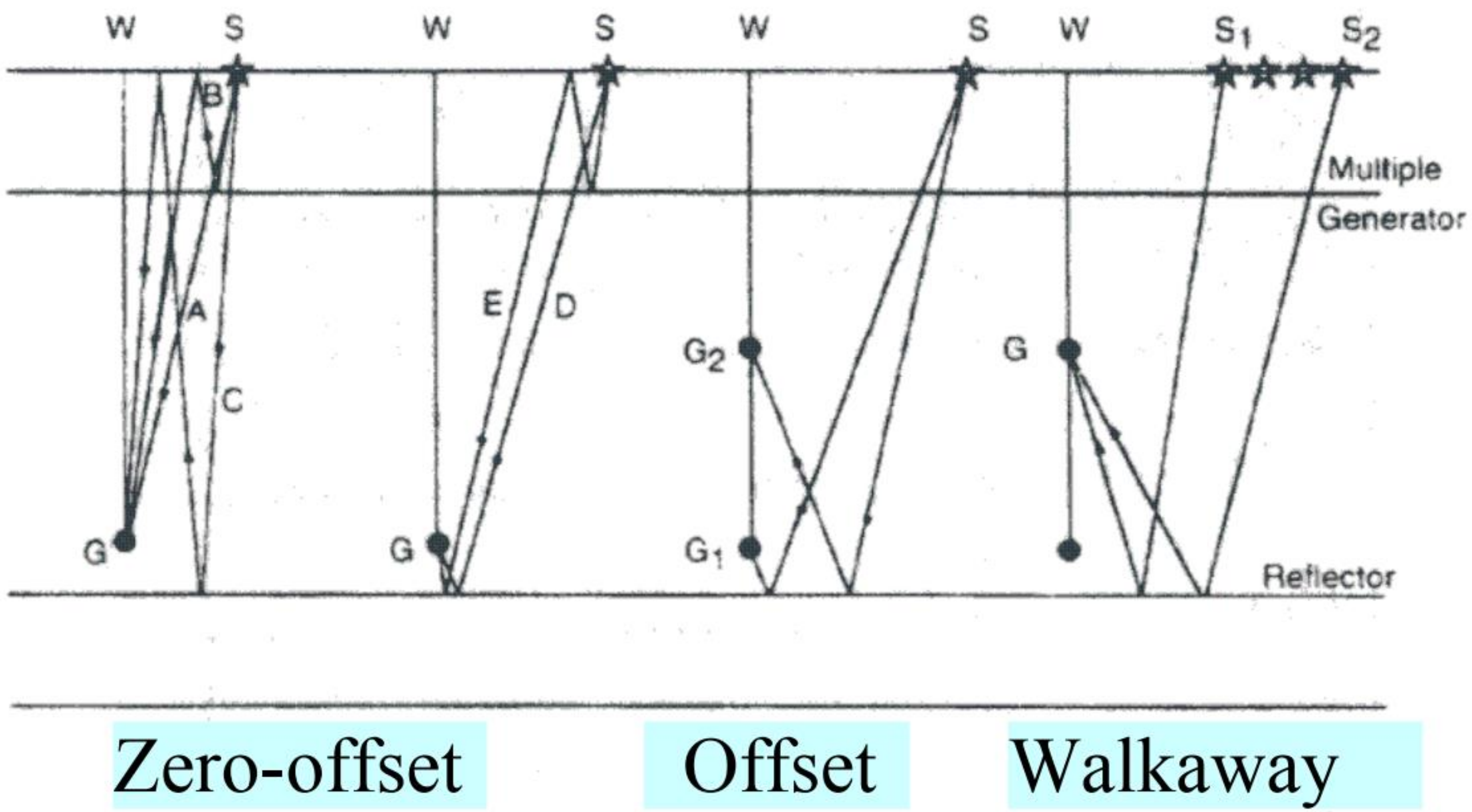

Different types of Vertical Seismic Profiles (VSP's)

A zero-offset VSP

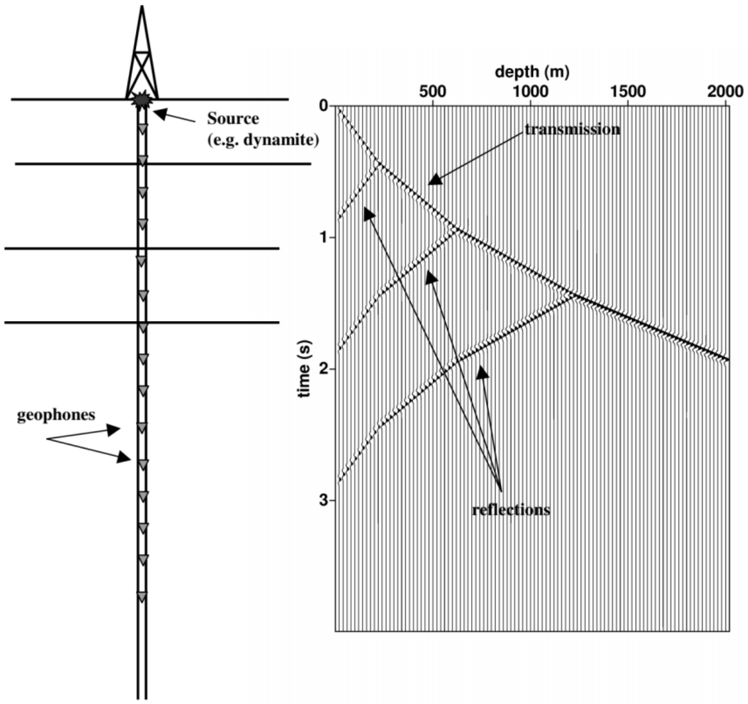

Figure 6.1: Zero-offset Vertical Seismic Profile; zero-offset means no horizontal distance between source position and the well.

- zero-offset means that the source is situated right on top of the borehole, i.e. no offset exists between the horizontal position of the borehole and the source.

- a linear event emerging from time t = 0 can be observed in the obtained recordings at depth, which can be interpreted as a direct wave from the surface to the receiver.

- we can use the slope of the event to determine the seismic velocity, either being the average velocity from the surface to the receiver, or the local seismic velocity between to successive receiver-positions.

Different types of Vertical Seismic Profiles (VSP's)

A zero-offset VSP

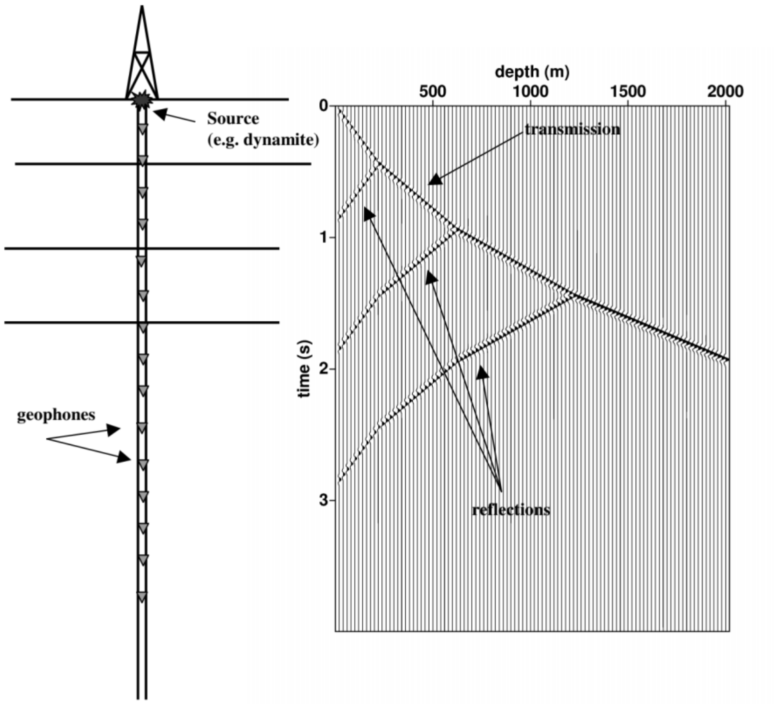

Figure 6.1: Zero-offset Vertical Seismic Profile; zero-offset means no horizontal distance between source position and the well.

- a reflector is also present in the recordings, this is the other linear event that has opposite slope than that of the direct arrival.
- the time is increasing with decreasing depth; this is clear since the wave is a reflection so is propagating upwards.
- the event "stops" at the direct arrival.
- This crossing of the direct and reflected arrival can be used to determine the depth of the reflector itself.
- that the slope of the reflected arrival is the same as the one from the direct arrival, the same, only of opposite sign.

Different types of Vertical Seismic Profiles (VSP's)

offset-VSP

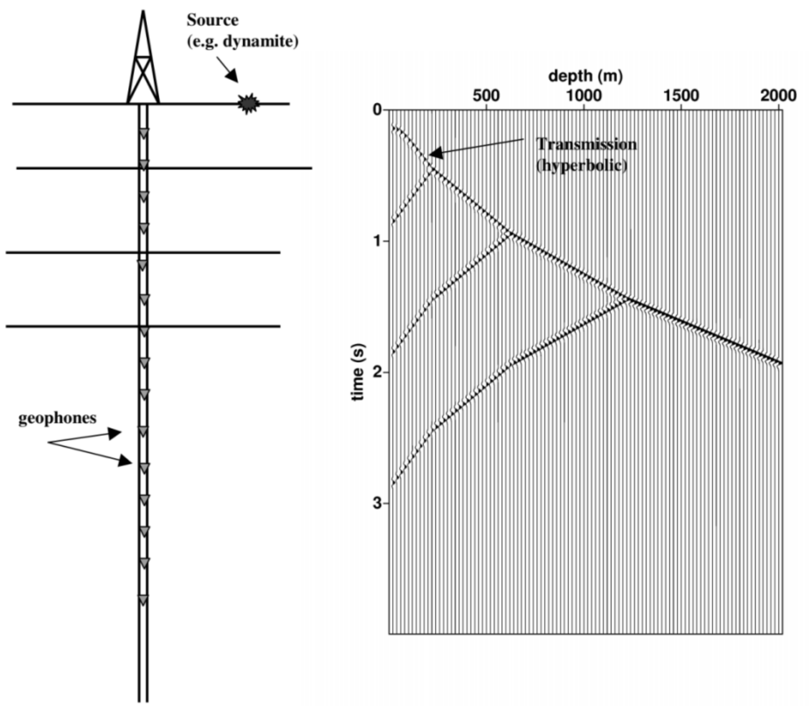

Figure 6.2: Offset Vertical Seismic Profile; offset means a fixed horizontal distance between source position and the well.

- the source is now not right above the borehole but is displaced in the horizontal direction, i.e., has some offset; hence the name offset-VSP.
- Usually, the offset is not too large compared to the depths of the receivers.
- the direct arrival shows some hyperbolicity in the shallow recordings. When the offset becomes relatively large compared to the depth of recording.
- one should be careful with interpreting the first arrival as the direct arrival: it could well be a refracted arrival from a deeper faster layer, comparable to a refraction in surface seismic.

Different types of Vertical Seismic Profiles (VSP’s)

a walk-away VSP

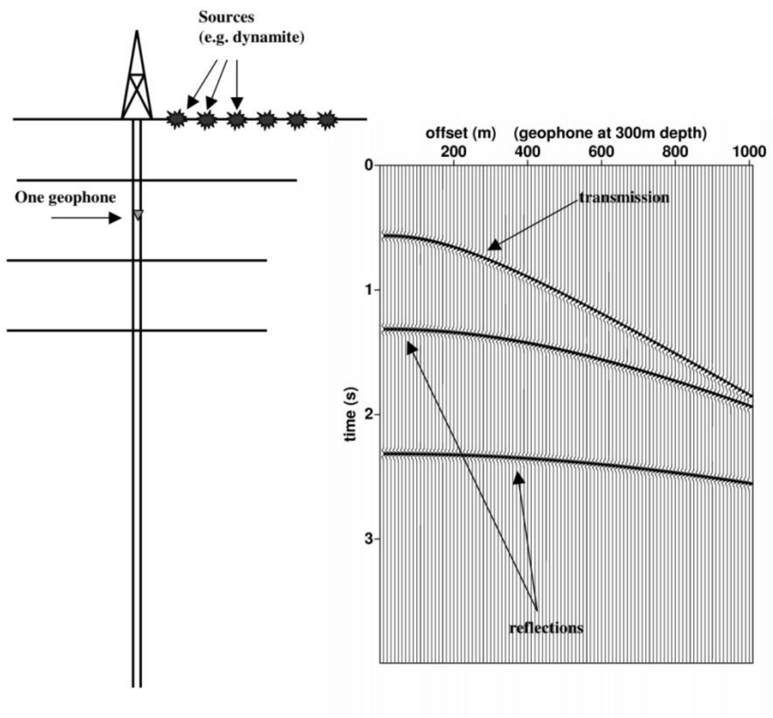

Figure 6.3: Walk-away Vertical Seismic Profile; walk-away means variable offset and fixed position (geophone) in the well.

- it is of course possible to let the source change position and keep the receiver position(s) fixed. This is called a walk-away VSP.
- The direct arrival becomes hyperbolic as the reflections.
- These recordings are pretty similar to surface-seismic recordings.
- Often, the resulting seismic section from the walk-away VSP can be "merged" into the surface-seismic section.

Processing of a Zero-Offset VSP

from this data two products are obtained:

1. Velocity profile as a function of depth;

- the direct or transmitted wave is used, while for the second product

2. Seismic trace, comparable to a surface-seismic trace.

- the reflected waves are used.

The Zero-Offset (VSP) processing flow

- At the beginning trace editing for bad trace with exclude the auxiliary traces too, and calculating of average and RMS velocities.
- the amplitude recovery
- an f-k filter has been used for the separation of the upgoing and downgoing waves.
- Afterwards, a waveshaping deconvolution that use the downgoing P waves took place in order to design the deconvolution operator to apply for the upgoing P waves.
- shifting to the TWT by doubling the first-break time of the upgoing P waves and
- finally the corridor stack has been resulted.

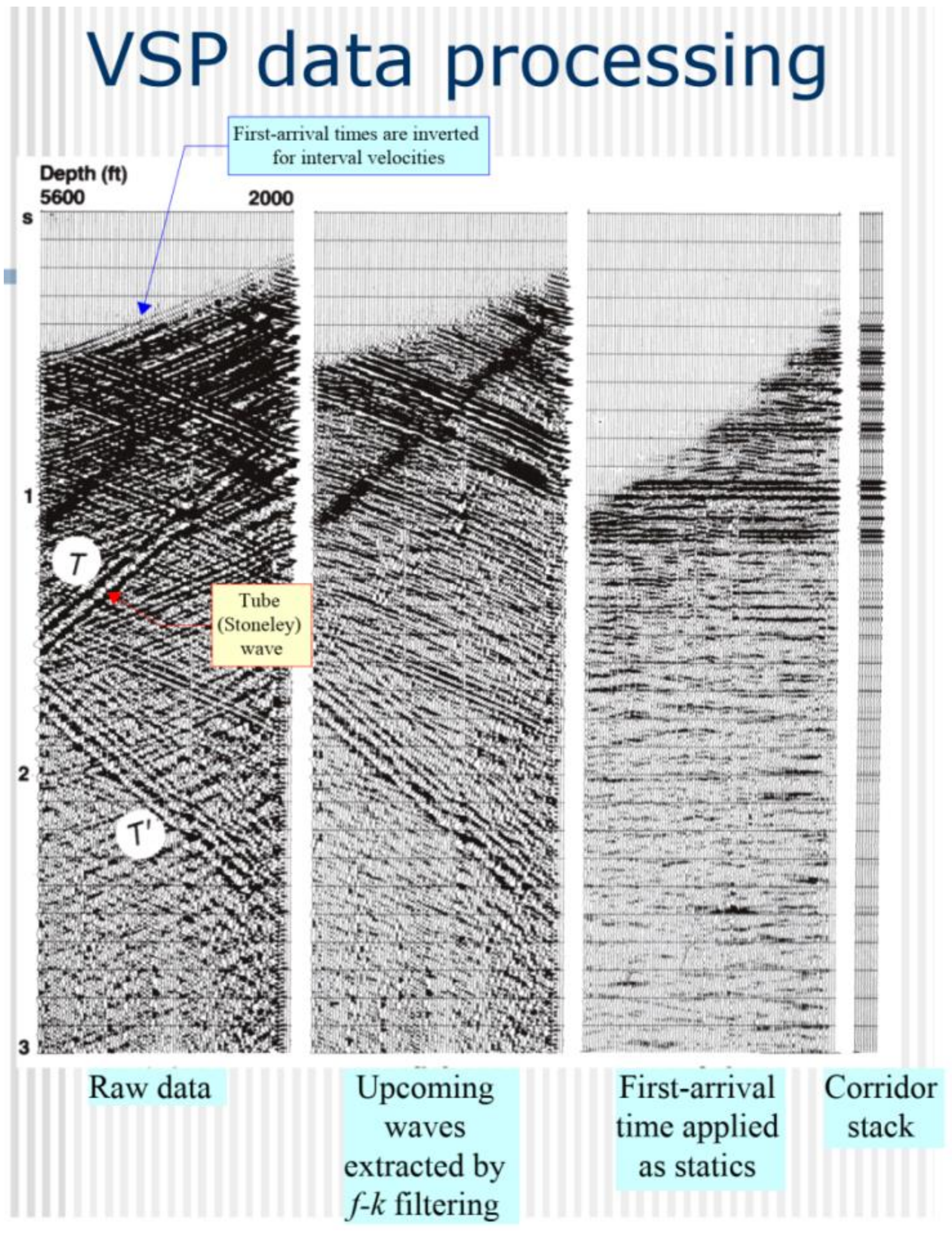

the basic steps in VSP processing

- After some trace editing, VSP processing starts with the separation of the downgoing waves from the upcoming waves (reflections).
- One separation technique is based on $f-k$ filtering.

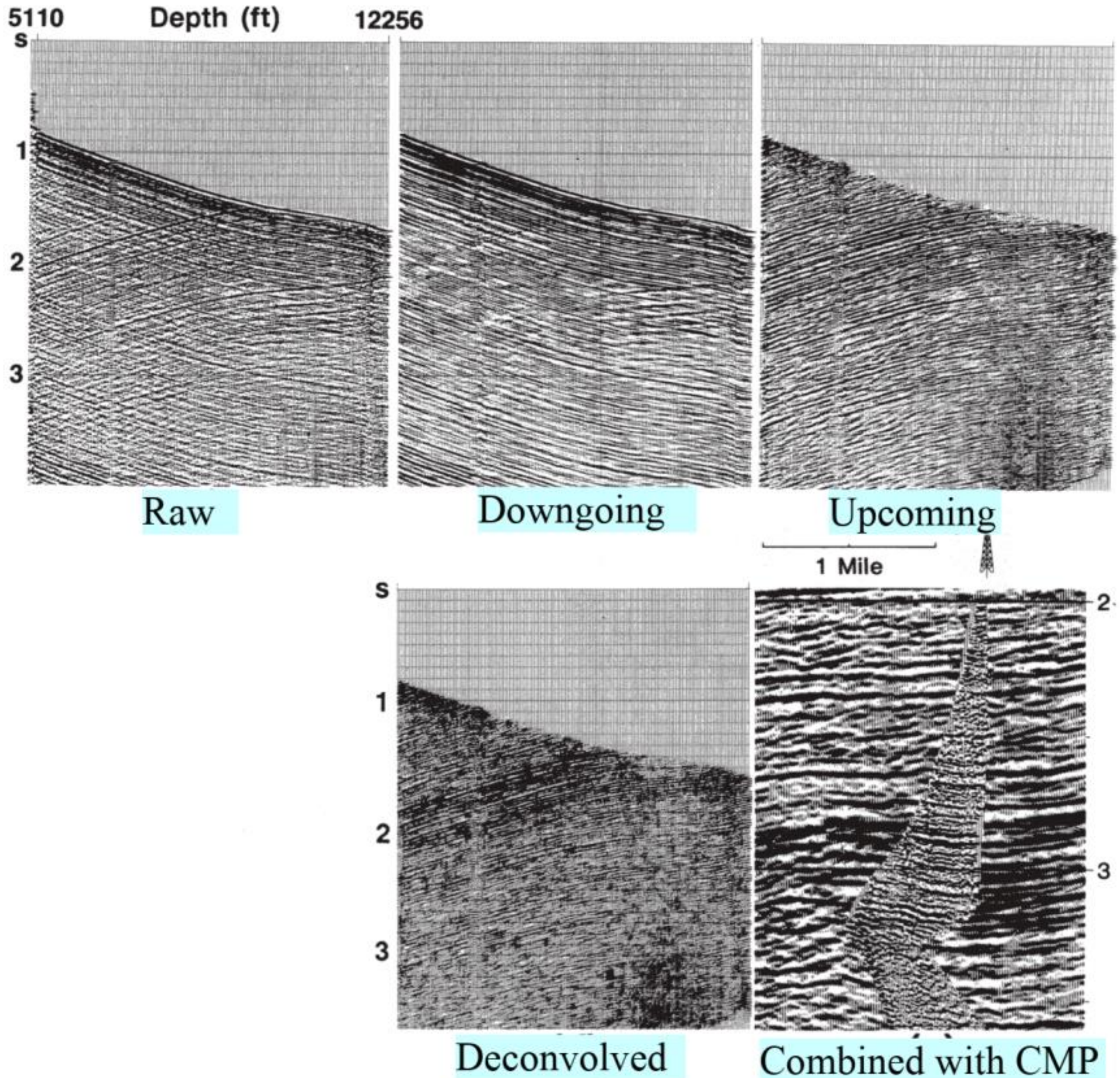
5110
Depth (ft)
12256
s
1
2
3
Raw
Downgoing
Upcoming
1 Mile
s
1
2
3
2
3
Deconvolved
Combined with CMP

Applications of vertical seismic profiling

Time-depth calibration
What depth are reflections coming from?
Primary and multiple identification
Does an interface actually produce a reflection?

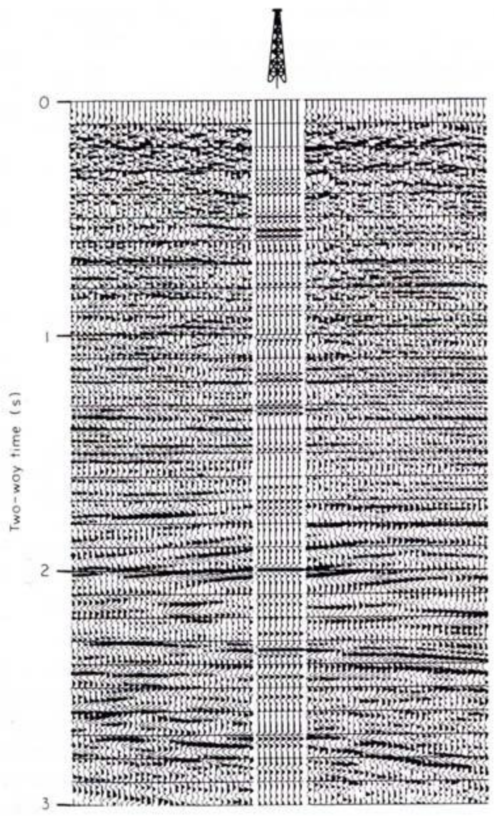

Higher resolution imaging

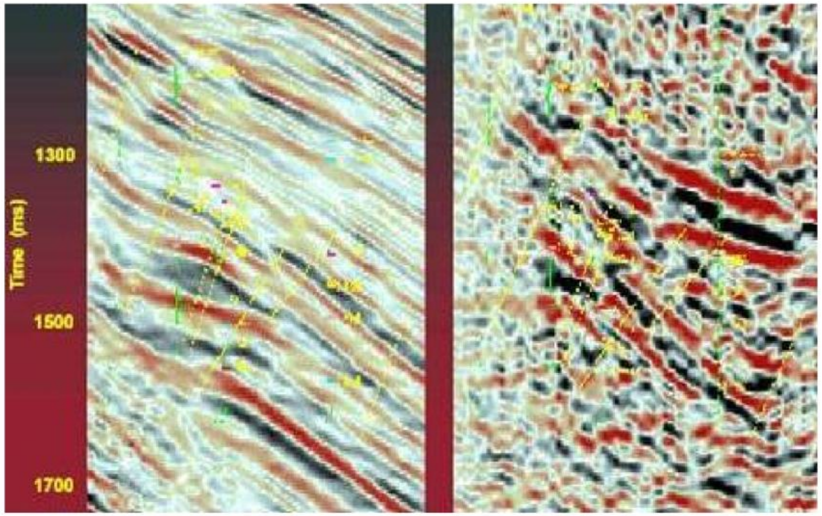

Surface 3-D VSP

Table 13.1 *Objectives of VSP surveys*

Objective	How achieved
Reflector identification Surface-to-borehole correlation Increased resolution at depth	Upgoing wave studies on zero-offset VSP
Time–depth conversion Enhanced velocity analysis Log calibration	First-break studies on zero-offset VSP
Multiple identification Deconvolution operator	Downgoing wave studies on zero-offset VSP
Improve poor data area	All types, especially offset VSP
Predict ahead of bit	Upgoing wave studies on zero-offset VSP
Structural imaging	Walkaway or offset VSP with presurvey modeling
Delineate salt dome	Proximity survey with source over dome
Seeing above/below bit on deviated wells	Zero-offset, offset, or walkaway VSP
Stratigraphic imaging (channels, faults, reefs, pinchouts)	Multiple-source locations with offset VSP
AVO studies	Research study on offset VSP with presurvey modeling
P/S-wave analysis Polarization studies Fracture orientation	Research study on offset VSP, three-component phone
Attenuation analysis	Research study on zero-offset VSP
Secondary recovery	Research study on offset VSP
Tomographic studies	Multiple wells, multiple offsets
Permeability studies	Tube-wave analysis research study

After Gilpatrick and Fouquet, 1989.

Hydrocarbon exploration with seismic reflection

Seismic processing includes the following:

(1) Filtering of raw data
(2) Selecting traces for CMP gathers
(3) Static corrections
(4) Velocity analysis
(5) NMO/DMO corrections
(6) CMP stacking.
(7) Deconvolution and filtering of stacked zero offset traces
(8) Migration (depth or time)

Processed seismic data can contribute to hydrocarbon exploration in several ways:

1. Seismic data can give **direct evidenc**e of the presence of hydrocarbons (*e.g.* bright spots, oil-water contact, amplitude-versus-offset anomalies).
2. Potential **hydrocarbon traps** can be imaged (*e.g.* reefs, unconformities, structural traps, stratiagraphic traps etc)
3. Regional structure can be understood in terms of depositional history and the timing of regression and transgression (seismic stratigraphy, seismic facies analysis).

1. Direct indicators of hydrocarbons (DHI)

1.1 Bright spots

- A gas reservoir can have a P-wave velocity that is significantly lower than that the surrounding rocks.
- This can lead to a high amplitude (negative polarity) reflection from the top of the reservoir.
- However, not all bright spots are hydrocarbons. They can be caused by sills of igneous rocks or other lithological contrasts.

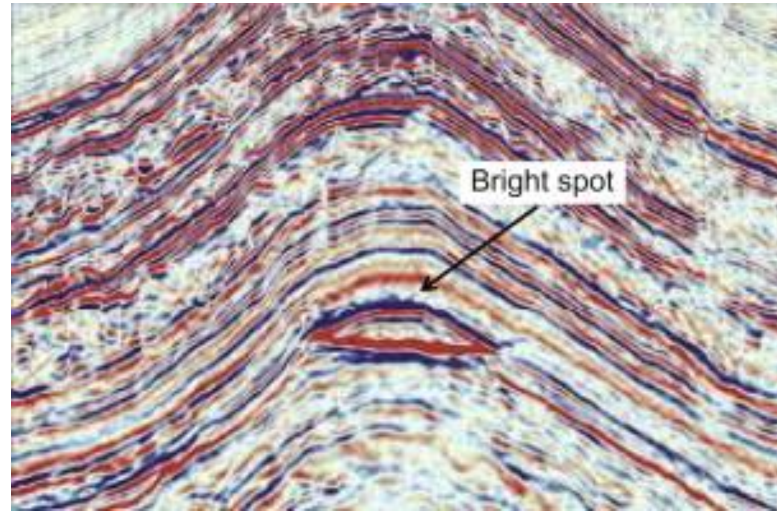

A 'bright spot' on the seismic section.

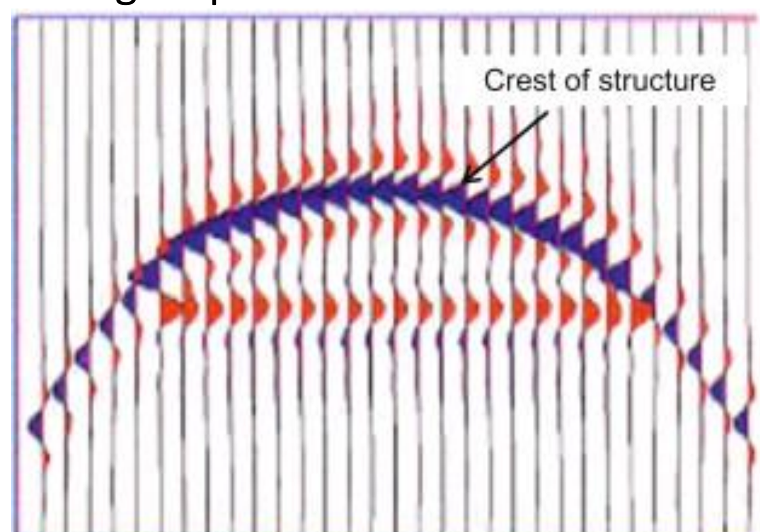

Model of a bright spot response, after M. Bacon et al. (2003).

1. Direct indicators of hydrocarbons

2 Hydrocarbon-water interface

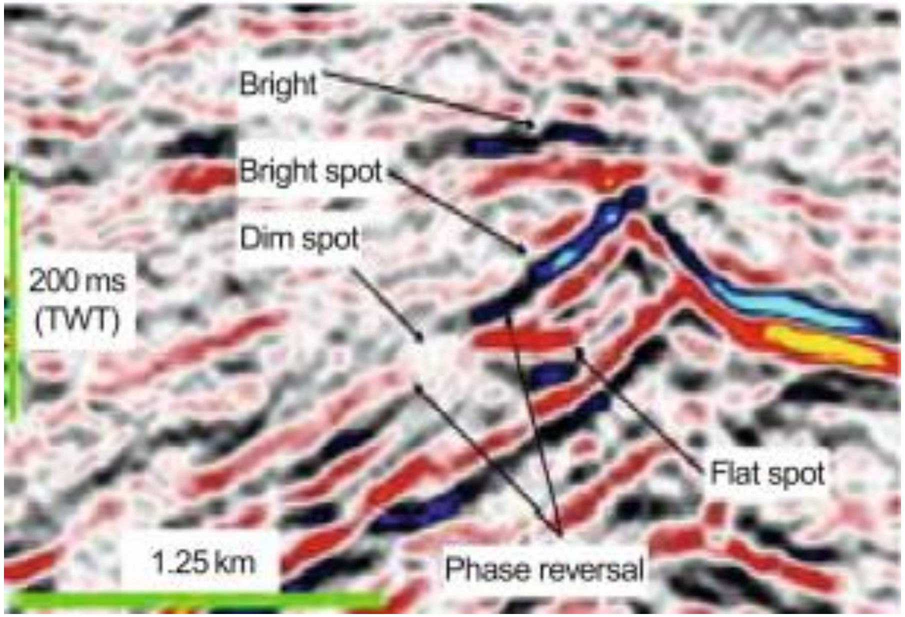

- A ‘flat spot’ is a seismic anomaly that appears as a horizontal reflector on a seismic section.
- Flat spots will occur when there is a contact between oil, gas and water in a limited area and the surrounding reflectors are not flat.

- ‘Flat spots’ can occur when hydrocarbon-saturated sand with a lower acoustic impedance overlies water-saturated sand with a higher acoustic impedance. The ‘flat spot’ is noticed at the hydrocarbon–water contact.

Fulmar field, North Sea

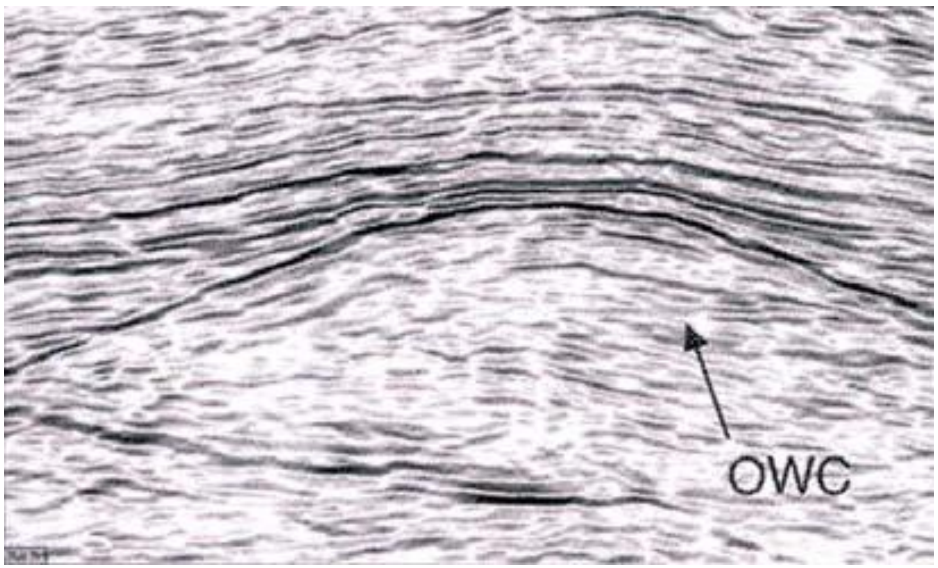

- The oil-water contact is flat in this depth section from the Fulmar field in the North Sea (Kearey 4-39). Note that it crosses reflectors in the anticline.

1. Direct indicators of hydrocarbons

3 Amplitude versus offset (AVO)

- Previously we computed reflection coefficients for seismic waves incident at normal incidence.
- However, the full Zoeppritz equations predict that the reflection coefficient will **vary with the angle of incidence**.

- **Example 1**

  Both P-wave and S-wave velocities **increase** across the interface.

  Remember that at non-normal incidence, an incident P-wave will generate 4 new waves. These are the reflected and transmitted P-waves **and** the reflected and transmitted S-waves.

  The reflection coefficient of the P-wave decreases with angle in this example.

Increase in P-wave and s-wave velocity

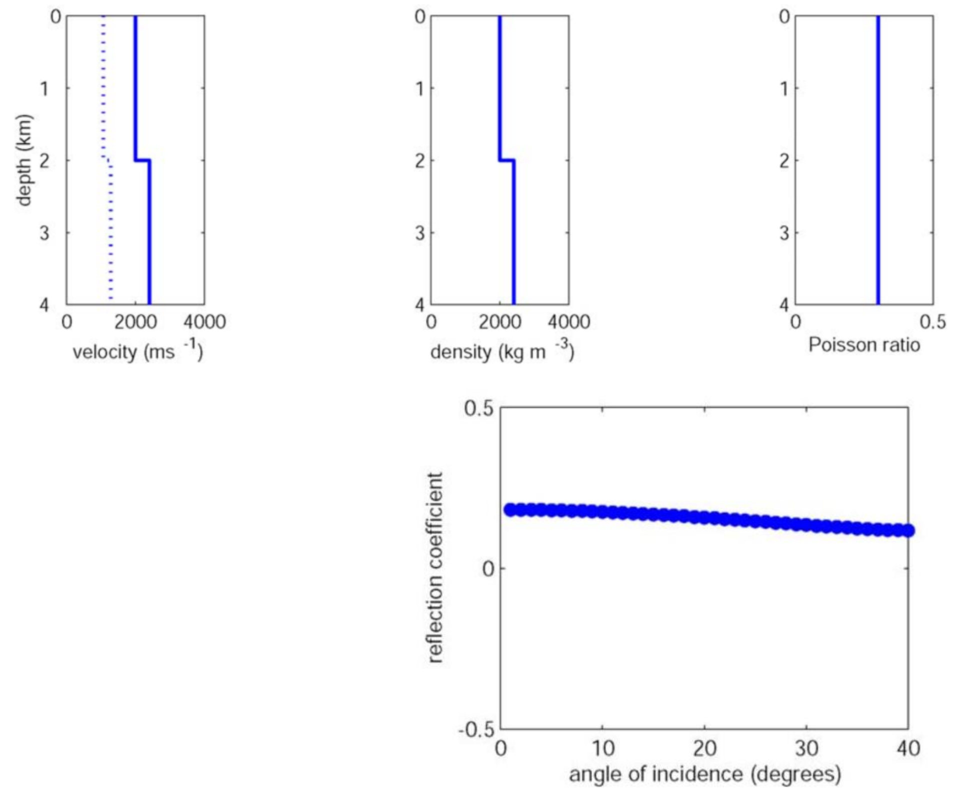

1. Direct indicators of hydrocarbons

3 Amplitude versus offset (AVO)

- **Example 2**
- This example simulates the effect of shale overlying a gas saturated sand reservoir. The P-wave velocity **decreases**, giving a **negative reflection coefficient** at normal incidence.
- The S-wave velocity **increases** from the shale into the gas sand. Can show that this corresponds to a **decrease** of Poisson's ratio.
- In this case, the P-wave reflection coefficient becomes larger as the angle of incidence increases.

Reflection from the top of gas sand reservoir

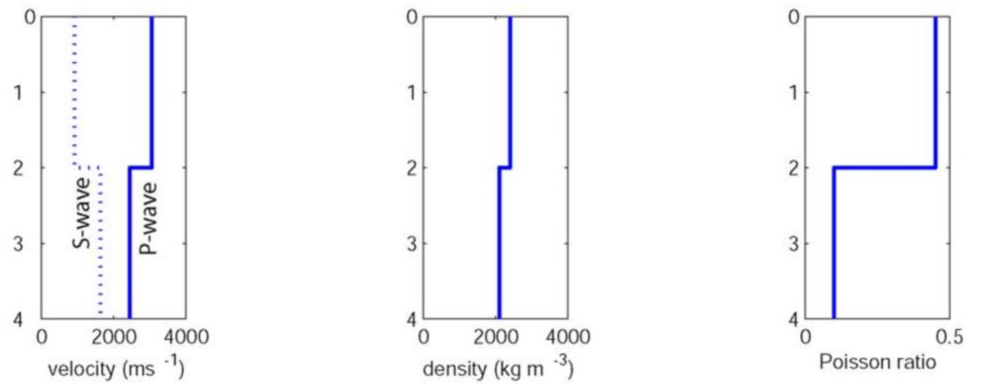

$$\sigma = \frac{(v_P / v_S)^2 - 2}{2((v_P / v_S)^2 - 1)}$$

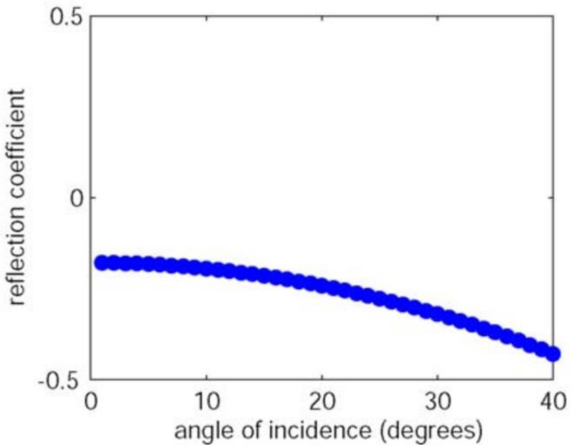

Since an **increase in angle** corresponds to a **greater source-receiver offset**, this is called an amplitude-versus offset (AVO) anomaly.

Data examples of AVO

These effects are often present in field data and can indicate the presence of oil or gas with more reliability than normal incidence reflection data.

- The following example is taken from *Ostrander* (1984) and shows a reflection from a known gas reservoir at a depth of 6700 feet in the Sacramento Valley, California.
- The amplitude **increases** with offset on a number of CDP gathers

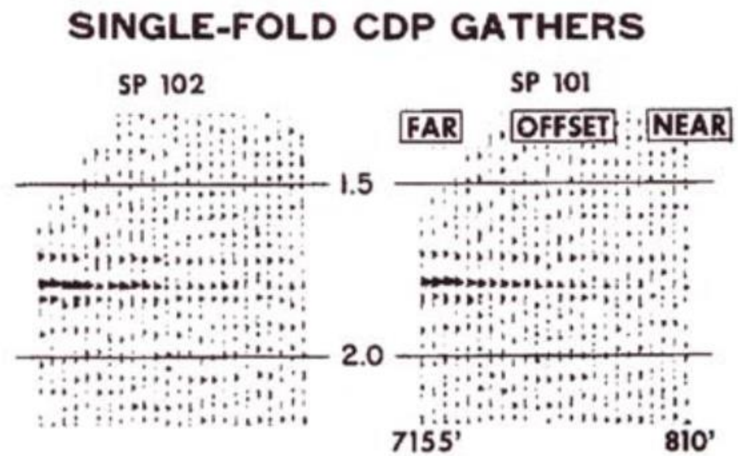

- In this example, also from *Ostrander* (1984), a high amplitude reflection in a sedimentary basin in Nevada was analysed.
- The amplitude **decreases** with offset, suggesting that the layer had a normal Poisson's ratio.
- It was subsequently drilled and shown to be 160 feet of basalt.

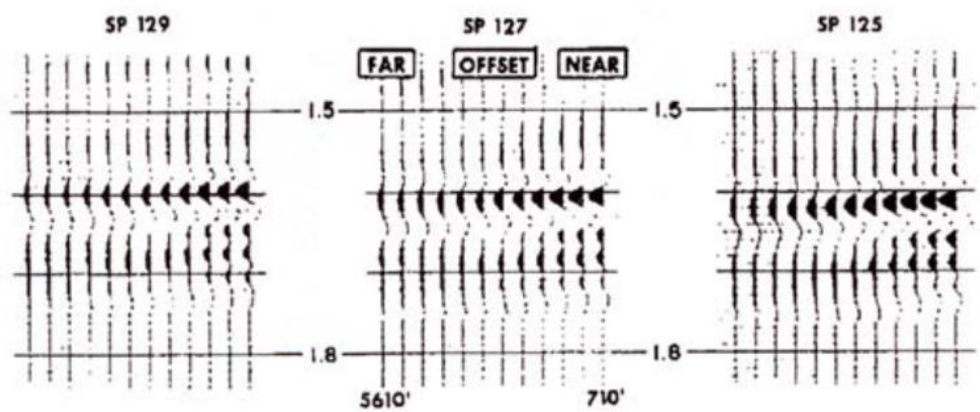

2 Images of hydrocarbon reservoirs on seismic sections

2.1 Extensional environment – North Sea

- Viking gas field, North Sea, *Kearey 4.61*. Gas reservoir is located in a faulted anticline. The most prominent reflections in a seismic section are called markers.
- These are correlated across the section though a comparison of their character and sequence.
- They are tied to lithologic units through measuring well logs and computing synthetic seismograms.
- Vertical seismic profiles can also be used in this respect.

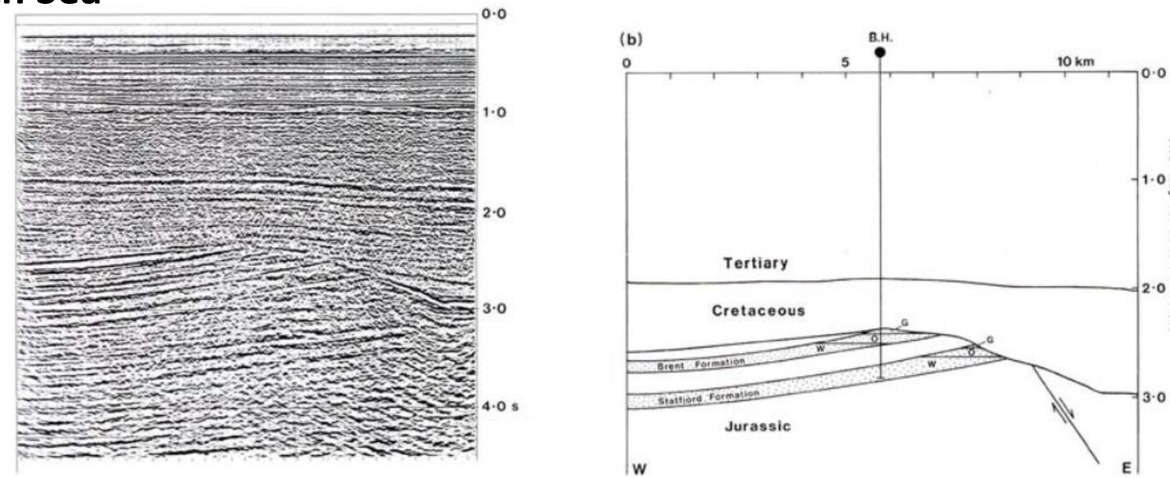

Brent oilfield, North Sea, *Kearey Figure 4.62*

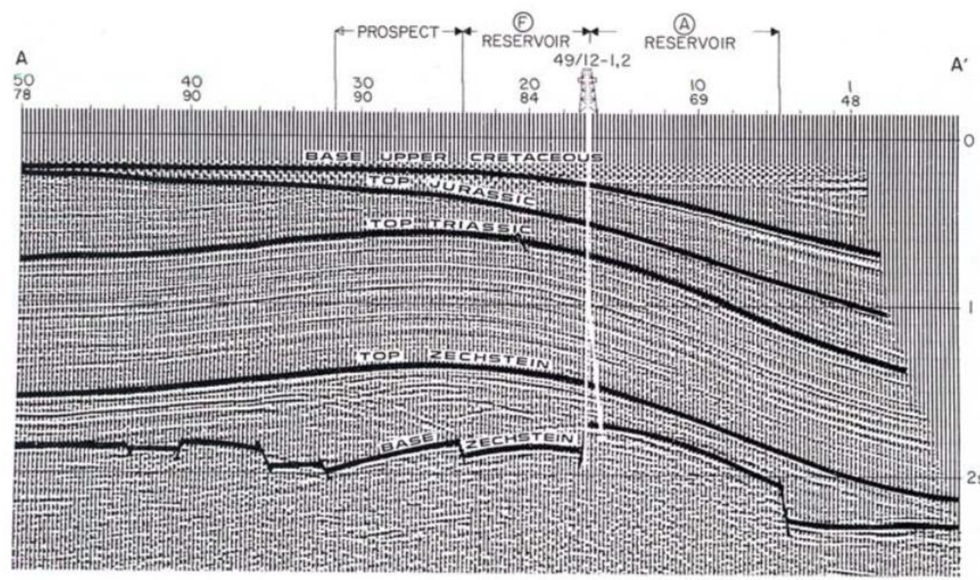

2.2 Fold and Thrust belts

- Tracing reflectors across a series of faults

Rocky Mountain Foothills
Turner Valley *Anderson et al*, 1989, page 165

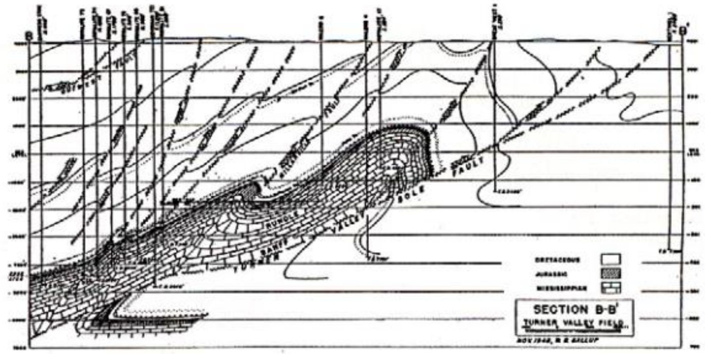

(After Gallup, 1951)

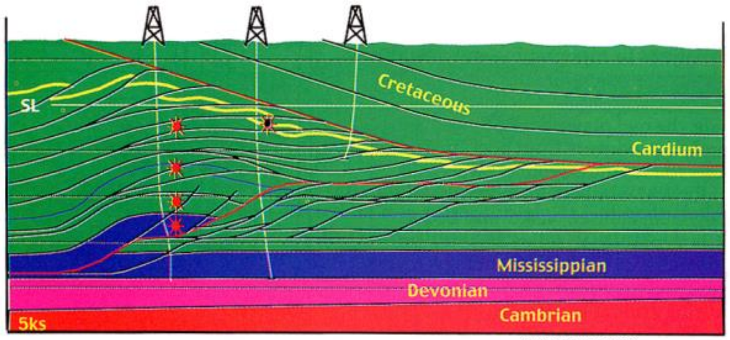

(After Teal, 1983)

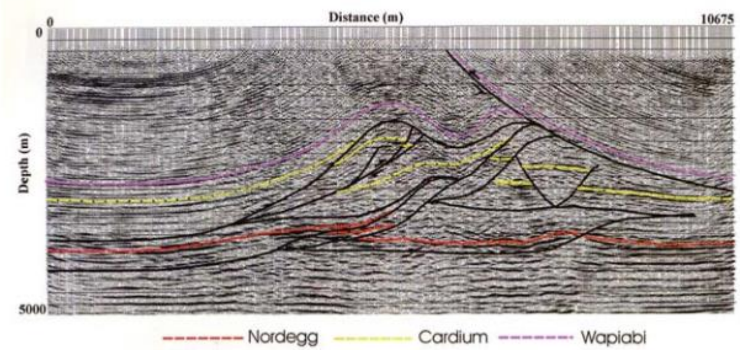

Yan and Lines, *The Leading Edge*, (2001)

2.3 Reefs

- Reefs are often a zone of high porosity in a carbonate layer and make good hydrocarbon reservoirs.
- Seismic characteristics of the reef are draping of overlying sediments and upper surface.
- Note also that the base of the reef does not appear as a flat feature. It is **pulled up** because of the higher velocity within the reef.

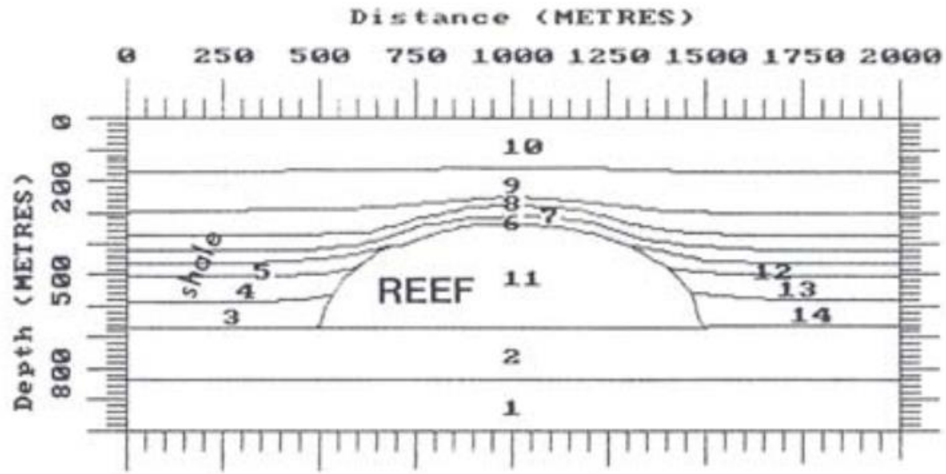

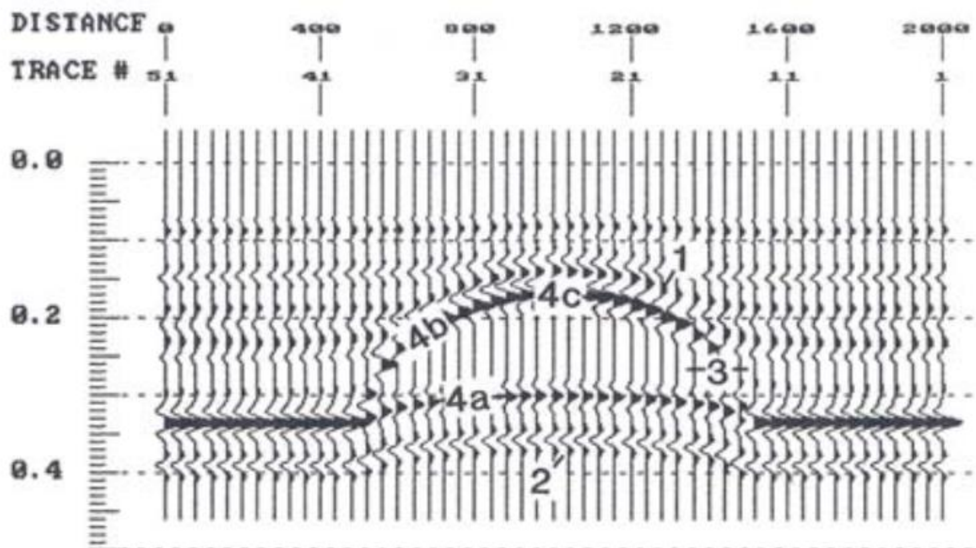

2.4 Salt related hydrocarbon reservoirs

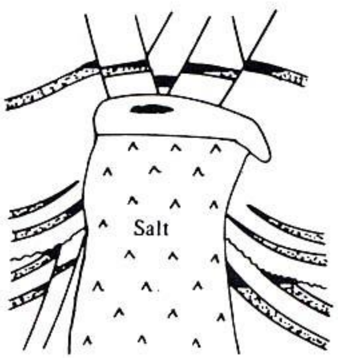

Salt can produce significant hydrocarbon traps when sedimentary units are deformed in salt tectonics.

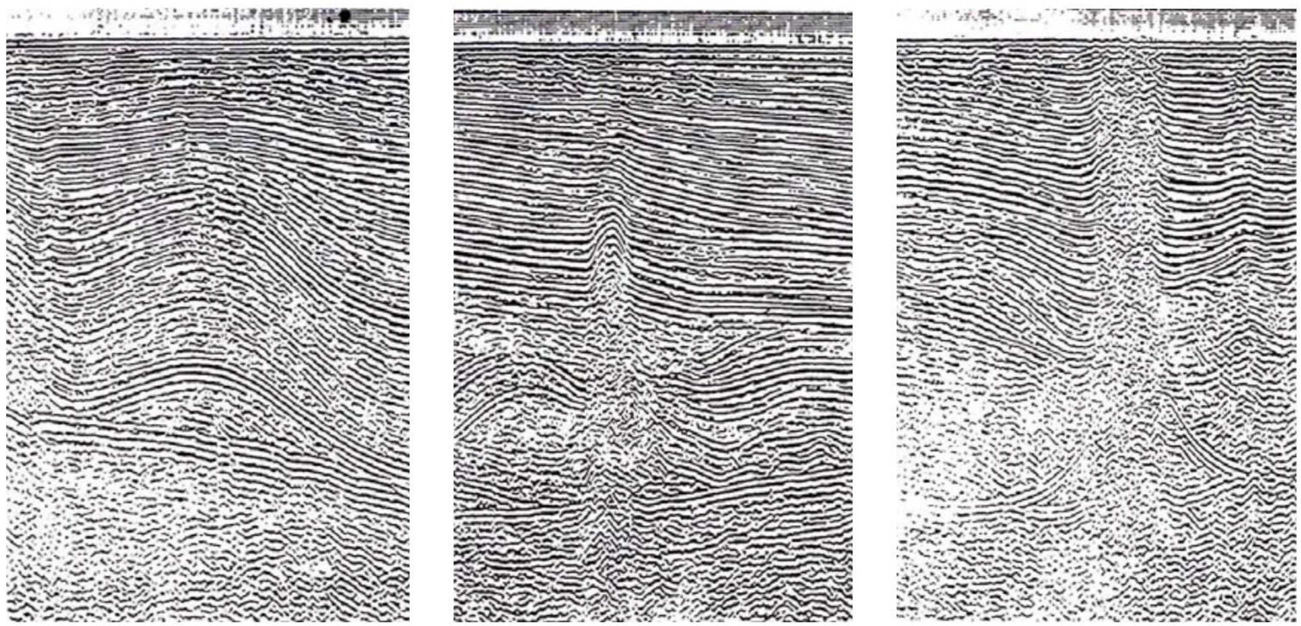

Salt creeps under mechanical loading and salt sheets can flow horizontally.
Salt diapers can rise in a column to the surface.
The figure above shows 4 second seismic reflection data that reveals the evolution of a salt sheet, progressing from a salt swell, to a diapir that penetrates the sediments, and finally to the surface *(North Sea, Telford figure 4.102)*

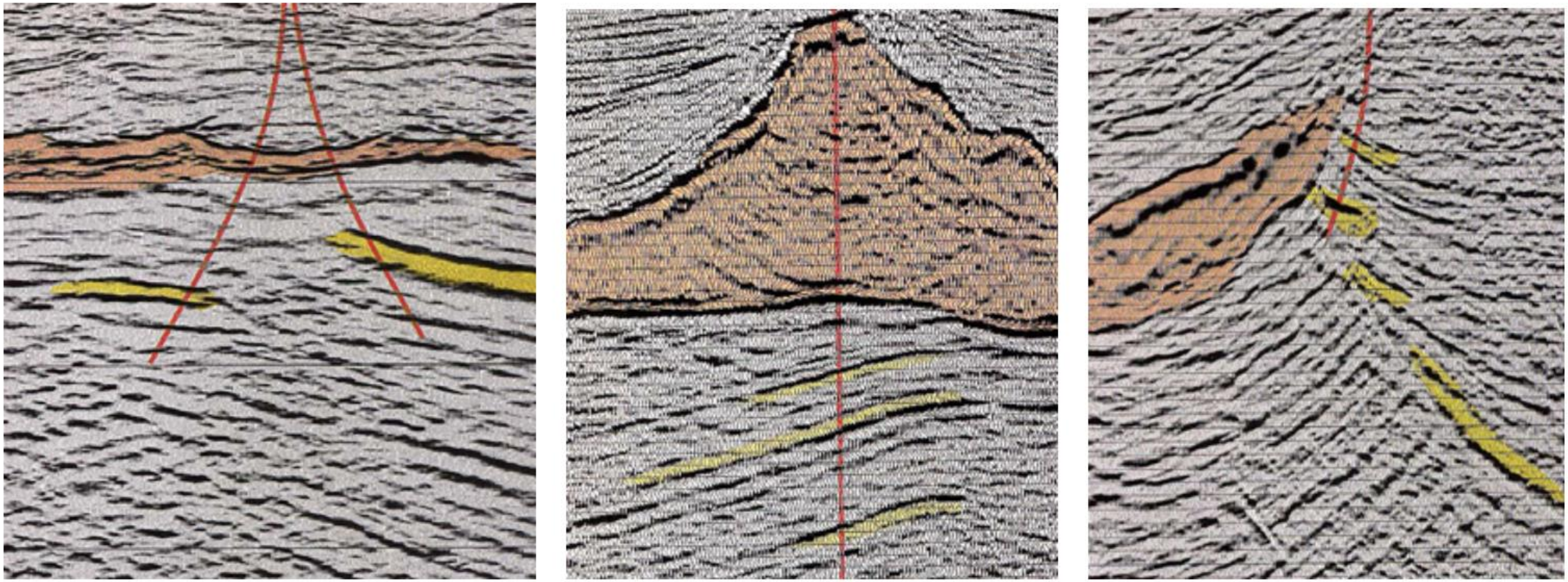

Hydrocarbon reservoirs may be located in the sedimentary sequence beneath a salt layer. However, the high velocity of a salt body makes it difficult to image these reservoirs.

Brown denotes the salt body and yellow the reservoir.
Imaging techniques such as pre-stack depth migration have made a big improvement in this type of exploration problem

General Review

Q1

- **How does a migrated reflection seismic section differ from an unmigrated one? In what circumstances would they be the same?**

Answer

- Migration is the spatial repositioning (migration) of seismic arrivals from the initial assumption that the arrivals come from flat and continuous layers. Migrations do three primary things:

a) steepens dipping layers,

b) collapses diffractions,

c) moves reflectors to deeper levels.

Q2

How can a primary reflection be distinguished from a multiple one?

Answer

- Multiple reflections have greater temporal moveout compared to primary reflections.
- Thus, multiples stack with a lower velocity.

Q3

What are the main purposes of stacking?

Answer

- Stacking is the seismic equivalent of ‘averaging’ numbers to improve one’s estimate of the quantity.
- Stacking constructively adds together the signal, while the random noise tends to cancel, thereby increasing the signal to noise ratio.

Q4

How many synclines and anticlines appear in an unmigrated seismic section?

Answer

- It depends on the individual seismic section! Would have to study a section to identify them.
- Anticlines appear spatially broader on an unmigrated section.
- The signature of a syncline depends on its depth relative to its curvature. If it is shallower than the radius of curvature, it tends to be narrower on the unmigrated section. If the reflector is deeper than the radius of curvature, it produces the 'bow tie' on the unmigrated section.

Q5

Seismic sections are not always what they appear.

Explain how an apparent reflector may

(a) have an incorrect slope,

(b) may have an incorrect curvature, or

(c) may not exist at all,

while

(d) three horizontal reflectors spaced equally one above the other may not be equally spaced, in reality?

Answer

- (a) Unmigrated sections have lesser dips.

  (b) Synclines (concave up) and anticlines (concave down) will have their curvatures modified in unmigrated sections.

  (c) Multiple reflections can produce an apparent reflector

  (d) The scale on a seismic section is TWT, not distance. TWT=2(*thickness)/velocity*, hence, variations in the combination of thickness and velocity can make it appear that they are equally spaced, when in reality, they are only equally spaced in TWT.

Q6

Why is a very strong horizontal reflection usually indicative of a gaswater interface?

Why may a gas water interface not always appear as a horizontal reflector?

Answer

- Because the acoustic impedance of a gas-liquid is very different than the surrounding rock, it can produce a ‘bright spot’ on a section.
- Since gas-liquid is generally less dense than the surrounding rock, it will tend to move upward until it reaches an impermeable boundary, which is often horizontal.
- However, traps can exist that are not horizontal, therefore the interface may not always be horizontal.

Q7

Explain why a seismic interface may not be a lithological boundary, and viceversa.

Give an example of each.

Answer

- A seismic interface may be an artifact from reflective interference of several layers.
- An example is alternating layers of sandstone and shale, which can produce false reflectors.
- A lithologic boundary may not produce a seismic reflector because the combination of density and velocity (impedance) may not be such as to produce a significant reflector even though they are distinctly different.

Q8

Why do marine seismic reflection surveys not record (a) Swaves? (b) refracted rays?

Answer

a) For ideal fluid, μ=0, thus, $v_s^2 = \mu/\rho = 0$.

b) Reflection offsets are at offset less than the critical refraction distance.

Q9

How can a reflection coefficient be negative? How can it be recognized?

Answer

The sign of the reflection coefficient depends on the seismic impedence difference between the lower layer (assuming downgoing wave) and the upper layer.

$$R = \frac{a_{reflected}}{a_{incident}} = \frac{\rho_2 v_2 - \rho_1 v_1}{\rho_2 v_2 + \rho_1 v_1}$$

Thus, if $Z_2 = \rho_2\ v_2 > Z_1 = \rho_1\ v_1$, then R>0.

If $Z_2 = \rho_2\ v_2 < Z_1 = \rho_1\ v_1$, then R<0.

The way that a negative reflection coefficient is manifested in a seismogram, is that the wave is inverted.

Processing Potential Field Data

- Processing Objectives
- 1D Fourier Transform
- 2D Fourier Transform
- Discrete Fourier Transform
- Aliasing
- Fourier transform of a monopole
- Fourier transform of a dipole

Processing

- Low pass filtering
- Directional filtering
- Upward continuation
- Downward continuation
- Horizontal and vertical derivatives
- Reduction to pole

Processing of Potential Field Data.

Data in map format 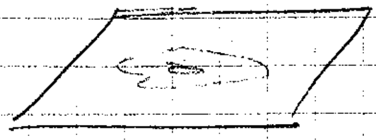

Things to do

(i) Upward continue the fields (see what they look like at a higher level)
- (a) needed for inversion
- (b) get away from near surface contamination
- (c) see deep structure.

Important concept: High frequency (wave number) components of the field are preferentially attenuated with upward continuation height

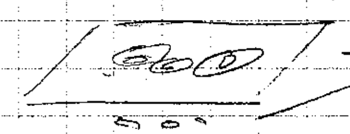 high frequency data is caused by small objects close to the surface.

(ii) Filter data
- (a) remove noise
- (b) accentuate or eliminate features with a particular strike.
- (c) separate high frequency and low frequency components of data

(iii) Downward continuation
- (a) see what the data would be like on a plane beneath the measurement plane

(iv) Calculation of spatial derivatives

(v) Reduction to pole.
- (a) See what magnetic data would be if the same magnetic bodies were at the magnetic pole.

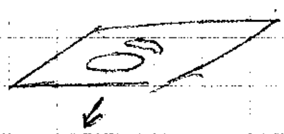

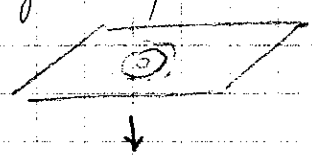

Most of the processing is done using Fourier transforms. Therefore

(i) Review 1d FT

(ii) 2D - FFT

(iii) FT of a: monopole (for gravity)
dipole (for magnetics)

(iv) Power spectrum (radial power spectrum for 2d maps)

chapter 11

(v) Data processing:
(a) Filtering
(b) Upward/downward continuation
(c) Calculation of spatial derivative
(d) Reduction to pole.

General procedure for Fourier Domain filtering

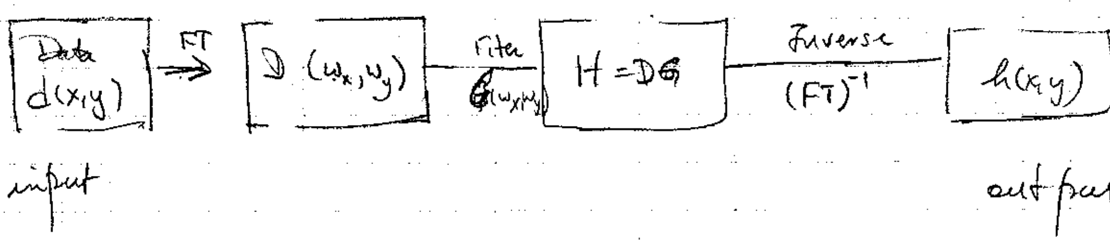

eg

$$h(x) = d(x) \otimes g(x) \qquad h(x) = \int_{-\infty}^{\infty} d(u)\, g(x-u)\, du$$

$$H(k) = D(k) \cdot G(k)$$

$$h(x) = \mathcal{F}^{-1}\left[H(k) \right]$$

Fourier Transform: Notation and Review.

Remark: The material in Chapter 11 in Blakely is well presented. The following is a review of main items.

1D Fourier transform.

Let $f(x)$ be defined on $(-\infty, \infty)$ such that $\int |f(x)|\, dx < \infty$ then

$$F(k) = \int_{-\infty}^{\infty} f(x) e^{-ikx}\, dx$$

$$f(x) = \frac{1}{2\pi} \int_{-\infty}^{\infty} F(k) e^{ikx}\, dk$$

where $k = \frac{2\pi}{\lambda}$ is the (circular) wave number

The quantity $F(k)$ is complex and can be written as

$$F(k) = F_R + i F_I \quad \text{(Real \& Imaginary parts)}$$

$$F(k) = |F| e^{i\theta(k)}$$

$$|F| = \sqrt{F_R^2 + F_I^2} \qquad \text{Amplitude}$$

$$\theta(k) = \tan^{-1}\left(\frac{F_I}{F_R}\right) \qquad \text{Phase}$$

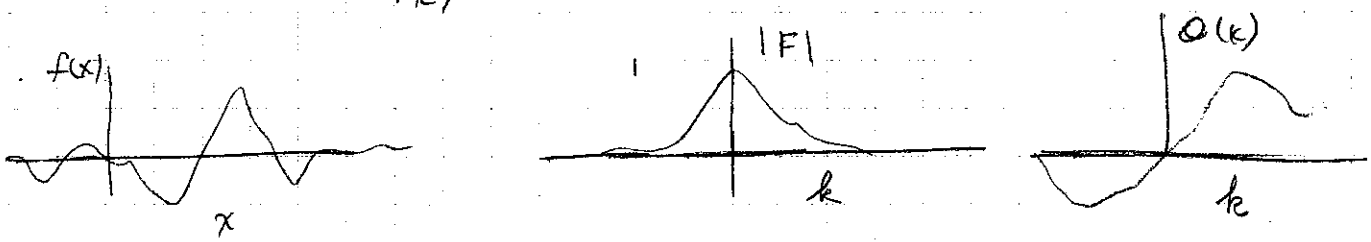

Properties: $f(x) \leftrightarrow F(k)$ denote Fourier transform pair

(1) $f(x)$ is real $\quad F(k) = F(-k)^*$

(2) $f(ax) \leftrightarrow \frac{1}{|a|} F\left(\frac{k}{a}\right)$ (Scaling)

(3) Shifting, $f(x-x_0) \Leftrightarrow F(k)\,e^{-ix_0 k}$

(4) Differentiation $\frac{d}{dx^n} f(x) \Leftrightarrow (ik)^n F(k)$

(5) Linearity $\left[a_1 f_1(x) + a_2 f_2(x)\right] \Leftrightarrow \left[a_1 F_1(k) + a_2 F_2(k)\right]$

Convolution

$$h(x) = f(x) \otimes g(x)$$

$$h(x) = \int_{-\infty}^{\infty} f(u)\, g(x-u)\, du = \int_{-\infty}^{\infty} g(u)\, f(u-x)\, du$$

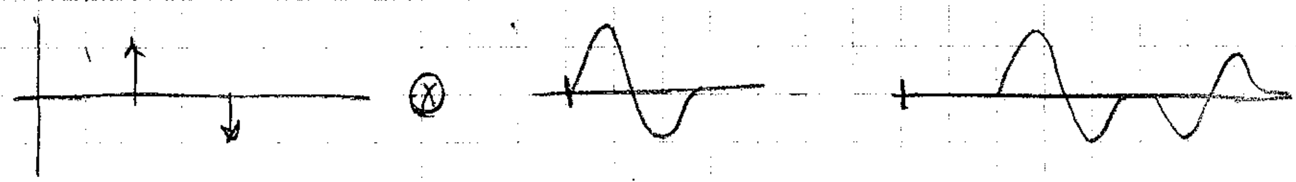

Process is one of (i) reversing
(ii) shifting
(iii) multiplying

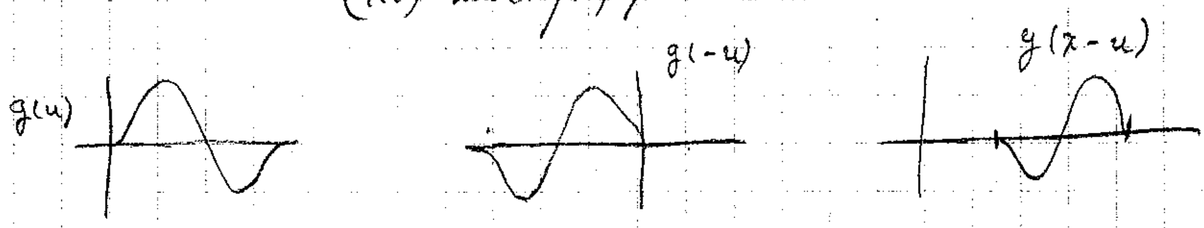

(6) Convolution theorem: $h(x) = f(x) \otimes g(x)$ (1)

$$h(x) \Leftrightarrow H(k)$$
$$f(x) \Leftrightarrow F(k)$$
$$g(x) \Leftrightarrow G(k)$$

then
$$\left.\begin{aligned} H(k) &= F(k)\cdot G(k) \\ h(x) &= \frac{1}{2\pi}\int_{-\infty}^{\infty} H(k)\, e^{ikx}\, dk \end{aligned}\right\} \quad (2)$$

So we can obtain the convolution in either of two ways. Directly by (1) or using the FT as per (2). $h(x) = \mathcal{F}^{-1}\left[F(k)\,G(k)\right]$.

(7). Parseval's formula

$$\int_{-\infty}^{\infty} |f(x)|^2 dx = \frac{1}{2\pi} \int |F(k)|^2 dk.$$

2D Fourier Transforms.

Consider a function $f(x,y)$

$$F(k_x, k_y) = \int_{-\infty}^{\infty}\int_{-\infty}^{\infty} f(x,y)\, e^{-i(k_x x + k_y y)}\, dx\, dy$$

$$f(x,y) = \frac{1}{4\pi^2}\int_{-\infty}^{\infty}\int_{-\infty}^{\infty} F(k_x, k_y)\, e^{i(k_x x + k_y y)}\, dk_x\, dk_y$$

$$k_x = \frac{2\pi}{\lambda_x} \qquad k_y = \frac{2\pi}{\lambda_y}$$

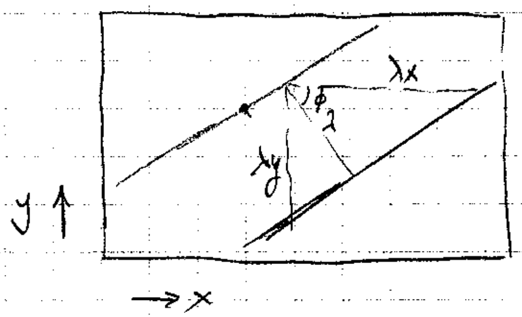

$$\lambda = \lambda_x \cos\phi \qquad \lambda_x = \frac{\lambda}{\cos\phi}$$

$$\lambda = \lambda_y \sin\phi \qquad \lambda_y = \frac{\lambda}{\sin\phi}$$

$$k_x = \frac{2\pi}{\lambda_x} = \frac{2\pi}{\lambda}\cos\phi = k\cos\phi \qquad \boxed{k_x = k\cos\phi}$$

$$k_y = \frac{2\pi}{\lambda_y} = \frac{2\pi}{\lambda}\sin\phi = k\sin\phi \qquad \boxed{k_y = k\sin\phi}$$

Fourier Transform: Notation and Definition Comments

Possible notations: general f^{n} $g(x)$

① $$G(k) = \int_{-\infty}^{\infty} g(x)\, e^{-ikx}\, dx$$ k: circular wave number $k = \frac{2\pi}{\lambda}$

$$g(x) = \frac{1}{2\pi} \int_{-\infty}^{\infty} G(k)\, e^{ikx}\, dk$$

If the signal is in the time domain: general function $g(t)$

(2) $$G(\omega) = \int_{-\infty}^{\infty} g(t)\, e^{-i\omega t}\, dt$$ ω: angular frequency (radians)

$$g(t) = \frac{1}{2\pi} \int G(\omega)\, e^{i\omega t}\, d\omega$$

Comment: sometimes the signs in the exponentials will change. For instance we could define

(3) $$G(\omega) = \int_{-\infty}^{\infty} g(t)\, e^{i\omega t}\, dt$$

$$g(t) = \frac{1}{2\pi} \int_{-\infty}^{\infty} G(\omega)\, e^{-i\omega t}\, d\omega$$

So $|G|$ will be the same in (2) and (3) but the phase $\arg G$ will be different

Practical comment: Be careful! This is especially true for geophysical electromagnetic data.

Many authors use linear wavenumber/frequency in the definition

$$(4) \qquad G(\tilde{k}) = \int_{-\infty}^{\infty} g(x)\, e^{-i2\pi \tilde{k} x}\, dx \qquad \tilde{k} \text{ is linear wave number}$$

$$g(x) = \int_{-\infty}^{\infty} G(\tilde{k})\, e^{i2\pi \tilde{k} x}\, d\tilde{k} \qquad \tilde{k} = 1/\lambda$$

* Comment: I have written $\tilde{k}$ in the above equations to distinguish between case (1) and (4). Usually the symbol k will be used so you need to know which definition is used.

(5) For signals in the time domain

$$G(f) = \int_{-\infty}^{\infty} g(x)\, e^{-i2\pi f t}\, dt$$

$$g(t) = \int_{-\infty}^{\infty} G(f)\, e^{i2\pi f t}\, df \qquad f = 1/T \quad \text{Hz}.$$

Discrete Fourier Transform:

Suppose we have a time-sequence or spatial sequence

$$f_r = f(x_r) = f(r\Delta x) \qquad r = 0, N_x - 1 \qquad (N_x \text{ samples})$$

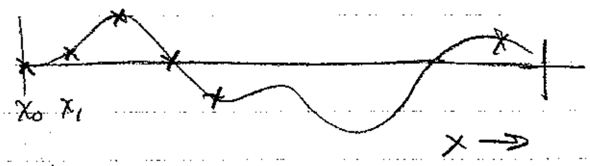

Discrete Fourier transform

$$\boxed{\begin{aligned} F_j &= \sum_{r=0}^{N_x-1} f_r\, e^{-i2\pi rj/N_x} \\ f_r &= \frac{1}{N_x} \sum_{j=0}^{N_x-1} F_j\, e^{i2\pi rj/N_x} \end{aligned}}$$

$j = 0, N_x - 1$

$r = 0, N_x - 1$

Remark: The above assumes that the data are periodic with period $L_x = \Delta_x N_x$

The linear wavenumbers are

$$\tilde{k}_j = \frac{j}{N_x \Delta x} = \frac{j}{L_x} \qquad j = 0, \dots N_x - 1$$

Note that this is a linear wavenumber $\quad 2\pi \tilde{k}_j = k_j$

As you saw in your introductory time series analysis, the wave numbers corresponding to $j = 0, \dots N_x - 1$ pertain to positive and negative wavenumbers (frequencies)
The output from the N_x numbers in the digital FT is ordered like:

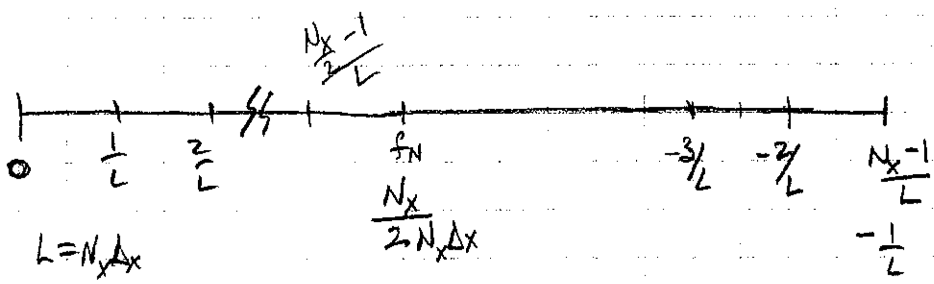

$f_N = \dfrac{1}{2\Delta x} = \vec{k}_{xN}$ is the Nyquist frequency.

Note the ordering for understanding the Fourier components F_j

$j=0$ corresponds to dc

$j=1 \quad \vec{k} = \dfrac{1}{L}$

$j = \dfrac{N_x}{2} \quad \dfrac{\frac{N_x}{2}}{L} = \dfrac{N_x}{2N_x\Delta x} = \dfrac{1}{2\Delta x}$ is the Nyquist

$j = \dfrac{N_x}{2}+1 \quad \dfrac{\frac{N_x}{2}+1}{L} = -\left(\dfrac{\frac{N_x}{2}-1}{L}\right)$

$j = N_x - 1 \quad \dfrac{N_x-1}{L} = -\dfrac{1}{L}$

So the spectrum comes out "folded"

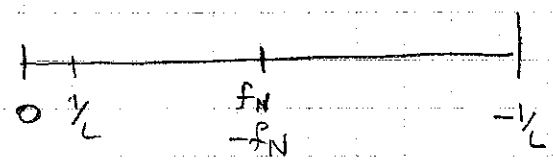

Spectrum

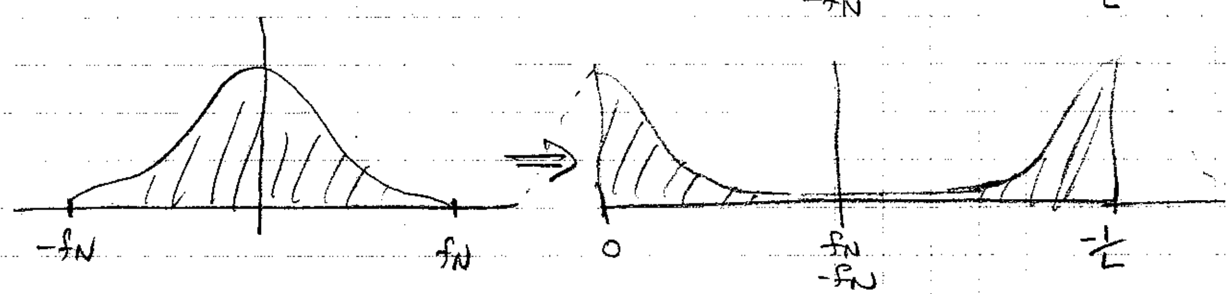

Remark. Note that because of the folding $-f_N \equiv f_N$.

<u>2D - DFT</u>:

$f(x,y)$ sampled at increments $\Delta x, \Delta y$

N_x : number of points in x-direction

N_y : number of points in y-direction

$$F_{j\ell} = \sum_{r=0}^{N_x-1}\sum_{s=0}^{N_y-1} f_{rs}\, e^{-i2\pi\left(rj/N_x + s\ell/N_y\right)}$$

$$f_{rs} = \frac{1}{N_x N_y}\sum_{j=0}^{N_x-1}\sum_{\ell=0}^{N_y-1} F_{j\ell}\, e^{i2\pi\left(rj/N_x + s\ell/N_y\right)}$$

$\tilde{k}_{x_j} = \frac{j}{N_x \Delta x} = \frac{j}{L_x}$ $j = 0, \dots N_x - 1$ $\tilde{k}_{N_x} = \frac{1}{2\Delta x}$ is Nyquist in x direct.

$\tilde{k}_{y_l} = \frac{l}{N_y \Delta y} = \frac{l}{L_y}$ $l = 0, \dots N_y - 1$ $\tilde{k}_{N_y} = \frac{1}{2\Delta y}$ is Nyquist in y

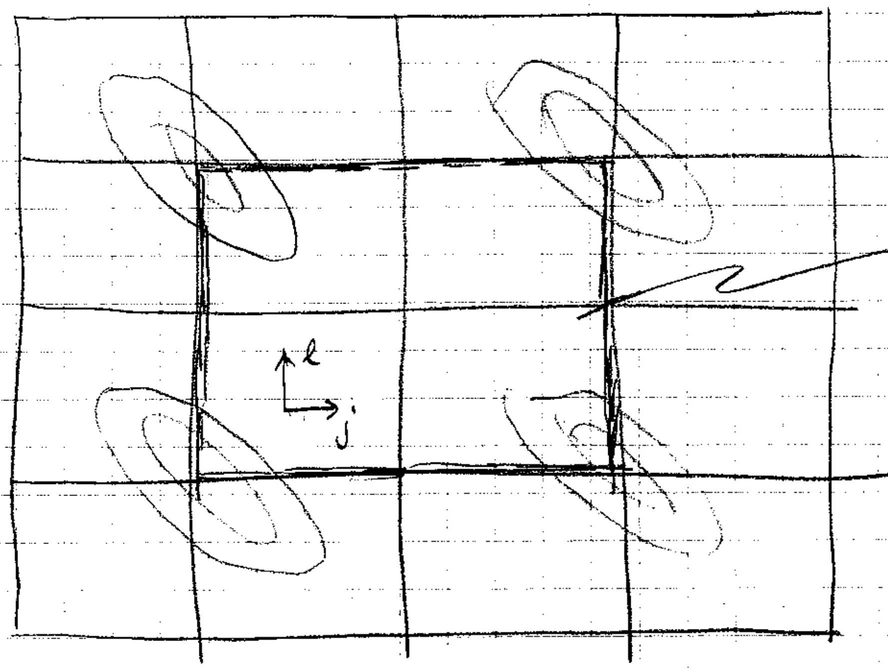

This is what come out from the DFT

Remark: Understanding the output of the DFT and how everything is folded is important.

Tutorial example:

Aliasing

The highest frequency that we can capture with a sampling interval Δ is $\tilde{k}_N = \frac{1}{2\Delta x}$ (the Nyquist frequency)

If data contain frequencies higher than the Nyquist, they will appear as lower frequencies

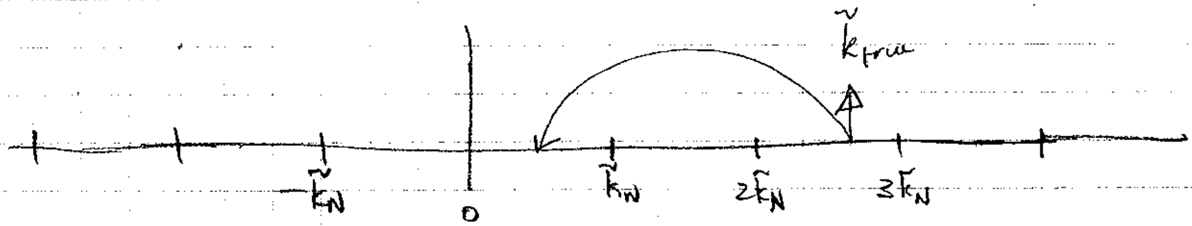

$$\tilde{k}_{rec} = \tilde{k}_{true} \pm \frac{n}{\Delta x} \qquad n = \pm 1, \pm 2, \dots$$

in circular wavenumber

$$k_{rec} = k_{true} \pm \frac{2\pi n}{\Delta x}$$

If $F(k)$ is the true fourier transform then the digital transform is the sum of all of the aliased energy, ie

$$\boxed{F_D(k) = \frac{1}{\Delta x} \sum_{j=-\infty}^{\infty} F\left(k - \frac{2\pi j}{\Delta x}\right)}$$

Remark: The relationship between the discrete and continuous F.T. is
$F_j = \frac{1}{\Delta} F\left(k = \frac{2\pi j}{L}\right)$

Power Spectrum

$$\boxed{P(\tilde{k}_j) = |F(\tilde{k}_j)|^2}$$ is the descrete power spectrum.

Fourier Transform of Basic Source

For gravity and magnetics can have simple sources of monopoles, dipoles, lines. We are interested in what the signature of these elements are in the Fourier domain. These depend upon the 1/r f$^{\underline{o}}$.

$\mathcal{F}[\frac{1}{r}]$:

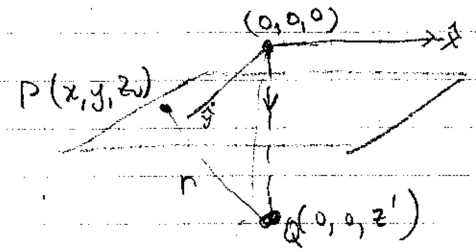

Consider a source point Q at a point (0,0,z') and an arbitrary point P at a depth z_0 $(z' > z_0)$

$$\mathcal{F}\left[\frac{1}{r}\right] = \int_{-\infty}^{\infty}\int_{-\infty}^{\infty} \frac{1}{\sqrt{x^2+y^2+(z_0-z')^2}} e^{-i(k_x x + k_y y)} dx\,dy$$

$$\boxed{\mathcal{F}\left[\frac{1}{r}\right] = 2\pi \frac{e^{|k|(z_0-z')}}{|k|} \qquad z' > z_0 \quad |k| \neq 0}$$

p 272

$$|k| = \sqrt{k_x^2 + k_y^2}$$

Fourier Spectrum of a monopole.

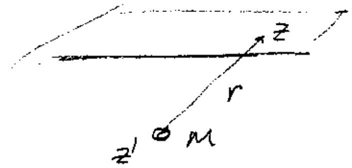

z = observer

(γ is Newtons Gravitational constant.)

$$\phi(r) = \frac{\gamma M}{r}$$

$$\mathcal{F}[\phi] = \gamma M \, \mathcal{F}\left[\frac{1}{r}\right]$$

$$\boxed{\mathcal{F}[\phi] = 2\pi \frac{\gamma M}{|k|} e^{|k|(z-z')}} \qquad z' > z \qquad \text{and } k \neq 0 \qquad (1)$$

Vertical component of gravity field $\boxed{g_z = \frac{\partial}{\partial z}\phi(r)}$

$$\mathcal{F}[g_z] = \mathcal{F}\left[\gamma M \frac{\partial}{\partial z}\left(\frac{1}{r}\right)\right] = \gamma M \frac{\partial}{\partial z} \mathcal{F}\left[\frac{1}{r}\right] \qquad \left(\mathcal{F}_{2d} = \iint_{x\,y} \quad dx\,dy\right)$$

$$\boxed{\mathcal{F}[g_z] = 2\pi \gamma M e^{|k|(z-z')}} \qquad z' > z$$

(1)

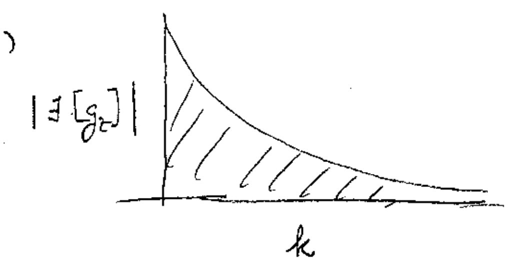

(1) Maximum value occurs at $|k| = 0$ and is proportional to the mass

(2) Energy decreases according to $|k|(z-z')$

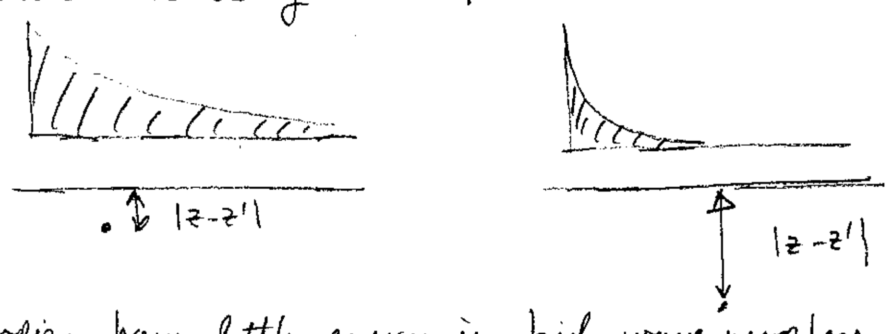

Deeper bodies have little energy in high wave numbers (short wavelength)

Remark: Because of superposition, we can use this result to produce the spectrum from line sources or discrete multiple bodies

Magnetic Dipole

This is the second building block

$$\phi(r) = -\frac{\mu_0}{4\pi} \vec{m} \cdot \nabla_p\left(\frac{1}{r}\right) \qquad \left(\vec{m} = m\hat{m}\right)$$

$$= -\frac{\mu_0}{4\pi} m \left(\hat{m}_x \frac{\partial}{\partial x}\left(\frac{1}{r}\right) + \hat{m}_y \frac{\partial}{\partial y}\left(\frac{1}{r}\right) + \hat{m}_z \frac{\partial}{\partial z}\left(\frac{1}{r}\right)\right)$$

For any f^{cn} $f(x,z)$

$$\mathcal{F}\left[\frac{\partial}{\partial x} f(x,z)\right] = \iint \frac{\partial}{\partial x} f(x,z)\, e^{-i(k_x x + k_y y)} dx\,dy = ik_x \mathcal{F}[f(x,y)]$$

$$\left\{ \int \frac{df(x)}{dx} e^{-ikx} dx = f(x) e^{-ikx} \Big|_{-\infty}^{\infty} - \int_{-\infty}^{\infty} f(x)(-ik) e^{-ikx} dx = ik\mathcal{F}[f] \right\}$$

So $$\mathcal{F}[\phi(r)] = -\frac{\mu_0 m}{4\pi}\left[\hat{m}_x ik_x \mathcal{F}\left[\frac{1}{r}\right] + \hat{m}_y ik_y \mathcal{F}\left[\frac{1}{r}\right] + \hat{m}_z \frac{\partial}{\partial z}\mathcal{F}\left[\frac{1}{r}\right]\right]$$

$$\mathcal{F}\left[\frac{1}{r}\right] = \frac{2\pi e^{|k|(z-z')}}{|k|} \qquad \frac{\partial}{\partial z}\mathcal{F}\left[\frac{1}{r}\right] = 2\pi e^{|k|(z-z')}$$

$$\mathcal{F}[\phi(r)] = -\frac{\mu_0}{2} m \left[\frac{\hat{m}_x ik_x}{|k|} + \frac{\hat{m}_y ik_y}{|k|} + \hat{m}_z\right] e^{|k|(z-z')}$$

$$\boxed{\mathcal{F}[\phi(r)] = -\frac{\mu_0 m}{2} \Theta_m e^{|k|(z-z')}}$$

where $$\boxed{\Theta_m = \left(\hat{m}_z + i\frac{\hat{m}_x k_x + \hat{m}_y k_y}{|k|}\right)}$$

is a complex function of k_x and k_y and depends only upon the orientation of the dipole.

The magnetic field is related to the potential by $B = -\nabla_p \phi$, and any component; say in the $\hat{l}$ direction is obtained by

$$B_l = \hat{l} \cdot \vec{B} = -\hat{l} \cdot \nabla_p \phi$$

Perhaps B_l represents the total magnetic field anomaly.

$$\mathcal{F}[B_l(x,y)] = \mathcal{F}\left[-\hat{l}_x \frac{\partial}{\partial x}\phi - \hat{l}_y \frac{\partial}{\partial y}\phi - \hat{l}_z \frac{\partial}{\partial z}\phi\right]$$

$$= ik_x\left[-\hat{l}_x \mathcal{F}[\phi]\right] - ik_y \hat{l}_y \mathcal{F}[\phi] - \hat{l}_z \frac{\partial}{\partial z}\mathcal{F}[\phi]$$

$$\mathcal{F}[\phi] = -\frac{\mu_0 m}{2} \Theta_m e^{|k|(z-z')}$$

$$\frac{\partial}{\partial z}\mathcal{F}[\phi] = -\frac{\mu_0 m}{2} \Theta_m |k| e^{|k|(z-z')}$$

$$\mathcal{F}[B_l(x,y)] = -\left[\hat{l}_z |k| + ik_x \hat{l}_x + ik_y \hat{l}_y\right]\left(-\frac{\mu_0 m}{2}\Theta_m e^{|k|(z-z')}\right)$$

$$= +\left[l_z + \frac{ik_x \hat{l}_x + ik_y \hat{l}_y}{|k|}\right]|k| \frac{\mu_0 m}{2} \Theta_m e^{|k|(z-z')}$$

Let $\quad \Theta_l = l_z + \dfrac{ik_x \hat{l}_x + ik_y \hat{l}_y}{|k|}$

So $$\boxed{\mathcal{F}[B_l(x,y)] = \frac{\mu_0 m}{2} \Theta_m \Theta_l |k| e^{k(z-z')}} \qquad z < z'$$

(1) Orientations of the source dipole and the receiver are in Θ_m, Θ_l

(2) Depth of the dipole is exclusively in the exponential term.

(3) Spectrum of a dipole is complicated

Consider: $\Theta_M = \left(m_z + i \left(\frac{\hat{m}_x k_x + \hat{m}_y k_y}{|k|} \right) \right)$

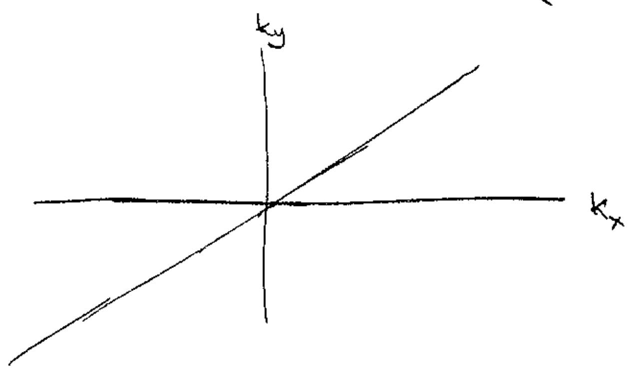

Real $\{ \Theta_m \} = m_z =$ constant

Im $\{ \Theta_m \}$ is complicated

Consider $k_y = \alpha k_x$

Imaginary part $\frac{\hat{m}_x k_x + \hat{m}_y \alpha k_x}{k_x (1+\alpha^2)^{1/2}} = \frac{\hat{m}_x + \alpha \hat{m}_y}{\sqrt{1+\alpha^2}}$ is constant for any k_x

If $\alpha < 0$ then imaginary part behaves as $\frac{\hat{m}_x - |\alpha| \hat{m}_y}{\sqrt{1+\alpha^2}}$

So imaginary part is discontinuous at the origin

$(|k|, \theta)$

Or write $k_x = |k| \cos\theta$ Polar coordinates
$k_y = |k| \sin\theta$

$$\text{Im}\{ \Theta_M \} = \frac{\hat{m}_x |k| \cos\theta + \hat{m}_y |k| \sin\theta}{|k|} = \hat{m}_x \cos\theta + \hat{m}_y \sin\theta$$

is independent of $|k|$.

Average value of Θ_M in a circle around the origin

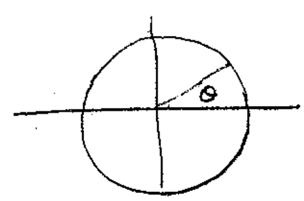

$$\boxed{\begin{aligned} &\frac{1}{2\pi} \int_0^{2\pi} \left(\hat{m}_x \cos\theta + \hat{m}_y \sin\theta \right) d\theta = 0 \\ &\frac{1}{2\pi} \int_0^{2\pi} \hat{m}_z \, d\theta = \hat{m}_z \end{aligned}}$$

Θ_m is not radially symmetric but the average value along any concentric circle is independent of radius of the circle

Consider Θ_m in complex plane

$$|\Theta_m| = \sqrt{\hat{m}_z^2 + \left(\hat{m}_x \cos\theta + \hat{m}_y \sin\theta\right)^2} \qquad \text{independent of } k$$

$$\mathcal{F}\left[B_\ell(x,y)\right] = \frac{\mu_0 m}{2}\, \Theta_m\, \Theta_\ell\, |k|\, e^{k(z-z')}$$

$$\boxed{\left|\mathcal{F}\left[B_\ell(x,y)\right]\right| = \frac{\mu_0 m}{2}\, |\Theta_m|\, |\Theta_\ell|\, |k|\, e^{k(z-z')}}$$

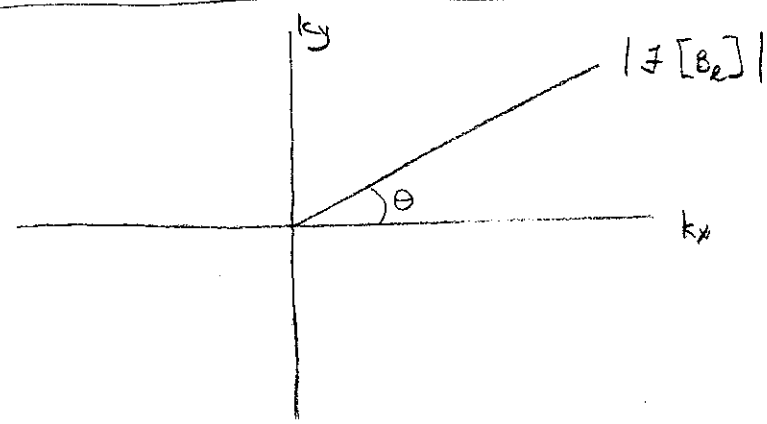

Amplitude spectra of $\mathcal{F}[B_\ell]$ will have the same shape, independent of θ. Spectra for different θ will differ only by a constant.

The radially averaged power spectrum is proportional to spectrum along each radius extending from the origin.

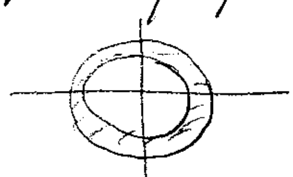

$$P(|k|) = \int_0^{2\pi} P(|k|,\theta)\, |k|\, d\theta$$

✱ So the shape of the amplitude spectrum as a function of $|k|$ depends only on the term $|k|\, e^{k(z-z')}$

which depends upon depth of burial of the dipole.

The shape is independent of orientation of the dipole and orientation of receiver.

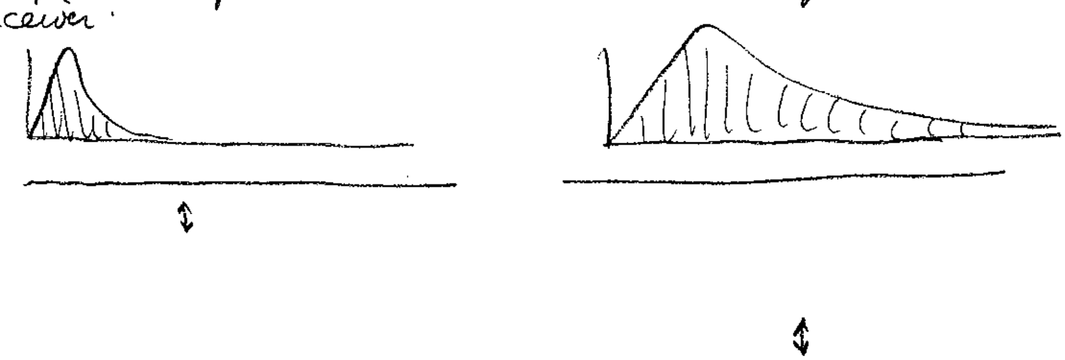

Processing of Potential Field Data

A: Low pass / high pass filtering

Uses: remove noise
: separate regional and local anomalies

e.g. input data — $\boxed{\text{low pass filter}}$ — regional field

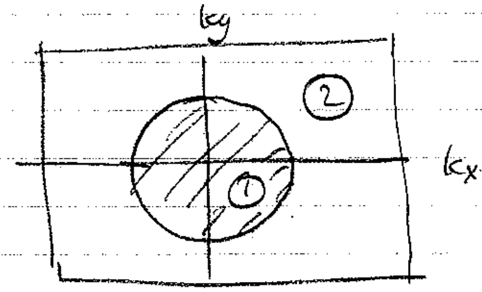

Ideal low pass filter $\quad H(k_x, k_y) = 1 \quad (k_x^2 + k_y^2)^{1/2} < k_o$

$\qquad\qquad\qquad\qquad\qquad\qquad = 0 \quad > k_o$

Ideal high pass $\quad H(k_y, k_y) = 0 \quad |k| < k_o$

$\qquad\qquad\qquad\qquad\qquad = 1 \quad |k| > k_o$

Remark: In designing filters you must take the same precautions as with 1-d filters. Don't want sidelobes $\Rightarrow$ use ramps for transitions rather than abrupt cuts.

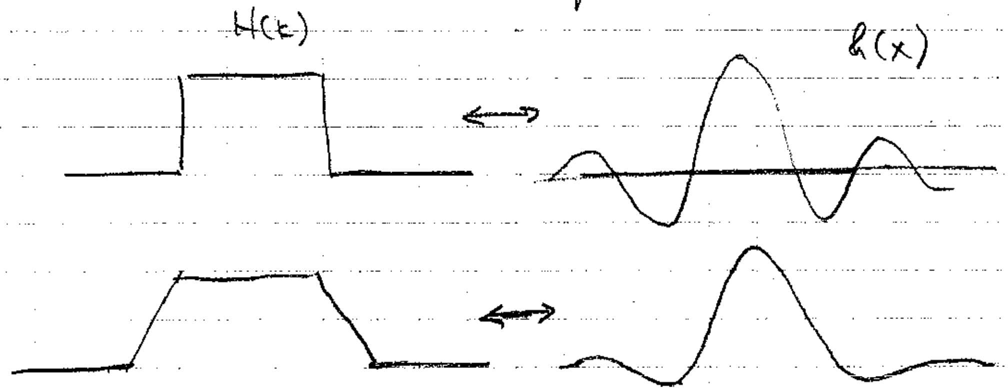

Directional Filtering (Dip filtering)

Maps are sometimes dominated by features in a particular direction. It is often desirable to

(i) accentuate those features by removing signal that does not have that trend

(ii) see the residual field obtained by removing the linear features.

map

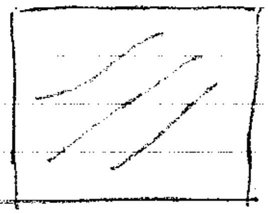

To carry out directional filtering, we first calculate the Fourier transform of a straight line

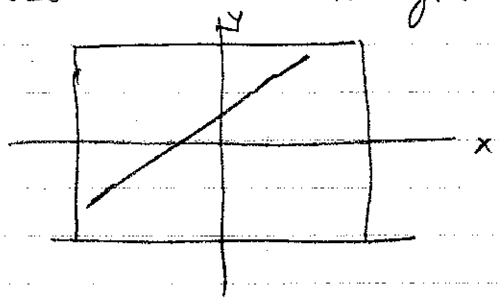

$y = ax + b$

$$f(x,y) = \delta\left(y - (ax+b)\right) = \delta(y - ax - b)$$

$$F[k_x, k_y] = \int_{-\infty}^{\infty}\int_{-\infty}^{\infty} \delta(y-ax-b)\, e^{-i(k_x x + k_y y)}\, dx\, dy$$

do y-integral

$$= \int_{-\infty}^{\infty} e^{-i(k_x x + k_y(ax+b))}\, dx$$

$$= \int_{-\infty}^{\infty} e^{-ik_y b}\, e^{-i(k_x + ak_y)x}\, dx$$

$$= e^{-ik_y b} \int_{-\infty}^{\infty} e^{-i(k_x + ak_y)x}\, dx$$

$$\boxed{F[k_x, k_y] = 2\pi e^{-ik_y b}\, \delta(k_x + ak_y)}$$

In the last step we have used the relationship

$$\boxed{\delta(k) = \frac{1}{2\pi}\int_{-\infty}^{\infty} e^{-i2\pi k x}\, dx} \qquad (1)$$

$$\boxed{\mathcal{F}[k_x, k_y] = 2\pi e^{-ik_y b}\, \delta(k_x + a k_y)} \qquad (2)$$

$k_x + a k_y = 0$

$k_y = -\frac{1}{a} k_x$

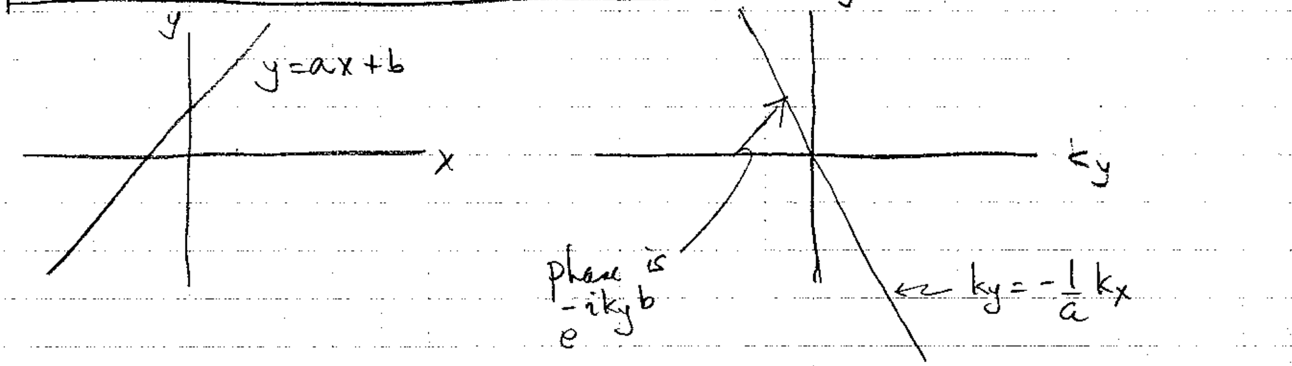

So a line with slope 'a' in the spatial domain appears as a line with slope $-1/a$ in the Fourier domain!

Remark: One way to validate equation (1) is to begin with the Fourier integrals

$$F(k) = \int_{-\infty}^{\infty} f(x)\, e^{-ikx}\, dx$$

$$f(x) = \frac{1}{2\pi}\int_{-\infty}^{\infty} F(k)\, e^{ikx}\, dk$$

Substitute

$$F(k) = \int_{-\infty}^{\infty}\left(\frac{1}{2\pi}\int_{-\infty}^{\infty} F(k')\, e^{ik'x}\, dk'\right) e^{-ikx}\, dx$$

$$= \int_{-\infty}^{\infty} F(k') \underbrace{\left(\frac{1}{2\pi}\int_{-\infty}^{\infty} e^{-i(k-k')x}\, dx\right)}_{\delta(k-k')} dk$$

(k') (x)

$$= \int F(k')\, \delta(k-k')\, dk$$

$$\equiv F(k)$$

So $$\boxed{\delta(k) = \frac{1}{2\pi}\int_{-\infty}^{\infty} e^{-ikx}\,dx}$$

Dip Filters, Pie-Slice Filters

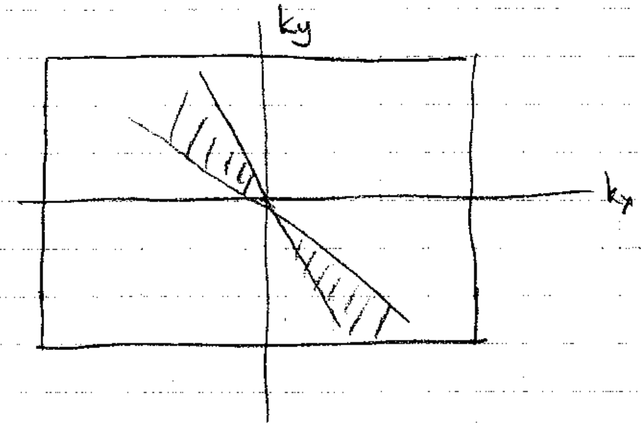

for data

Again: Good practise to not make cuts severe; taper the boundaries.

Upward Continuation

- Compare surface and airborne data
- provide fields at a height above the surface (as a possible prelude to inversion)
- accentuate deep seated anomalies
- attenuate the shallow-source anomalies
- estimation of regional

Green's Third Identity:

If u is harmonic in R

$$u(P) = \frac{1}{4\pi}\int_S \left(\frac{1}{r}\frac{\partial u}{\partial n} - u\frac{\partial}{\partial n}\left(\frac{1}{r}\right)\right)ds$$

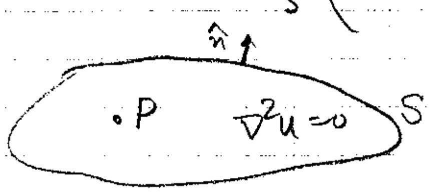

This says if we know u and $\frac{\partial u}{\partial n}$ on the boundary then we can compute $u(P)$ at any location in R.

So consider

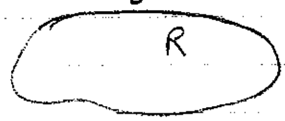

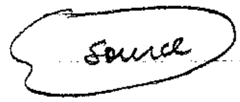

gravity or magnetic sources have potentials and fields outside that are harmonic

How can we use this? Consider R to be a hemisphere.
Bottom plane is at $z = z_0$

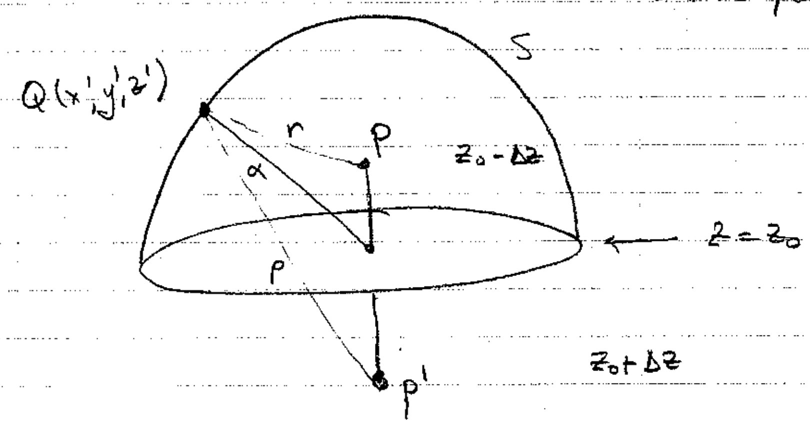

$P(x, y, z_0 - \Delta z)$: is the point at which we want to evaluate the u
$Q(x', y', z')$: is a point on S
$P'(x, y, z_0 + \Delta z)$: is a mirror (or image) point that is a reflection of P across the plane

$$\int_S = \int_{\text{dome}} + \int_{\text{flat bottom}}$$

for gravity fields $u \propto \frac{M}{r}$

for magnetic fields $u \propto \frac{m}{r^2}$

$$\int_{\text{dome}} \frac{1}{r}\frac{\partial u}{\partial n}\, dS \;\to 0 \text{ as } \alpha \to \infty$$

$$\int_{\text{dome}} u \frac{\partial}{\partial n}\left(\frac{1}{r}\right) dS \to 0 \text{ as } \alpha \to \infty$$

So the contribution to $u(P)$ from the top part of the hemisphere becomes negligible as the radius $\alpha \to \infty$.

So working with the bottom of the hemisphere

$$\boxed{u(x,y,z_0-\Delta z) = \int_{-\infty}^{\infty}\int_{-\infty}^{\infty}\left(\frac{1}{r}\frac{\partial u(x',y',z_0)}{\partial z'} - u(x',y',z_0)\frac{\partial}{\partial z'}\left(\frac{1}{r}\right)\right)dx'dy'} \quad (1)$$

$$r = \sqrt{(x-x')^2 + (y-y')^2 + (z_0-\Delta z - z')^2}$$

Difficulty: Equation (1) requires knowledge of u and $\frac{\partial u}{\partial n}$ on the boundary. This degree of information is rarely available.

Green's second identity

If u and V are both harmonic in R then

$$\frac{1}{4\pi}\int_S\left(V\frac{\partial u}{\partial n} - u\frac{\partial V}{\partial n}\right)ds = 0$$

Add this to Green's third identity $\quad u(P) = \frac{1}{4\pi}\int_S\left(\frac{1}{r}\frac{\partial u}{\partial n} - u\frac{\partial}{\partial n}\left(\frac{1}{r}\right)\right)ds$
to get

$$u(P) = \frac{1}{4\pi}\int_S\left[\left(V+\frac{1}{r}\right)\frac{\partial u}{\partial n} - u\frac{\partial}{\partial n}\left(V+\frac{1}{r}\right)\right]ds$$

To eliminate the first term we need to find a function V that is harmonic in R and for which $V+\frac{1}{r}=0$ on S

Let $\quad V = -\frac{1}{\rho}$

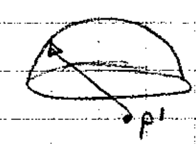

$$\rho = \sqrt{(x-x')^2 + (y-y')^2 + (z_0+\Delta z - z')^2}$$

is the distance from the mirror point to any point on the bdy.

(1) $\nabla^2\left(\frac{1}{\rho}\right) = 0$ inside R

(2) on the dome: $\left(V+\frac{1}{r}\right)\to 0$ as $\alpha\to\infty$

(3) on the flat bottom $V+\frac{1}{r} = 0$
$z'=z_0$

So

$$U(x,y,z_0-\Delta z) = -\frac{1}{4\pi}\iint u(x',y',z_0)\,\frac{\partial}{\partial z'}\left(\frac{1}{r}-\frac{1}{\rho}\right)dx'dy'$$

Carrying out the derivative yields

$$\boxed{U(x,y,z_0-\Delta z) = \frac{\Delta z}{2\pi}\int_{-\infty}^{\infty}\int_{-\infty}^{\infty}\frac{U(x',y',z_0)}{\left((x-x')^2+(y-y')^2+\Delta z^2\right)^{3/2}}\,dx'dy'} \quad (1)$$

$\underline{\Delta z > 0}$

So the upward continuation can be achieved by a weighted summation (or integration) of the existing data

Integration formula (along any direction in the xy plane looks like

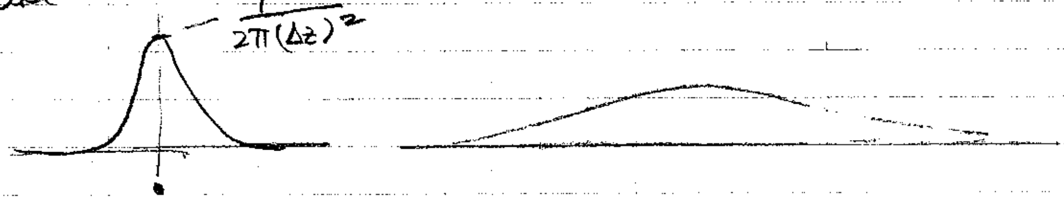

Small $\Delta z \Rightarrow$ upward continued value depends only on close neighbors

• large $\Delta z \Rightarrow$ upward continued value depends on values far away.

Upward Continuation in the Fourier Domain

We note that eq (1) is a 2D convolution

Let $\boxed{\psi_u(x,y,\Delta z) = \frac{\Delta z}{2\pi}\,\frac{1}{\left(x^2+y^2+(\Delta z)^2\right)^{3/2}}}$

Then $\boxed{U(x,y,z_0-\Delta z) = \iint U(x',y',z_0)\,\psi_u(x-x',y-y',\Delta z)\,dx'dy'}$

Thus we can write

$$\mathcal{F}\left[u(x,y,z_0-\Delta z)\right] = \mathcal{F}\left[u(x,y,z_0)\right]\cdot\mathcal{F}\left[\psi(x,y,\Delta z)\right]$$

$$\psi(x,y,\Delta z) = \frac{\Delta z}{2\pi}\,\frac{1}{(x^2+y^2+\Delta z^2)^{3/2}} = \frac{\Delta z}{2\pi r^3} \qquad r=\sqrt{x^2+y^2+(\Delta z)^2}$$

$$\frac{\partial}{\partial \Delta z}\left(\frac{1}{r}\right) = \frac{\partial}{\partial \Delta z}\,\frac{1}{(x^2+y^2+(\Delta z)^2)^{1/2}} = -\frac{1}{2}\,\frac{2\Delta z}{r^3} = \frac{-\Delta z}{r^3}$$

So $$\boxed{\psi(x,y,\Delta z) = \frac{-1}{2\pi}\frac{\partial}{\partial \Delta z}\left(\frac{1}{r}\right)}$$

$$\mathcal{F}\left[\psi(x,y,\Delta z)\right] = \frac{-1}{2\pi}\frac{\partial}{\partial \Delta z}\,\mathcal{F}\left[\frac{1}{r}\right]$$

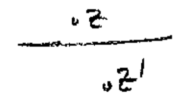

But we previously had derived $\mathcal{F}\left[\frac{1}{r}\right] = \frac{2\pi e^{|k|(z-z')}}{|k|} \equiv \frac{2\pi}{|k|}e^{-|k|\Delta z}$

$$\mathcal{F}\left[\psi(x,y,\Delta z)\right] = -\frac{1}{\cancel{2\pi}}\frac{\partial}{\partial \Delta z}\left(\frac{\cancel{2\pi}}{|k|}e^{-|k|\Delta z}\right) = e^{-|k|\Delta z}$$

So $$\boxed{\mathcal{F}\left[\psi(x,y,\Delta z)\right] = e^{-|k|\Delta z} \qquad \Delta z > 0}$$

Thus level to level continuation of the fields can be obtained by multiplying the FT of the data by the upward continuation filter

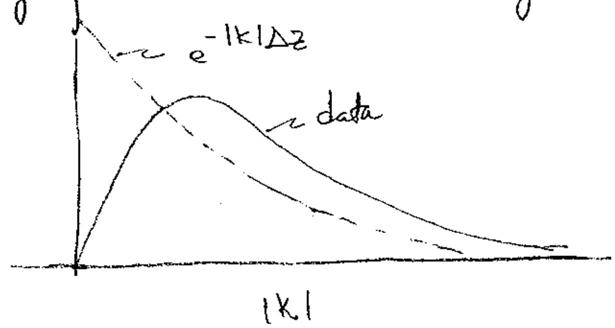

So we can see how the high frequencies will be attenuated with upward continuation.

The higher the upward continuation height ⇒ the greater the attenuation will be.

Downward Continuation

The upward continuation formula is a relationship between the Fourier transform of the field at two heights (z_0, $z_0 - \Delta z$)
The formula is valid so long as there are no sources between the two levels:

$z_0 - \Delta z$

no sources

z_0

It follows, that if the field is known at $z_0 - \Delta z$ we can find the field at z_0 by

$$\mathcal{F}\left[u(x,y,z_0)\right] = \frac{\mathcal{F}\left[u(x,y,z_0-\Delta z)\right]}{\mathcal{F}\left[\psi(x,y,\Delta z)\right]} = e^{|k|\Delta z}\,\mathcal{F}\left[u(x,y,z_0-\Delta z)\right]$$

The downward continuation filter $e^{|k|\Delta z}$ will greatly accentuate the high frequency data (which is often associated with noise)

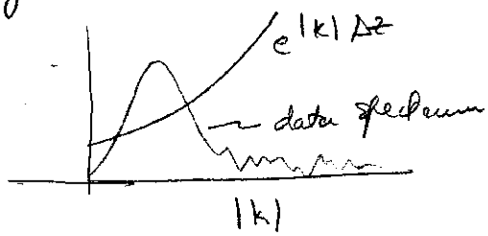

Comments:

(1) Downward continuation is valid so long as there is no source between the data plane and the level of downward continued data

(2) Downward continuation can enhance resolution

(3) Downward continuation enhances the high frequency

(4) Downward continuation is basically unstable filtering. Use it with extreme caution.

☆ Downward continuation should be done as an inverse problem.

Horizontal and Vertical Derivatives

When viewing data in map form it is often worthwhile to look at spatial gradients.

Example: Gravity map of Canada

Horizontal derivatives are easy to compute using Fourier analysis

$$\mathcal{F}\left[\frac{d^n\phi}{dx^n}\right] = (ik_x)^n \mathcal{F}[\phi]$$

$$\mathcal{F}\left[\frac{d^n\phi}{dy^n}\right] = (ik_y)^n \mathcal{F}[\phi]$$

First derivative maps $\sqrt{\left(\frac{d\phi}{dx}\right)^2 + \left(\frac{d\phi}{dy}\right)^2}$ are used to accentuate structu

eg

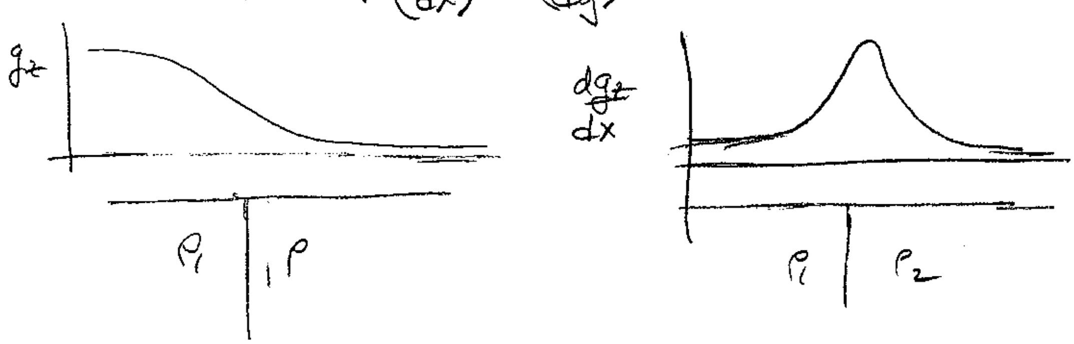

First derivative would show a peak over a contact zone.

2^{nd} Vertical Derivative $\left(\frac{d^2\phi}{dz^2}\right)$

It is straightforward to obtain the second vertical derivative since ϕ is harmonic

$$\nabla^2\phi = 0$$

$$\frac{\partial^2\phi}{\partial x^2} + \frac{\partial^2\phi}{\partial y^2} + \frac{\partial^2\phi}{\partial z^2} = 0$$

So
$$\frac{\partial^2\phi}{\partial z^2} = -\frac{\partial^2\phi}{\partial x^2} - \frac{\partial^2\phi}{\partial y^2}$$

$$\mathcal{F}\left[\frac{\partial^2\phi}{\partial z^2}\right] = \left[-(ik_x)^2 - (ik_y)^2\right]\mathcal{F}[\phi] = (k_x^2 + k_y^2)\mathcal{F}[\phi]$$

So
$$\boxed{\mathcal{F}\left[\frac{\partial^2\phi}{\partial z^2}\right] = |k|^2\mathcal{F}[\phi]}$$

So the Fourier filter for the second derivative also accentuates high wave numbers.

Remark: We can get any order of vertical derivative. This must be true since we showed how to upward continue the data. Consider the first vertical derivative

$$\frac{\partial}{\partial z}\phi(x,y,z) = \lim_{\Delta z\to 0}\frac{\phi(x,y,z) - \phi(x,y,z-\Delta z)}{\Delta z}$$

So
$$\mathcal{F}\left[\frac{\partial\phi}{\partial z}\right] = \lim_{\Delta z\to 0}\frac{\mathcal{F}[\phi] - e^{-|k|\Delta z}\mathcal{F}[\phi]}{\Delta z} = \lim_{\Delta z\to 0}\frac{1}{\Delta z}\left(1 - e^{-|k|\Delta z}\right)\mathcal{F}[\phi]$$

$$= \lim_{\Delta z\to 0}\frac{1}{\Delta z}\left(1 - (1 - |k|\Delta z)\right)\mathcal{F}[\phi]$$

$$\boxed{\mathcal{F}\left[\frac{\partial\phi}{\partial z}\right] = |k|\mathcal{F}[\phi]}$$

Thus we have
$$\boxed{\mathcal{F}[\nabla\phi] = (ik_x, ik_y, |k|)\mathcal{F}[\phi]}$$

Reduction to Pole.

A common filtering operation applied to magnetic maps is to "reduce them to pole". This makes signatures easier to interpret

Consider

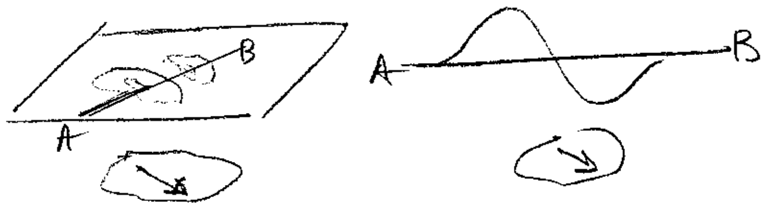

Profile over the body has +ve & -ve

It would be easier to interpret if we had a total field anomaly that corresponded to the magnetization being vertical.

eg

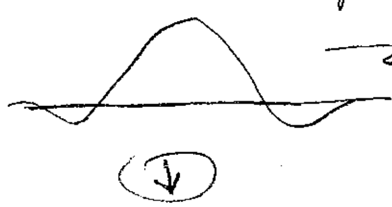

now the peak lies directly over the body.

Procedure: Take the measured magnetic field and transform it so that you obtain the field that would have been measured if the inducing field had been vertical. That is, if the survey had been done at the magnetic pole.

To do this, we first need to find an expression, using Fourier transforms, to model arbitrary magnetizations.

First Step: Modelling of a 3D density distribution using $\mathcal{F}T$.

Remember:

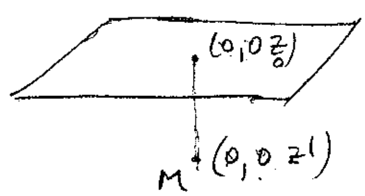

$z' > z_0$ z_0: observation plane

$$\mathcal{F}[g_z(x,y)] = 2\pi\gamma M e^{|k|(z_0 - z')}$$

If the mass is not beneath the coordinate origin but at a location (x', y', z') the

$$\mathcal{F}[g_z(x,y)] = 2\pi\gamma M e^{|k|(z_0 - z')} e^{i(k_x x' + k_y y')}$$ (shift thm)

$$f(x - x') \longleftrightarrow e^{ikx'} \mathcal{F}[x]$$

Now think of

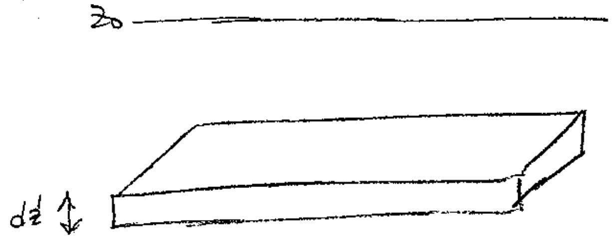

$$M \rightarrow \rho(x', y, z')\,dx'dy'dz$$

Then by superposition,

$$\mathcal{F}[g_z(x,y)] = \int_{-\infty}^{\infty}\int_{-\infty}^{\infty} 2\pi\gamma\,\rho(x',y',z')\, e^{|k|(z_0 - z')} e^{i(k_x x' + k_y y')}\,dx'dy'dz'$$

$$= 2\pi\gamma\, e^{|k|(z_0 - z')} \underbrace{\iint \rho(x',y',z')\, e^{i(k_x x' + k_y y')}\,dx'dy'}$$

but

$$\boxed{\mathcal{F}[\rho(z')] = \int_{-\infty}^{\infty}\int_{-\infty}^{\infty} \rho(x',y',z')\, e^{i(k_x x' + k_y y')}\,dx'dy'}$$

is the 2d FT of the mass sheet at z'.

Now use superposition in the vertical direction
Response from the whole volume is

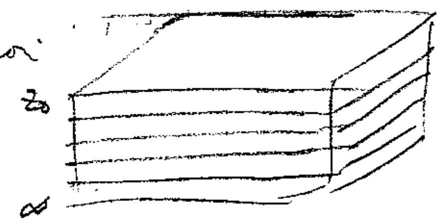

$$\mathcal{F}[g_z(x,y)] = \int_{z_0}^{\infty} (\text{Response of sheet})\,dz'$$

$$\boxed{\mathcal{F}[g_z(x,y)] = 2\pi\gamma\, e^{|k|z_0} \int_{z_0}^{\infty} \mathcal{F}[\rho(z')]\, e^{-|k|z'}\,dz'}$$

So we integrate the FT due to separate layers and then take the inverse FT to get the final field.

Remark: This can be quite computationally efficient for large problems

In a completely analagous vein we can derive the magnetic field for 3d bodies

FT of a dipole of strength m at a depth Δz below the observer was

$$\boxed{\mathcal{F}[\Delta T] = \frac{\mu_0}{2} m\, \Theta_m\, \Theta_f\, |k|\, e^{-|k|\Delta z}} \qquad \Delta z > 0$$

This translate in

$$\boxed{\mathcal{F}[\Delta T] = \frac{\mu_0}{2}\, \Theta_m\, \Theta_f\, |k|\, e^{-|k| z_0} \int_{z_0}^{\infty} \mathcal{F}[M(z')]\, e^{-|k|z'}\, dz'} \qquad \star$$

where $\mathcal{F}[M(z')]$ is the 2d FT of the magnetization on one horizontal slice through the body at depth z'

Note that the information about the strength of the magnetization $M = \kappa H$ is in the integral. The information about the direction of magnetization and the direction in which the data are acquired is stored in Θ_m, Θ_f

where

$$\Theta_m = \hat{m}_z + i\left(\frac{\hat{m}_x k_x + \hat{m}_y k_y}{|k|}\right) \qquad \hat{m} = (\hat{m}_x, \hat{m}_y, \hat{m}_z)$$

$$\Theta_f = \hat{f}_z + i\left(\frac{\hat{f}_x k_x + \hat{f}_y k_y}{|k|}\right) \qquad \hat{f} = (\hat{f}_x, \hat{f}_y, \hat{f}_z)$$

Suppose we wanted to generate the data corresponding to a different field component and due to a different direction of the inducing field. $\hat{f}' = (\hat{f}_x', \hat{f}_y', \hat{f}_z')$ $\quad \hat{m}' = (\hat{m}_x', \hat{m}_y', \hat{m}_z')$

Say

$$\Theta_m' = \hat{m}_z' + i\left(\frac{\hat{m}_x' k_x + \hat{m}_y' k_y}{|k|}\right)$$

$$\Theta_f' = \hat{f}_z' - i\left(\frac{\hat{f}_x' k_x + \hat{f}_y' k_y}{|k|}\right)$$

So if

$$\mathcal{F}[\Delta T_t] = \frac{\mu_0}{2} \Theta_m' \Theta_f' |k| e^{|k| z_0} \int_{z_0}^{\infty} e^{-|k| z'} \mathcal{F}[M(z')]\, dz'$$

then the filter which converts the original data set to the new data set is

$$\mathcal{F}[\Delta T_t] = \mathcal{F}[\Delta T] \cdot \mathcal{F}[\psi_t]$$

$$\boxed{\mathcal{F}[\psi_t] = \frac{\Theta_m' \Theta_f'}{\Theta_m \Theta_f}}$$

In reduction to pole, for total field data $\hat{m}' = \hat{f}' = (0,0,1)$